THEORETICAL INVESTIGATION ON MIXED CONVECTION INSIDE HORIZONTAL TUBES WITH NOMINALLY UNIFORM HEAT FLUX

By

CHANGLIN ZHANG

Master of Science

Xi'an Jiaotong University

Xi'an, China

1982

Submitted to the Faculty of the
Graduate College of the
Oklahoma State University
in partial fulfillment of
the requirements for
the degree of
DOCTOR OF PHILOSOPHY
December, 1990

THEORETICAL INVESTIGATION ON MIXED CONVECTION INSIDE

HORIZONTAL TUBES WITH NOMINALLY

UNIFORM HEAT FLUX

Thesis Approved:

Thesis Adviser

Dean of Graduate College

ACKNOWLEDGMENTS

First of all, I would like to express my sincere gratitude to my advisor, Dr. Kenneth J. Bell, for his intelligent guidance, inspirational dedication to research and teaching, great human understanding, kindest concern and invaluable help through out my doctoral program.

I am grateful to members of my advisory committee, Drs. Ruth C. Erbar, Cecil C. Gentry, Afshin J. Ghajar, Arland H. Johannes, and Jan Wagner for their advisement. Special thanks are due to Dr. Johannes for permitting me to use his computers.

Particular thanks are due to Dr. Jerry Taborek for his valuable suggestion on development of the correlation, and Dr. David G. Lilley and Dr. Khaled Gasem for their discussions about the computer program. Special thanks are due to Mark A. Young, Bin Fang, and Xiaojian Tao for their help in many ways.

I am thankful to the School of Chemical Engineering for the financial support I received during the course of this work. I am also thankful to all faculty and staff in the School for their kindness and friendship.

My wife, Weiping, and my son, Carl, deserve my deepest appreciation for their encouragement and understanding.

TABLE OF CONTENTS

LIST OF TABLES

LIST OF FIGURES

Figure Page

Figure Page

LIST OF SYMBOLS

A	area, or a function defined in Eq. (4-9)
a	discretization coefficient
c_p	specific heat
D	diffusion conductance
d_i	inside tube diameter
Gr	Grashof number, $g\beta\rho^2 d_i^3(T_w - T_b)/\mu^2$
F	flow rate, Eq. (4-14)
f	a function, Eq. (4-43), or Fanning friction factor
g	gravitational acceleration
h	heat transfer coefficient
k	thermal conductivity
L	length, or convection term, Eqs. (4-10) and (4-11)
m	mass flow rate
Nu	Nusselt number, hd_i/k
Pr	Prandtl number, $c_p\mu/k$
P	Peclet number, $\rho uL/\Gamma$
p	pressure
Q	defined by Eq. (4-43)
q''_w	heat flux on inside tube wall
R	inside tube radius
r	radial coordinate
Ra	Rayleigh number, $GrPr$

Re	Reynolds number, $\rho w_b d_i/\mu$
S	source term
T	temperature,
	or diffusion terms, Eqs. (4-17) and (4-18)
T_b	bulk temperature at a cross section
T_{in}	uniform entrance temperature
u	velocity component in θ direction
v	velocity component in r direction
w	velocity component in z direction
w_b	average axial velocity at a cross section
z	axial coordinate
β	thermal expansion coefficient
Γ	diffusion coefficient
θ	angular coordinate
μ	viscosity
ρ	density
ϕ	a general dependent variable

<u>Subscripts</u>

e,n,s,w	control volume faces, Fig. 13
E,N,S,W	grid points, Fig. 13
D	down stream
i	along θ direction
j	along r direction
k	along z direction
U	up stream

CHAPTER I

INTRODUCTION

Convection is defined as the transport of mass and energy by potential gradients and by gross fluid motion. If the fluid motion arises "naturally" from the effect of a density difference, i. e., buoyancy, resulting from a temperature difference in the gravitational field, then the process is termed natural convection, or free convection. On the other hand, if the motion of the fluid is induced by some external means such as fluid machinery, the process is generally called forced convection.

In a shell-and-tube heat exchanger where the tube-side fluid is moved by a pump or a compressor and there is a temperature difference between the tube wall and the fluid, the effect of natural convection always exists no matter how small it is, compared with the forced convection effect. The effect of natural convection would be superposed on the forced convection. This combined forced convection and natural convection process is called mixed convection.

Within the gravity field of the earth, one would say that mixed convection is the most general type of phenomenon, while pure forced or pure free convection are only the limiting cases when either type of mixing motion can be neglected in comparison to the other. However, for convenience of analysis, one prefers to use a correction factor on the limiting case unless both free and forced convection effects are of comparable order of magnitude. For instance, in the case of turbulent flow inside a small diameter tube usually the natural convection can be neglected and a pure forced convection prediction can be used. On the other hand, for most heat exchangers used in some solar energy systems or electronic element cooling systems where the velocity of working fluid is relatively slow and the flow is in laminar or transition region, the effect of natural convection should be taken into account using a method for mixed convection.

When natural convection effects are pronounced, the orientation of the tube axis becomes important. For example, in vertical tubes the velocity due to buoyancy forces are parallel to the direction of the forced motion; thus, rotational symmetry is retained, and it is possible to solve analytically the equations of motion and energy even in the case of mixed convection. However, in the case of horizontal tubes, the buoyancy-induced motion is perpendicular to the forced main flow direction, resulting in the loss of rotational symmetry. The fluid motion is thus much more difficult to analyze, hence one can appreciate the mathematical difficulties encountered in solving the resultant problem. The horizontal tube situation is considered in this study.

When a flowing fluid is heated in a horizontal tube, the fluid near the wall is warmer, and therefore less dense, than the fluid further removed from the wall; it therefore flows upward along the wall, and continuity requires a downflow of the more dense fluid near the center of the tube. This buoyancy-induced motion composes a so-called secondary flow, compared with the primary forced flow. The motion will reverse during cooling. The three-dimensional streamlines exhibit a spiraling character down the tube as shown in Figure 1. In this case, it is expected that the heat transfer coefficient from the tube wall becomes larger than that estimated by the pure forced convection prediction.

To analyze mixed convection in tubes, the following two cases are usually considered as possible boundary conditions: uniform heat flux (UHF) and uniform wall temperature (UWT). With UHF, a wall-minus-fluid temperature difference exists throughout the tube; therefore, the secondary flow continues along the tube axis. This is quite different from the UWT where the secondary flow develops to a maximum intensity and then diminishes to zero as the temperature difference gradually decreases. So, investigation of mixed convection with UHF has more significant meaning and is generally closer to industrial applications.

Including the entrance length effect into the mixed convection study makes the problem more complex, and of course, more practical. Under these circumstances, the statement of "fully developed flow" is somewhat ambiguous.

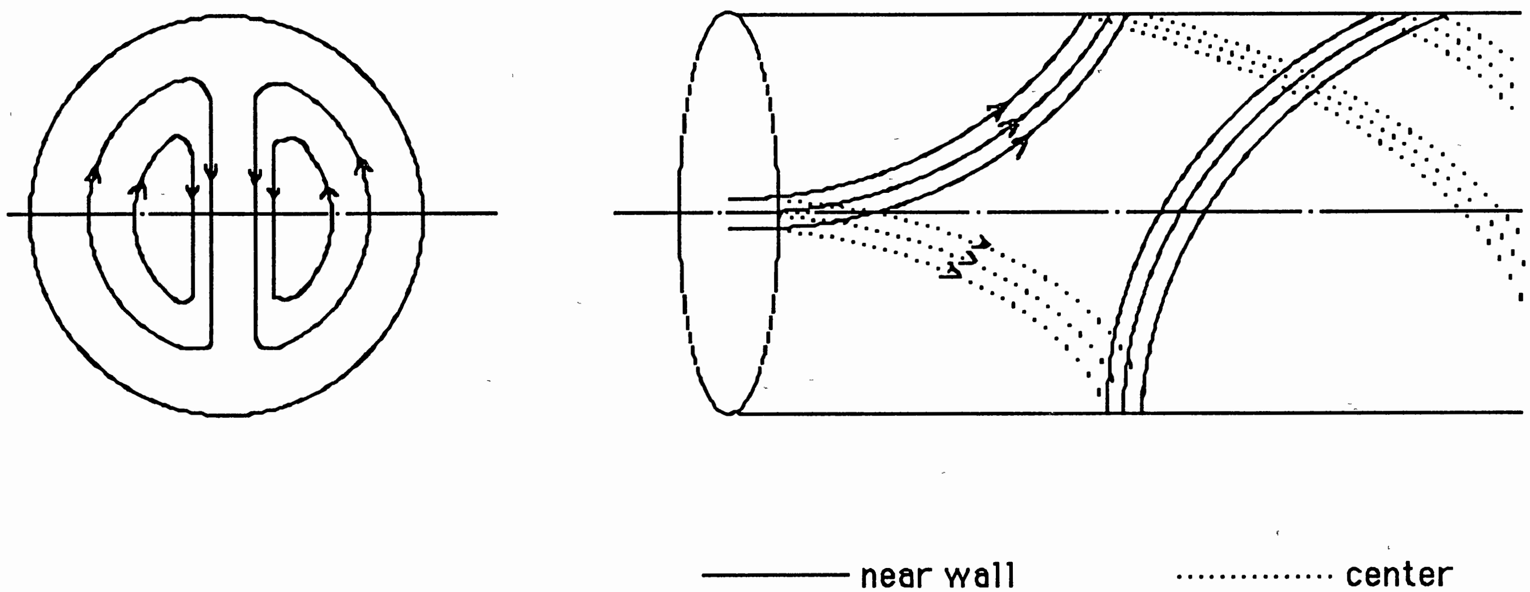

a) end elevation

b) horizontal elevation

Figure 1. Flow pattern inside a heated horizontal tube with mixed convection

One should distinguish the case of the fully developed velocity profile and temperature profile from the case of the fully developed velocity profile but developing temperature profile. Similarly, the concept of "entry length" can mean either fully developed velocity profile but developing temperature profile, or simultaneously developing velocity and temperature profiles, if the flow condition is not clearly specified. For most heat exchanger tubes, the simultaneously developing profiles case can simulate the real situation, but it is the most difficult problem to analyze.

Besides the temperature dependence of density which plays the key role in buoyancy-induced secondary flow, the temperature dependence of other physical properties, especially viscosity, also exerts considerable effect on the heat transfer problem, especially in the case of a large temperature difference between tube wall and the bulk fluid, or in the case of certain fluids whose properties are especially sensitive to temperature. In this study the constant property solution (CPS) would mean that every physical property of the working fluid, except density, is a constant calculated at a reference temperature, while the variable property solution (VPS) would take account of variations with temperature for each property. If the equations expressing the temperature dependence function are accurate enough, the VPS would approach the real situation.

In this thesis, theoretical analysis of mixed convection inside horizontal tubes with nominally uniform heat flux, including hydrodynamic and thermal entrance region and variable properties, will be carried out.

Because of the complexity of the problem, no analytical solutions can be expected and one can only use a numerical approach. This analysis is based on the principles of three-dimensional parabolic flow, which permits a marching procedure. A corresponding three-dimensional computer program in FORTRAN has been developed. Numerical analyses were conducted using conditions of Chen's (1988) experimental work. The computational results agree very well with experiments.

From the experimental results, a general correlation for laminar mixed convection, which is believed to fit most previous data better than previous correlations, has been derived. This correlation can be used directly in engineering design.

In addition, by further data reduction, improvements of the existing mixed convection flow regime maps have been suggested.

CHAPTER II

LITERATURE SURVEY

The effect of natural convection on forced convection heat transfer has drawn attention as early as the 1930's. Colburn (1933) is one of the pioneer workers studying combined forced and natural convection heat transfer. Afterwards, Sieder and Tate (1936), and Kern and Othmer (1943) modified and developed the original pioneering work. Eubank and Proctor (1951) first presented a mixed convection Nusselt number correlation. Since the late 60's, an increasing number of researchers have studied mixed convection, either experimentally or theoretically, or both. Many experimental data, analytical methods, and correlations have been published since then.

Experimental Approaches

Petukhov and Polyakov (1967) conducted an experimental study of laminar flow of water in a horizontal stainless steel tube (18.9 mm ID). The electrically heated (AC) length of 1.85 m (73 in.) was preceded by a 1.8 m (71 in.) calming length. Numerous thermocouples were attached to the tube wall at various axial and circumferential locations. The tube wall was also rotated to provide greater refinement of the measurement of circumferential temperature distribution. The experiments were performed for a range of Reynolds numbers from 50 to 2,400 and Rayleigh numbers from $2x10^5$ to $4x10^7$. All physical properties were evaluated at the axial local bulk temperature and the Grashof number was based on the average wall heat flux. Figure 2 shows their experimental data of average local Nusselt number versus (z/di)/(RePr). Compared to the pure forced convection prediction, these data clearly show that the higher the Rayleigh number, the higher the local heat transfer rate and the shorter the entrance length.

Siegwarth and Hanratty (1970) performed experimental studies of the effect of secondary flow on the fully developed temperature field and primary flow to support their analytical study (Siegwarth et al. 1969). They used a 10.97 m (36 ft) length of 64 mm (2.525 in.) ID tube with electrical heating on the outside of the tube. The wall temperature was measured at intervals along the entire length of the tube and at each axial station thermocouples whose junctions were approximately 2.4 mm (3/32 in.) from the inside wall, were spaced at 45^0 interval around the circumference of the tube. Because they used a relatively thick wall, 25.4 mm (1 in.), and a material of high thermal conductivity, aluminum, they assumed a constant temperature around the inside circumference at any axial location,

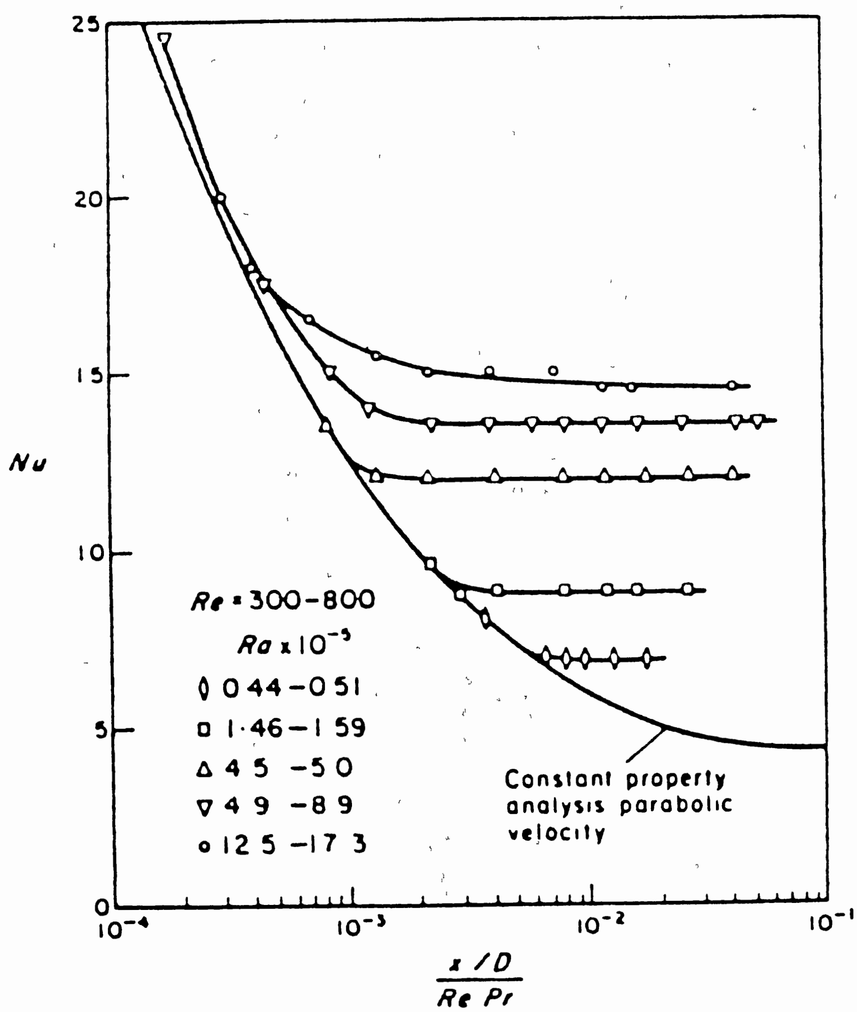

Figure 2. Local average heat transfer data
(Petukhov and Polyakov, 1967)

though they had found variations of the temperature around the inside wall. Tests were conducted under conditions where $T_w - T_b$ was constant over the last two meters of the heating section where they believed fully developed velocity and temperature profiles had been reached. Ethylene glycol was used. In addition, velocity and temperature profiles were measured near the end of the heating section. They found relatively large secondary flows for temperature differences between the wall and the fluid as low as 0.03°C (0.05°F).

Hussain and McComas (1970) made an experimental investigation of combined forced and free convection in a 25.4 mm ID, 3 m long uniformly heated horizontal tube preceded by a 2.13 m length of brass tube calming section. They tested air at Reynolds numbers between 670 and 3,800 and Grashof numbers, based on the wall to bulk temperature difference, between 10,000 and 1,000,000. They found that, far from the thermal entrance and at Reynolds numbers below 1,200, the local Nusselt number was below the constant property pure forced flow prediction by Siegel et al. (1958). For the runs in the Reynolds number range from 1,500 to 2,300, the data follow the forced convection solution closely in the thermal entrance region. The experimental results then started to deviate from that prediction giving increasingly higher values until a maximum occurred, and then the Nusselt number decreased with axial distance in the latter portion of the tube. For Reynolds numbers between 2,300 and 3,800, the local Nusselt number was higher than predicted in the latter portion of the tube. They predicted a possible difference in the behavior of gases and liquids. Also, they observed significant peripheral temperature variations, the wall temperature at the top of the tube being as much as 7°C higher than at the bottom of the tube for the upper range of Grashof numbers investigated. They attributed this to free convection. In addition, they claimed that no fully developed condition exists in the presence of free convection.

Bergles and Simonds (1971) conducted visual and experimental investigations of water in a horizontal coated glass tube (11 mm ID, 0.76 m long) with constant heat flux. A 0.91 m (36 in.) length of copper tube was used for the entrance section and a dye injection needle was mounted on the tube centerline axially. They observed that the dye clearly delineated the spiraling streamlines characteristic of developing secondary flow. Raising the heat flux at constant flow rate tended to decrease the axial pitch of the streamlines, while the same effect was produced by decreasing the flow rate at constant heat flux. They suggested that the dye trajectories could be used as a crude test of fully developed flow, and that a fully developed condition occurred when the dye completed at least one spiral by the time it reached the end of the tube. They concluded that the thermal development length when secondary flow existed was shorter than that required by the pure forced convection prediction (Kays and Crawford, 1980).

Depew and August (1971) studied the influence of buoyancy forces on convection heat transfer in a horizontal, isothermal tube by cooling experiments. A constant wall temperature condition was achieved by boiling Freon-12 in the annular space around the testing section. (Whether this actually achieves an isothermal wall is very questionable). Working fluids were water, ethyl alcohol, and a mixture of glycerol and water. The cooling section was 0.57 m long of 19.9 mm ID copper tube, preceded by a 2.44 m long adiabatic inlet calming section to approach a fully developed velocity profile, which seems to be impractical in engineering applications. They pointed out that the influence of buoyancy forces was generally less in the uniform wall temperature situation than when a uniform heat flux was imposed.

Morcos and Bergles (1975) investigated the effects of property variations on fully developed laminar flow heat transfer and pressure drop in horizontal tubes. They identified two classifications of uniform heat flux boundary conditions: uniform heat flux axially and circumferentially, i.e., zero wall conductivity, (ZC) and uniform heat flux along the tube but uniform temperature at each axial location, i.e., infinite wall conductivity, (IC). They used a coated glass tube (10.6 mm ID, 1.03 m heat length) for the ZC condition and a stainless steel tube (10.2 mm ID, 1.22 m heat length) for the IC condition. Before the heating section, a 1.9 m long tube was used to meet the "fully developed velocity profile" assumption. Distilled water and ethylene glycol were used as working fluids. They observed a pronounced effect of free convection on heat transfer, as much as six times higher than the constant property prediction. They suggested that the Nusselt number was affected not only by Rayleigh number and other variations in the physical properties of the working fluids, but also by the circumferential conductance of the tube wall.

Kato, Watanabe, Ogura, and Hanzawa (1982) conducted a comprehensive study of the effect of natural convection on laminar flow heat transfer in horizontal tubes with a high uniform wall temperature. In their experimental apparatus, copper tubes(28 mm ID, and 47 mm ID) and a stainless steel tube (56 mm ID) were used. The length of those tubes was in the range of 0.5-1 m according to their inside diameter. A length of tube 40-50 times the inside diameter was used as the calming section. Temperature was measured at 13 points in one cross section at various distances from the inlet of the tube. Air or nitrogen gas was the working fluid. Wall temperature, Reynolds number and inlet temperature of gas were in the range of 50 to 500°C, 100 to 1,500, and 15 to 25°C, respectively. However, they did not find the peculiarity mentioned by Hussain and McComas (1970) (increasing and then decreasing Nusselt number) for air at low Re with constant heat flux. Their experimental data agreed well with the numerical results and an empirical equation was obtained which successfully correlated both liquid and gas data.

Coutier and Greif (1985) made an investigation of laminar mixed convection inside a horizontal isothermal tube. The copper test tube (25.4 mm OD,3 mm wall, and 1.52 m long) was immersed in a constant temperature water tank to ensure the uniform wall temperature boundary condition. A long piece of well-insulated tube preceded the entrance to the testing tube, ensuring that a fully developed velocity profile was a good assumption for their inlet conditions. Fluid and wall temperatures were measured at four axial locations. At each of the locations, five thermocouples were used. Two of them were inside the tube and recorded the fluid temperature at the tube centerline and at two-thirds of the radius. Three of them recorded outside wall temperature at θ=0°, 90°, and 180°. Water and a propylene-glycol solution were used as the working fluids in the cooling experiments. Reynolds numbers ranged between 40 and 1,160, and Rayleigh numbers from 1.6×10^6 to 9×10^6. They also conducted a numerical analysis and their results for the temperature profile agreed well with the experimental data. They concluded that in their study the flow was developing thermally throughout the entire length of the short tube, and over the range of conditions tested, the heat transfer in horizontal isothermal tubes was shown to be strongly dependent on the secondary flow.

In order to simulate more closely the real situation for horizontal tubes inside shell-and-tube heat exchangers, Chen(1988) performed an experimental study of heat transfer in high laminar,transition, and lower turbulent flow regimes in a horizontal tube. He used a stainless steel tube (16.07 mm ID, 3.95 m long) with a square-edged entrance and heated the tube by electrical D. C. current for almost the entire length of the tube. Outside surface temperatures were measured at 12 axial stations, and at each station 4 or 8 thermocouples were located around the circumference. Distilled water and diethylene glycol (DEG)-water solutions were used as the working fluids. The experiments covered local bulk Reynolds numbers between 121 and 12,400, Prandtl numbers between 3.5 and 285, and Grashof numbers, between 930 and 1.04×10^6. A total of 48 runs were conducted. Chen's data will form the major experimental support for this analysis.

Theoretical Approaches

Compared with experimental approaches, there are relatively few theoretical studies of mixed convection in horizontal tubes. The reported approaches include perturbation analysis, boundary layer approximation, vorticity analysis, and finite difference solution. Most of them have assumed a fully developed velocity profile at the start of heating. The usual boundary conditions for those studies are either uniform wall temperature (UWT) or uniform heat flux (UHF). The latter (UHF) has been further classified into the zero wall conductivity (ZC) model and the infinite wall conductivity (IC) model.

After pointing out the very limited applicability of a perturbation analysis by Morton (1959), Mori and Futagami (1967) studied mixed convection of fully developed velocity and temperature fields in uniformly heated horizontal tubes. The infinite conductivity boundary condition was used. Based on their experiments and visualizations, they divided the tube flow into two parts: a flow in a thin layer along the tube wall and a flow in a core region. In the thin layer, velocity and temperature fields were affected by viscosity and thermal conductivity, and a boundary layer approximation was applied in the analysis. On the other hand, in the core region, velocity and temperature fields were affected mainly by the secondary flow and the effect of viscosity and thermal conductivity could be disregarded. On these assumptions, a boundary layer integral method was used, and correlations between Nusselt number and ReRa were obtained in the region of Pr not far from unity (Table I). Theoretical results were in good agreement with their experimental data for air.

Faris and Viskanta (1969) made an analytical study of laminar mixed convection heat transfer in a horizontal tube. They observed that for UHF condition, fully developed heat transfer was reached asymptotically after a considerable starting length, e.g., $z/d > 700$ was needed to establish fully developed heat transfer profiles for water, (Shannon and Depew, 1968). However,their analysis was still confined to the fully developed velocity and temperature profile region, so that the reduced governing equations could be solved by a perturbation method. After comparing their theoretical predictions with available experimental data, they claimed the validity of the perturbation method. One of the conclusions in that paper is that for all liquids, excepting liquid metals, the assumption that the inside tube wall temperature was uniform circumferentially was justifiable for ordinary tube thicknesses in view of the fact that the ratio of the thermal conductivities of the tube wall to that of the fluid was usually very high. However, this conclusion seems to be contrary to the results of most experimental studies.

Newell and Bergles (1970) analyzed the problem of fully developed flow in uniformly heated horizontal tubes, with density as the only temperature-dependent property. They suggested that the development of the secondary flow could be considered to occur in two stages: at stage one, the temperature profile develops almost as a symmetric flow, but a nonuniform radial density distribution develops; at stage two, the body force (gravity) comes significantly into play. Their estimate for the length of stage one is $L1/d \leq 0.05RePr$.

After introducing the stream function, they solved the 2-D momentum equations and energy equation by a finite difference method. Their computational data revealed as high as 59°C (106°F) temperature difference between the top and bottom of the inside tube wall (Figure 3). Furthermore, they found that the wall temperature at the bottom can be less than the local bulk temperature (Figure 3). Both ZC and IC boundary conditions were considered. The interesting results for these two conditions are shown on Figure 4. They concluded that because of the complex nature of the problem, additional dimensionless groups would be required to correlate data for more than one fluid. They recommended developing and using a 3-D solution.

In Hieber's (1974,1981,1982) theoretical investigations, the development of the velocity and temperature fields within an isothermal horizontal tube consists of a succession of regions, proceeding in the axial direction: a "near region", where buoyancy is a small perturbation upon the forced flow; a "intermediate region", where natural convection is dominant and the thermal boundary layer is axially invariant; a "break-up region", where the core region interacts with the thermal boundary layer and the natural convection effects therefore diminish; and a "far region", where the forced convection reappears as the dominant transport mechanism and the fluid temperature approaches wall temperature asymptotically in a Graetz-like manner. He attempted to include all previous experimental

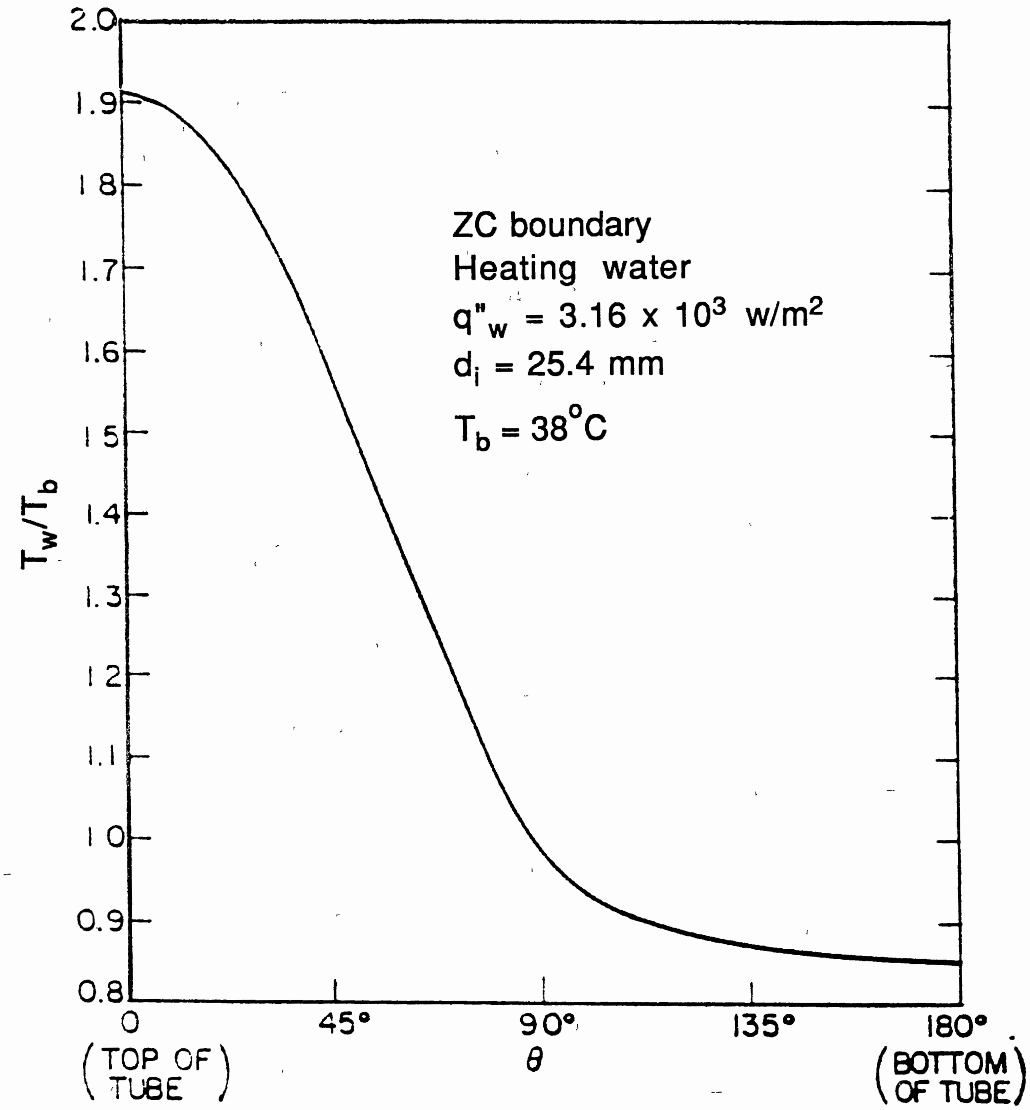

Figure 3. Circumferential inside wall temperature variation (Newell and Bergles, 1970)

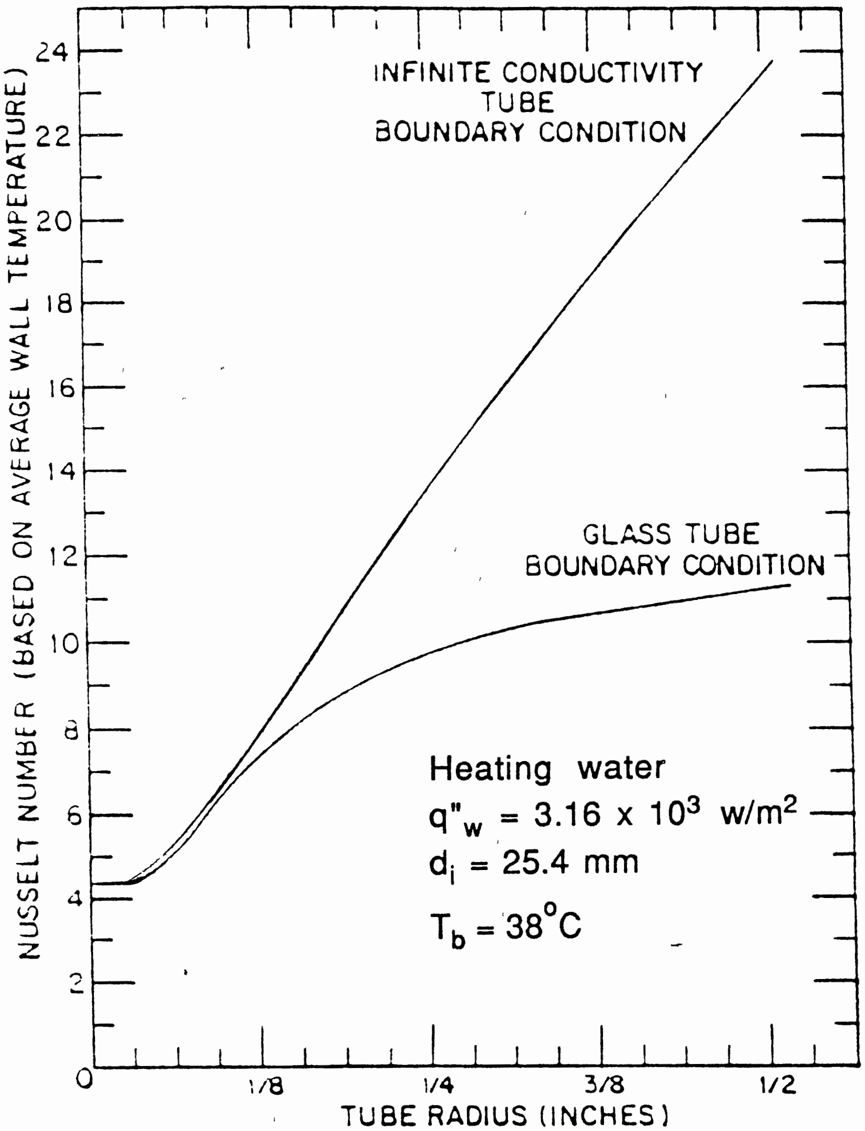

Figure 4. Influence of tube-wall boundary condition on Nu (Newell and Bergles, 1970)

data into a semi-analytical correlation with a different format, but his correlations are not easily acceptable because the definition of most of the parameters in his correlation differ from the ones in engineering applications. For example, the Grashof number and Nusselt number are based on the difference of T_w and T_{in}, which is always constant for a certain operating condition with UWT boundary.

While most of the analytical efforts concentrated on determining the effects of variable density, Hong and Bergles (1976) added effects of variable viscosity, which is another most important temperature-dependent property, into the fully developed mixed convection study. They used the two region (boundary layer and core) model and UHF boundary condition. They introduced a new viscosity parameter, $\gamma\Delta T$, and developed correlations for variable viscosity mixed convection.

Patankar, Ramadhyani, and Sparrow (1978) studied the effect of circumferentially nonuniform heating on fully developed, laminar mixed convection in a horizontal tube. Two heating conditions were investigated, one in which the tube was uniformly heated over the top half and insulated over the bottom, and the other in which the heated and insulated portions were reversed. The results were obtained numerically for a wide range of the governing buoyancy parameter and for Pr of 0.7 and 5. They found that bottom heating gives rise to a vigorous buoyancy-induced secondary flow, with the result that the average Nu were much higher than those of pure forced convection, while the local Nu were nearly circumferentially uniform. It was also demonstrated that the buoyancy effects were governed solely by the modified Gr, based on wall heat flux, without regard for the Re of the forced convection flow.

Numerical solutions for laminar mixed convection in the entrance region of a horizontal tube where the velocity and temperature profiles are developing simultaneously are available only in a few limited cases, due to the attendant complexities arising from the three-dimensionality of the flow. Hieber and Sreenivasan (1974), and Ou and Cheng (1977) obtained the solutions of the entry flow problem by using the large Prandtl number assumption. As the matter of fact, this assumption implies that the secondary flow is not significant in the momentum equations, but is important in the energy equation, so that one could neglect the nonlinear inertia terms in the momentum equations and avoid the chief difficulty in obtaining a numerical solution. Obviously, this assumption is unsatisfactory to describe the characteristics of fluid flow and heat transfer for ordinary gases and even smaller Prandtl number fluids.

Without the aid of a large Prandtl number assumption, Hishida, Nagano, and Montesclaros (1982) performed analytical studies on mixed convection in the entrance region of an isothermally heated horizontal tube. Numerical solutions were presented for the developing primary and secondary velocity profiles, developing temperature profiles, local wall shear stress, and local and average Nusselt numbers. Figure 5 shows the variation of the circumferential average Nusselt number with Grashof number (which is based on T_w-T_{in}) as a parameter. With the addition of free convection effects,the average Nu becomes higher than that for the pure forced convection (Gr=0). After reaching a local maximum value, Nu decreases again until the limiting value of Nu=3.66 is approached. It was claimed that increasing Gr decreases the entrance length prior to the onset of significant free convection effects and increases the local maximum of Nu.

Assuming uniform heat flux, Aihara and Maruyama (1986) carried out a numerical analysis of laminar mixed convection heat transfer in a vertical tube, taking into account the temperature dependence of the physical properties. They found that in the case of UHF ducts, the difference of heat transfer characteristics between constant property solution and variable property solution is not so large as in the case of UWT ducts. The difference of local Nu is less than 25% for air and 50% for transformer oil.

Most recently, Choudhury and Patankar (1988) presented a numerical study of the developing laminar flow and mixed heat transfer in an inclined isothermal tube with constant properties. Three independent parameters, Pr, Ra*, and a parameter related to the relative magnitude of buoyancy and inertial forces, appeared explicitly in the governing

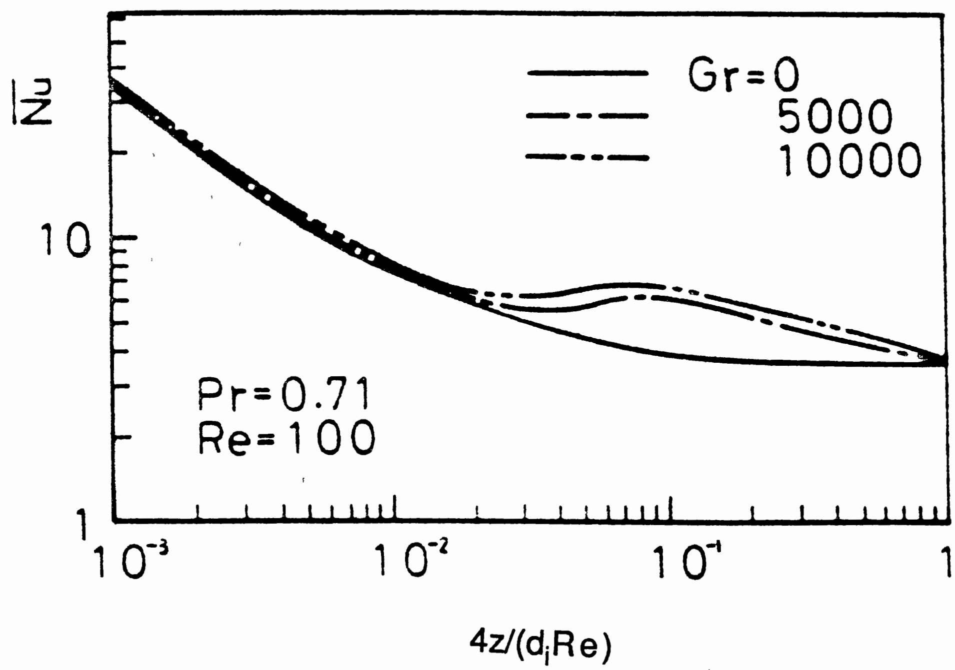

Figure 5. Local average Nu values for Gr=0, 5000, and 10000 (Hishida et al., 1982)

equations. With suitable choices of these parameters, the vertical and horizontal orientations of the heated tube could be recovered as limiting cases. The governing equations were solved numerically by a modified version of the finite-difference method for 3-D parabolic flow described by Patankar and Spalding (1972). The computations were carried out for Pr of 0.7, 5, and 10. Ra* was varied between 0 and 10^6 . This choice of parameters covers a wide range of possible combinations of fluid properties, flow rate, temperature difference, and inclination angles. The results obtained from the computation included Nu, friction factor, velocity profile, isotherm maps,and secondary flow patterns in the entrance region of the tube. Comparisons with numerical and experimental results for the vertical and horizontal tube orientations shown reasonably good agreement. They found that the buoyancy-induced secondary flow distorts the axial velocity and temperature distributions and the nature of the distortion depends on the relative magnitudes of Ra* and the inclination angle. But the effect of Pr is diminished for Pr greater than 10. The circumferential average Nu and the friction factor reached a local maximum at an axial location where the buoyancy effects were the most intense.

As for the entrance effect, on the other hand, Siegel, Sparrow, and Hallman (1958) solved the pure forced convection thermal-entry-length problem for fully developed laminar flow in circular tube with UHF condition. By using the method of separation of variables and Sturm-Liouville theory, they obtained an eigenvalue solution, which has been widely accepted and used as a standard reference case.

Correlations

A number of empirical correlations have been proposed, and some of them have been widely used in engineering applications, for the heating or cooling of various fluids in horizontal mixed convection tube flow with either UWT or UHF boundary conditions. According to the original experimental conditions,these correlations were individually applicable to fully developed velocity and temperature profiles, fully developed velocity profile but developing temperature profile, or simultaneously developing velocity and temperature profiles. Most of them were attempted with a view toward obtaining an axial average Nusselt number, though some of them gave local values. A summary of the important correlations and their experimental conditions, if given, is presented in Table I.

Flow Regime Maps

Exactly speaking, for laminar flow in horizontal tubes,mixed convection is the general case in most situations involving heat transfer. Pure forced convection or natural convection are only the extreme cases, when one

TABLE I

CORRELATIONS FOR MIXED CONVECTION IN HORIZONTAL TUBES

A. Fully Developed Velocity and Temperature Profiles

Reference	Boundary Conditions	Correlations	Range of Applicability
Ede (1961)	UHF	$Nu = 4.36\ (1 + 0.06Gr^3)$	$Re < 2300$
Petukhov & Polyakov(1966)	UHF	$Nu = 4.36[1 + Ra/(1.8 \times 10^4)]^{0.045}$	
Mori & Futagami (1967)	UHF	$Nu/Nu_F = 0.04085\ (ReRa^*)^{0.5}$ $Nu/Nu_F = 0.04823\ (ReRa^*)^{0.5}$	$Pr = 0.72$ $Pr = 1.0$
Morcos & Bergles (1975)	UHF	$Nu = \{(4.36)^2 + [0.145(GrPr^{1.35}/P_W{}^{0.25})]^2\}^{0.5}$	Ra: $3 \times 10^4 - 10^6$
Hong & Bergles (1976)	UHF(IC)	$Nu = [0.8823 + 0.0153\gamma\Delta T + 0.1481(\gamma\Delta T)^2 + 0.00334(\gamma\Delta T)^3]Ra^{0.25}$ $Nu = [0.877 + 0.0563\gamma\Delta T]Ra^{0.25}$	$1.5 \geq \gamma\Delta T \geq 0$ $0 > \gamma\Delta T \geq 1.0$
	UHF(ZC)	$Nu = [0.661 + 0.14\gamma\Delta T - 0.0098(\gamma\Delta T)^2 + 0.027(\gamma\Delta T)^3]Ra^{0.25}$ $Nu = [0.663+0.0886\gamma\Delta T+0.00526(\gamma\Delta T)^2]Ra^{0.25}$ where $\gamma = - d\mu/dT/\mu$	$2.0 \geq \gamma\Delta T \geq 0$ $0 > \gamma\Delta T \geq 1.0$

TABLE I (continued)

B. Fully Developed Velocity, but Developing Temperature Profiles

Reference	Boundary Conditions	Correlations	Range of Applicability
Colburn(1933)	UWT	$Nu(\mu_f/\mu_b)^{1/3} = 1.75Gz^{1/3}(1 + 0.015Gr^{1/3})$	Pr: 0.76 - 160
Sieder & Tate (1936)	UWT	$Nu = 1.75(\mu_w/\mu_b)^{0.14}Gz(1 + 0.01Gr^{1/3})$	
Kern & Othmer (1943)	UWT	$Nu(\mu_w/\mu_b)^{0.14} = 1.86(RePrd_i/L)^{1/3} \times 2.25(1 + 0.01Gr^{1/3})/Log(Re)$	
Eubank & Proctor(1951)	UWT	$Nu(\mu_w/\mu_b)^{0.14} = 1.75[Gz + 1.26(GrPrd_i/L)^{0.4}]^{1/3}$	
Oliver (1962)	UWT	$Nu(\mu_w/\mu_b)^{0.14} = 1.75[Gz + 5.6 \times 10^{-4}(GrPrL/d_i)^{0.7}]^{1/3}$	
Brown & Thomas (1965)	UWT	$Nu(\mu_w/\mu_b)^{0.14} = 1.75[Gz + 0.012(GzGr^{1/3})^{4/3}]^{1/3}$	
Depew & August (1971)	UWT	$Nu(\mu_w/\mu_b)^{0.14} = 1.75[Gz + 0.12(GzGr^{1/3}Pr^{0.36})^{0.88}]^{1/3}$	

TABLE I (continued)

B. Fully Developed Velocity, but Developing Temperature Profiles

Reference	Boundary Conditions	Correlations	Range of Applicability
Hong et al. (1974)	UHF	$Nu = 0.378Gr^{0.28}Pr^{0.33}/P_w^{0.12}$	
Kato et al. (1982)	UWT	$Nu(\mu_w/\mu_b)^{0.14} = 1.75[Gz + 0.63 \times 10^{-3}(GzGr^{0.83})^{0.97}]^{1/3}$	Re: 100-2000 Gr: $20 \times 10^3 - 5 \times 10^6$
Abdelmessih (1986)	UHF	$Nu = 4.364 + 0.3271(GrPr)^{0.25}(\mu_w/\mu_b)^{0.14}$	Re: 120 - 2500 Gr: 2500 1.13×10^6 Pr: 3.9 - 110

TABLE I (continued)

C. Simultaneously Developing Velocity and Temperature Profiles

Reference	Boundary Conditions	Correlations	Range of Applicability
Jackson et al. (1961)	UWT	$Nu = 2.67[Gz^2 + (0.0087)^2(GrPr)^{1.5}]^{1/6}$	Gz: 60 - 1300
Hieber (1982)	UWT	$Nu = (\mu_w/\mu_b)^{0.14}[Nu_B^{\ 3} + Nu_F^{\ 3}]^{1/3}$ $Nu_B = 2(GrPr)^{0.25}[\log(1 + 0.4785\sigma_L)]/2.2\sigma_L$ $Nu_F = 1.282(2L/d_iRePr)^{-1/3}\exp(-8.2L/d_iRePr)$ $+ 1.828[1 - \exp(-13.5L/d_iRePr)]$ $\sigma_L = (GrPr)^{0.25}(2L/d_iRePr)$	
Yousef & Tarasuk (1982)	UWT	$Nu(\mu_w/\mu_b)^{0.14} = 1.75[Gz$ $+0.245(Gz^{1.5}Gr^{1/3})^{0.882}]^{1/3}$ $Nu(\mu_w/\mu_b)^{0.14} = 0.969Gz^{0.82}$	where X = (x/D)/(RePr) $0.0073 < X < 0.04$ $0.04 < X < 0.25$
Chen (1988)	UHF	$Nu = [4.364 + 0.00106Re^{0.81}Pr^{0.45}(1$ $+ 14\exp(-0.063x/d_i)) + 0.268((GrPr)^{0.25}$ $(1 - \exp(-0.042x/d_i))](\mu_w/\mu_b)^{0.14}$	Re: 121 - 2100 Pr: 3.5 - 282.4 Gr: 930 - 67300

of the processes can be neglected. However, in the view of engineering applications, one wants to know exactly when the natural convection can be neglected and when it must be accounted for. In other words, one should be able to predict which regime a given application will be in --- forced, natural, or mixed convection. Metais (1963), and Metais and Eckert (1964) made an original exploration towards this goal. After a study of the available literature, they established criteria between these various regimes and presented empirical regime maps for vertical and horizontal tubes. The limits of the forced and natural convection regimes were defined in such a way that the actual heat flux under the combined influence of the forces did not deviate by more than 10 percent from the heat flux that would be caused by the external forces alone or by the body forces alone. Figure 6 is one of the maps they provided for the horizontal orientation. Since there were only a few experimental studies and no theoretical study for horizontal tubes at that time, they claimed that the results for horizontal tubes were more tentative than those for vertical tubes and they proposed further study in this area. But to the author's knowledge, these maps are the only ones on mixed convection flow regimes. The original regime maps have been widely applied, though they need further investigation, especially for horizontal tubes.

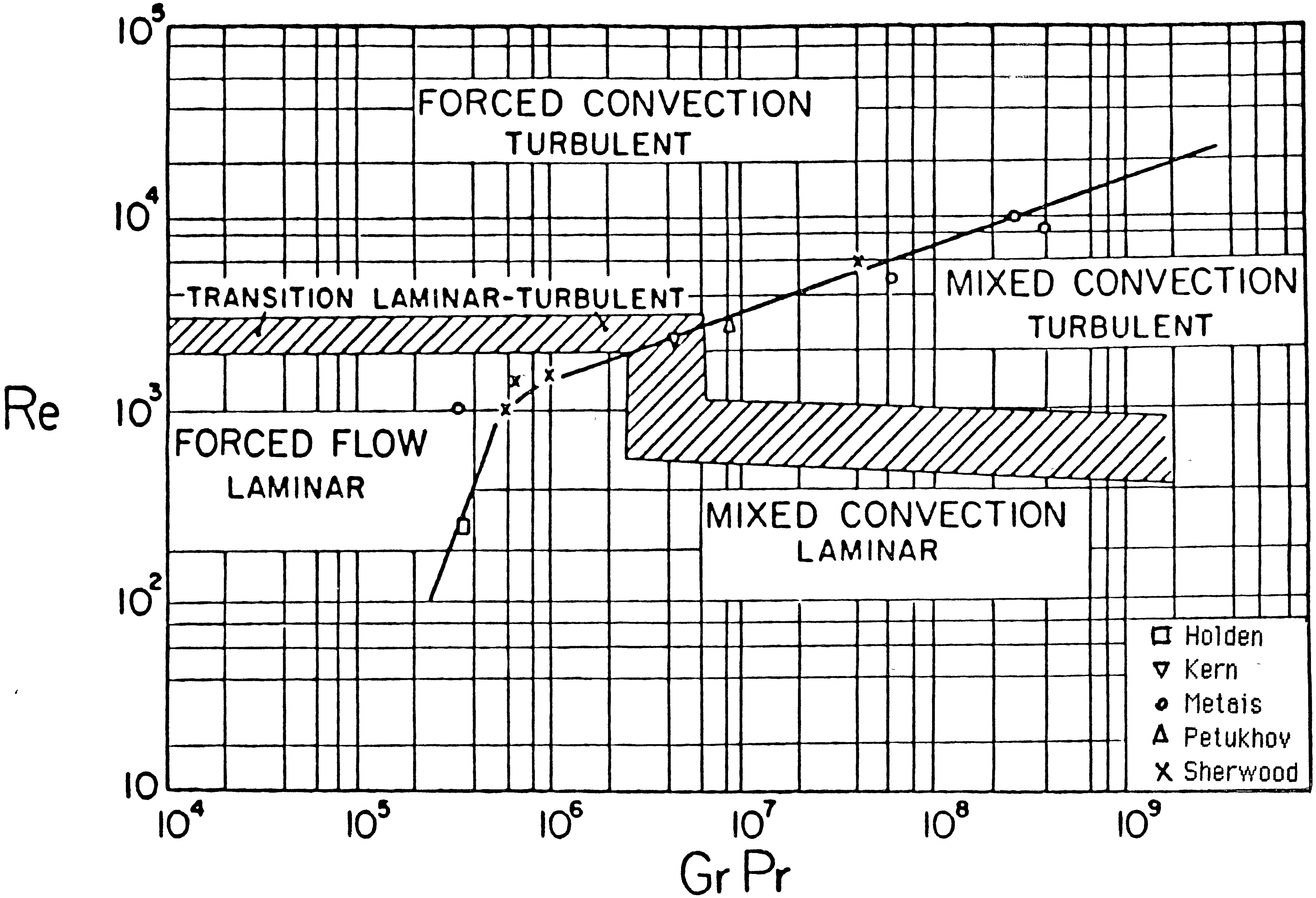

Figure 6. Regimes for free, forced, and mixed convection for horizontal tube (Metais and Eckert, 1964)

Summary of the Survey

1. Laminar mixed convection in horizontal tubes is a very complex phenomenon and it is worth further investigation.

2. With regard to this survey, there are more experimental studies on mixed convection than theoretical ones.

3. Most of the works surveyed have avoided the entrance length effect, especially on velocity profile, and used uniform tube wall temperature (at least circumferentially) boundary conditions.

4. To the author's knowledge, the only two 3-D numerical solutions for mixed convection including entrance length are for UWT boundary conditions (Hishida, Nagano, and Montesclaros, 1982, and Choudhury and Patankar, 1988). No 3-D solutions for UHF boundary conditions have been reported.

5. Generally speaking, each published correlation is only valid for its specific experimental condition and fluid, and may not be valid for others. No general correlation for mixed convection in horizontal tubes including entrance effect has been developed.

6. The current flow regime maps for mixed convection have been unchanged since 1964.

CHAPTER III

THEORETICAL ANALYSIS

Problem Statement

The horizontal tube in Chen's (1988) experimental apparatus (Figures 7 and 8) is the model for this analysis. This tube with a square-edged entrance closely simulates the tubes in most shell-and-tube heat exchangers. The fluid enters the tube with a uniform velocity w_{in} and at a uniform temperature T_{in}. The tube wall heat flux is held nominally constant at q''_w by passing D.C. current through the tube wall.

Since the gravitational force is perpendicular to the axis of the tube, the buoyancy-induced secondary flow acts at each cross section of the tube and superimposes on the primary flow, resulting in a three-dimensional spiraling movement. Therefore, the buoyancy force will appear in the governing equations for secondary flow.

Besides the density of the fluid, other properties, such as viscosity, may demonstrate significant temperature-dependence and have considerable effect on heat transfer and fluid flow. In this analysis, water and water-diethylene glycol solutions are employed as the example

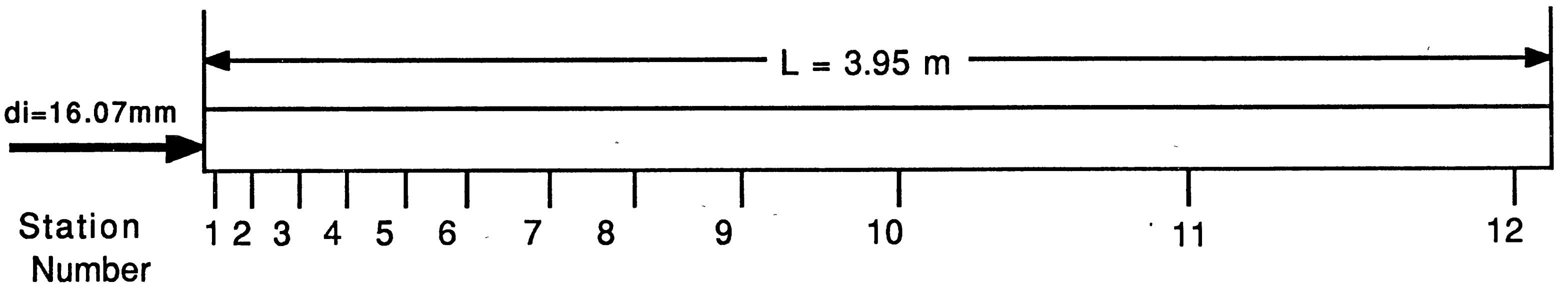

Station Number	1	2	3	4	5	6	7	8	9	10	11	12
z (m)	0.0386	0.114	0.215	0.418	0.62	0.823	1.025	1.229	1.634	2.039	2.849	3.926
Number of Thermocouples	4	8	8	4	8	4	8	4	4	4	4	4

Figure 7. Test section (Chen, 1988)

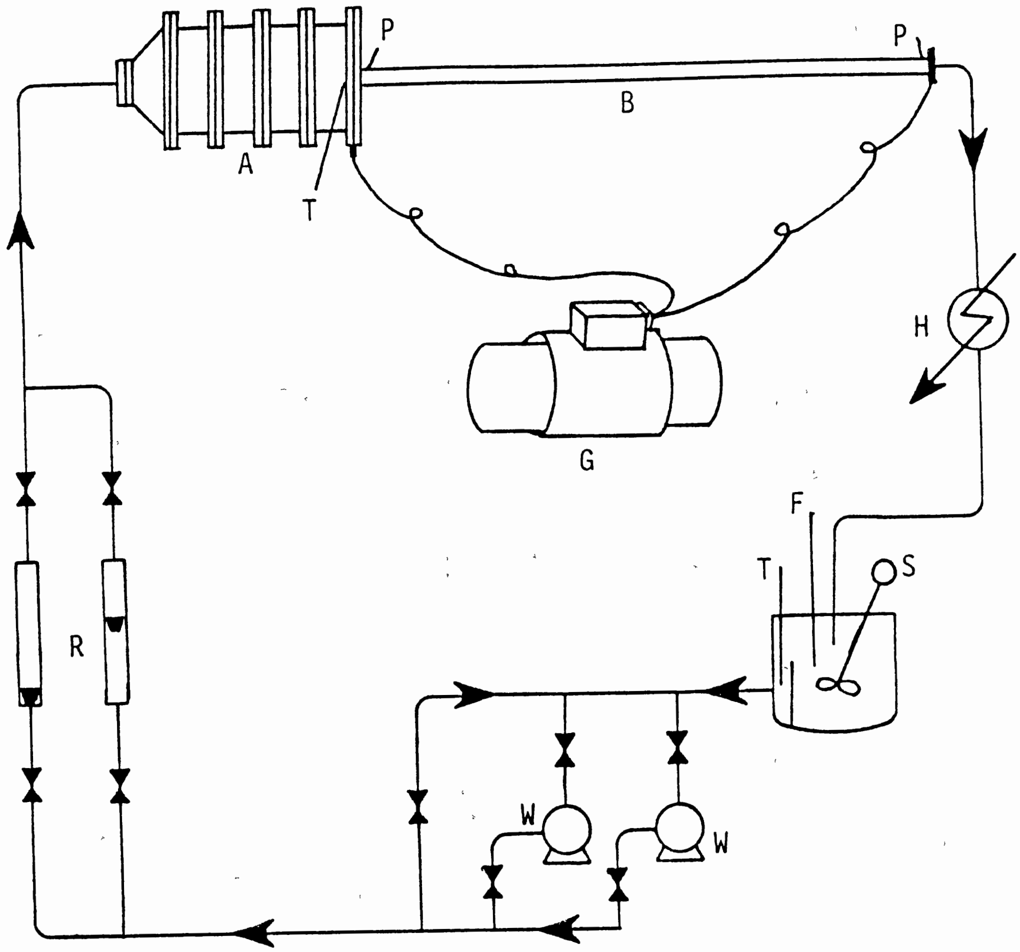

A: Entrance Chamber
B: Test Section
F: Heating Coil
G: Generator
H: Heat Exchanger

P: Pressure Gauge
R: Rotameter
S: Stirrer
T: Thermocouple
W: Pump

Figure 8. Experimental apparatus (Chen, 1988)

fluids for computation and property variation with temperature and composition has been taken into account.

In a word, the problem to be analyzed in this work is that of simultaneously developing laminar flow and heat transfer profiles of variable property fluids with appreciable buoyancy effects in a uniformly heated horizontal tube.

Figure 9 shows the cylindrical polar coordinate system and the corresponding velocity components for the present study. Because the gravitational force is exerted only in the vertical direction, symmetry about the vertical central surface is retained; hence, the calculation can be restricted to a solution domain that comprises one-half of the circular region as shown in Figure 9.

Three-Dimensional Parabolic Flow

In most cases tube side flows in shell-and-tube heat exchangers are characterized by the absence of reverse flow or separation and by a nearly uniform pressure over any cross section. Such flows can be treated as parabolic flow. Patankar and Spalding (1972) described the following conditions for parabolic flow:

1). There exists a predominant direction of flow, i.e., there is no reverse flow in that direction,

2). the diffusion of momentum, heat, mass, etc. is negligible in that direction, and

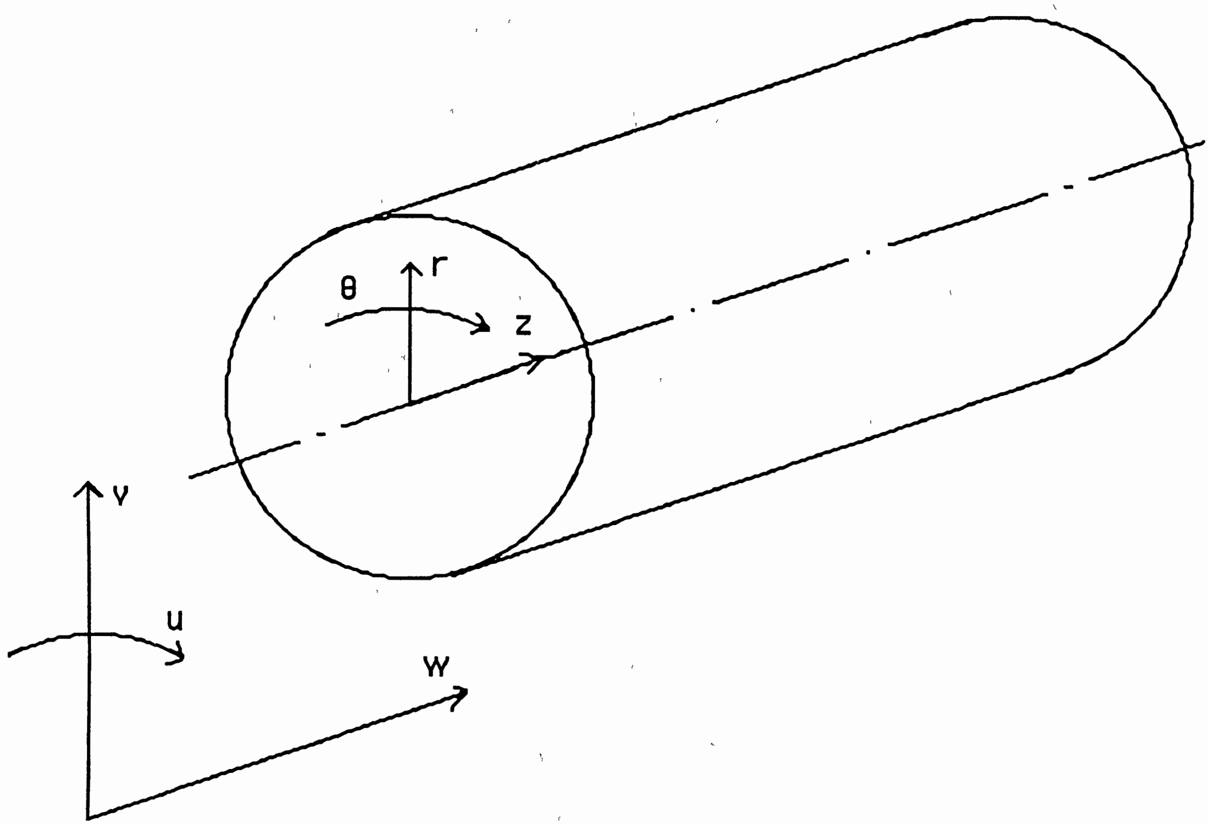

Figure 9. The coordinate system and corresponding velocity components

3). the downstream pressure field has little influence on the upstream flow conditions.

When these conditions are satisfied, the coordinate, z, in the main flow direction, becomes a 'one-way' coordinate; i.e., the upstream conditions can determine the downstream flow properties, but not vice versa. It is this convenient behavior of the parabolic flow that enables one to employ a marching procedure starting at the inlet plane and proceeding to successive cross-sectional planes downstream along the z-direction.

The advantage of a marching or parabolic procedure is that, although the flow domain is three-dimensional, the entire tube need not be considered at once. At any given station, the computational problem is to obtain, from the known values of the variables on an upstream plane, the unknown values of the variables on the next downstream plane. Successive repetition of this basic operation is used to cover the total length of the tube. Restriction of the basic computational module to the region between two planes implies that computer storage is needed for the variables only on the two planes and not throughout the entire tube.

For a three-dimensional parabolic flow, the pressure variations across the cross section are so small that they would have negligible effect if included in the streamwise momentum equation. Thus, cross section pressure variations have been neglected in the streamwise momentum equation. On the other hand, these small pressure variations are included in the θ- and r-direction momentum equations since they play an important role in the distribution of the generally small components of the secondary flow velocity at the cross section.

Assumptions

Concerning the mixed convection problem in this study, the following assumptions are made:

1). It is a parabolic flow in the z-direction.

2). It is a steady state laminar flow.

3). Working fluids are Newtonian and properties of the fluids are not dependent on pressure.

4). Energy dissipation is neglected.

Governing Equations

1). Continuity Equation

$$\frac{1}{r}\frac{\partial}{\partial\theta}(\rho u) + \frac{1}{r}\frac{\partial}{\partial r}(\rho r v) + \frac{\partial}{\partial z}(\rho w) = 0 \qquad (3\text{-}1)$$

2) Momentum Equations

θ-component

$$\frac{1}{r}\frac{\partial}{\partial\theta}(\rho uu) + \frac{1}{r}\frac{\partial}{\partial r}(\rho r v u) + \frac{\partial}{\partial z}(\rho w u) + \frac{1}{r}(\rho u v)$$
$$= -\frac{1}{r}\frac{\partial p}{\partial\theta} + \frac{1}{r^2}\frac{\partial}{\partial\theta}(\mu\frac{\partial u}{\partial\theta}) + \frac{\partial}{\partial r}(\frac{\mu}{r}\frac{\partial(ru)}{\partial r}) + \frac{2\mu}{r^2}\frac{\partial v}{\partial\theta} + \rho g\beta(T_w - T)\sin\theta$$

(3-2)

r-component

$$\frac{1}{r}\frac{\partial}{\partial\theta}(\rho uv) + \frac{1}{r}\frac{\partial}{\partial r}(\rho r vv) + \frac{\partial}{\partial z}(\rho wv) - \frac{1}{r}\rho u^2$$
$$= -\frac{1}{r}\frac{\partial p}{\partial r} + \frac{1}{r^2}\frac{\partial}{\partial\theta}(\mu\frac{\partial v}{\partial\theta}) + \frac{\partial}{\partial r}(\frac{\mu}{r}\frac{\partial(rv)}{\partial r}) - \frac{2\mu}{r^2}\frac{\partial u}{\partial\theta} - \rho g\beta(T_w - T)\cos\theta$$

(3-3)

z-component

$$\frac{1}{r}\frac{\partial}{\partial\theta}(\rho uw) + \frac{1}{r}\frac{\partial}{\partial r}(\rho r vw) + \frac{\partial}{\partial z}(\rho ww)$$
$$= -\frac{\partial p}{\partial z} + \frac{1}{r^2}\frac{\partial}{\partial\theta}(\mu\frac{\partial w}{\partial\theta}) + \frac{1}{r}\frac{\partial}{\partial r}(r\mu\frac{\partial w}{\partial r})$$

(3-4)

3). Energy Equation

$$\frac{1}{r}\frac{\partial}{\partial\theta}(\rho u T) + \frac{1}{r}\frac{\partial}{\partial r}(\rho r v T) + \frac{\partial}{\partial z}(\rho w T)$$
$$= \frac{1}{r^2}\frac{\partial}{\partial\theta}\left(\frac{k}{C_p}\frac{\partial T}{\partial\theta}\right) + \frac{1}{r}\frac{\partial}{\partial r}\left(r\frac{k}{C_p}\frac{\partial T}{\partial r}\right)$$

(3-5)

Boundary Conditions

At inlet

$z=0$, $w=w_{in}$, $T=T_{in}$, $u=v=0$

At tube wall

$r=R$, $u=v=w=0$, $T=T_w$, q''_w is given (constant or variable)

At vertical symmetry plane

$\theta=0$ and $\theta=\pi$, $u=0$, $\partial v/\partial\theta=\partial w/\partial\theta=\partial T/\partial\theta=0$

CHAPTER IV

DEVELOPMENT OF THE NUMERICAL METHOD

The General Mathematical Model

Looking through Equations (3-2) to (3-5), one can find that those equations can be expressed by one general model. Let ϕ denote the dependent variables u, v, p, T, and w in sequence; then the general differential equation is

$$\frac{1}{r}\frac{\partial}{\partial\theta}(\rho u\phi) + \frac{1}{r}\frac{\partial}{\partial r}(\rho r v\phi) + \frac{\partial}{\partial z}(\rho w\phi)$$
$$= \frac{1}{r^2}\frac{\partial}{\partial\theta}\left(\Gamma\frac{\partial\phi}{\partial\theta}\right) + \frac{1}{r}\frac{\partial}{\partial r}\left(r\Gamma\frac{\partial\phi}{\partial r}\right) + S \tag{4-1}$$

Where Γ is the diffusion coefficient and S stands for the source term. Γ and S are specific to a particular meaning of ϕ (see Table II). The terms on the left-hand side of Equation (4-1) are the convection terms, representing the flux of ϕ convected by the mass flow rate. The terms on the right-hand side of the equation are known as the diffusion terms and the source term, respectively. By the assumption of parabolic flow, the diffusion term in the main stream direction has been omitted.

The source term S is primarily meant for representing the mechanisms for the generation (or destruction) of ϕ. But it can also be used as a general 'dumping' ground; whatever cannot be conveniently expressed through the convection or diffusion terms can always be lumped into the source term. Because of this flexibility, the assumption that every dependent variable ϕ is governed by Equation (4-1) does not limit the physical processes or the types of the dependent variable that can be accommodated in the calculation procedure. It provides great convenience for computer programming---one solver can deal with a wide variety of problems.

Sometimes the source term depends on the variable ϕ itself. In order that the resulting discretization equation remains (at least nominally) linear, the source term S can be expressed as a linear function of ϕ.

$$S = S_c + S_p\phi_p \tag{4-2}$$

where S_p is the coefficient of ϕ_p, and S_c is the part of S that does not explicitly depend on ϕ.

Comparing Equations(3-2) to (3-5) with the general model and assertions above, diffusion coefficients and source terms corresponding to each individual variable in this study are listed in Table II.

TABLE II

Γ AND S FOR EACH VARIABLE

Variable	Γ	Sc	Sp
u	μ	$-\frac{1}{r}\frac{\partial p}{\partial \theta}+\frac{2\mu}{r^2}\frac{\partial v}{\partial \theta}+\rho g\beta(T_w-T)\sin\theta$	$-\frac{\mu}{r^2}-\frac{\rho v}{r}$
v	μ	$-\frac{\partial p}{\partial r}-\frac{2\mu}{r^2}\frac{\partial u}{\partial \theta}+\frac{\rho u^2}{r}-\rho g\beta(T_w-T)\cos\theta$	$-\frac{\mu}{r^2}$
T	k/Cp	Sc(i,M1) = q''_w/Cp	
w	μ	- dp/dz	

Grid and Control Volumes

The aim of the numerical method is to calculate the values of the relevant dependent variables at a set of chosen grid points. In this practice, the computational domain is first divided into subdomains, i.e., control volumes. Figure 10 shows the scheme of grid and control volumes; the dashed lines denote the control volume boundaries, the solid lines are the grid lines, and the dots denote the grid points. The currently considered grid point is marked by P. Its four neighboring points at a cross section are marked by N, S, W, E sequentially. And its upstream neighbor is P' (Figure 11).

Because of the characteristic of parabolic flow, each grid point is placed at the geometric center of the downstream face of the corresponding control volume; therefore, the value of ϕ at the grid point is dominant over the whole control volume except on the upstream face. Under these circumstances, a given grid point communicates with its five neighboring grid points, N, S, W, E, and P', through the five faces of the control volume.

The situation with a near-boundary control volume is somewhat different; such a control volume is shown shaded in Figure 10. Here, one face of the control volume coincides with the boundary of the calculation domain, and a boundary grid point is placed at the center of the

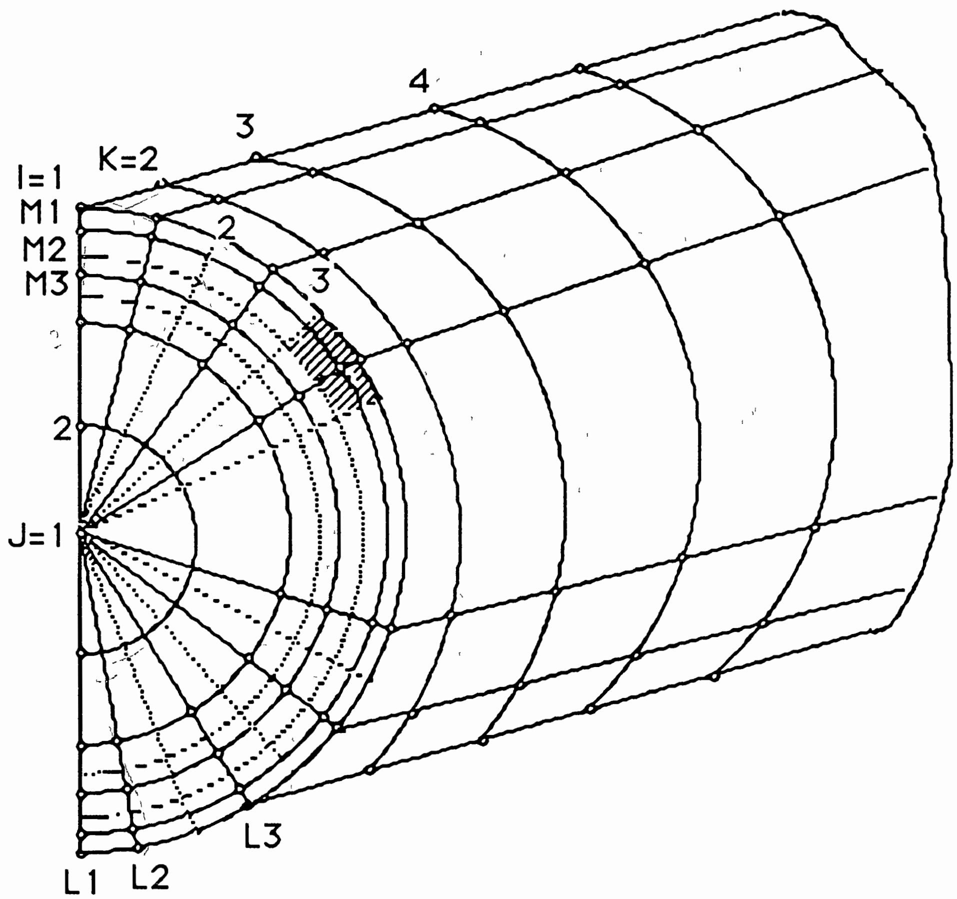

Figure 10. The scheme of grid points

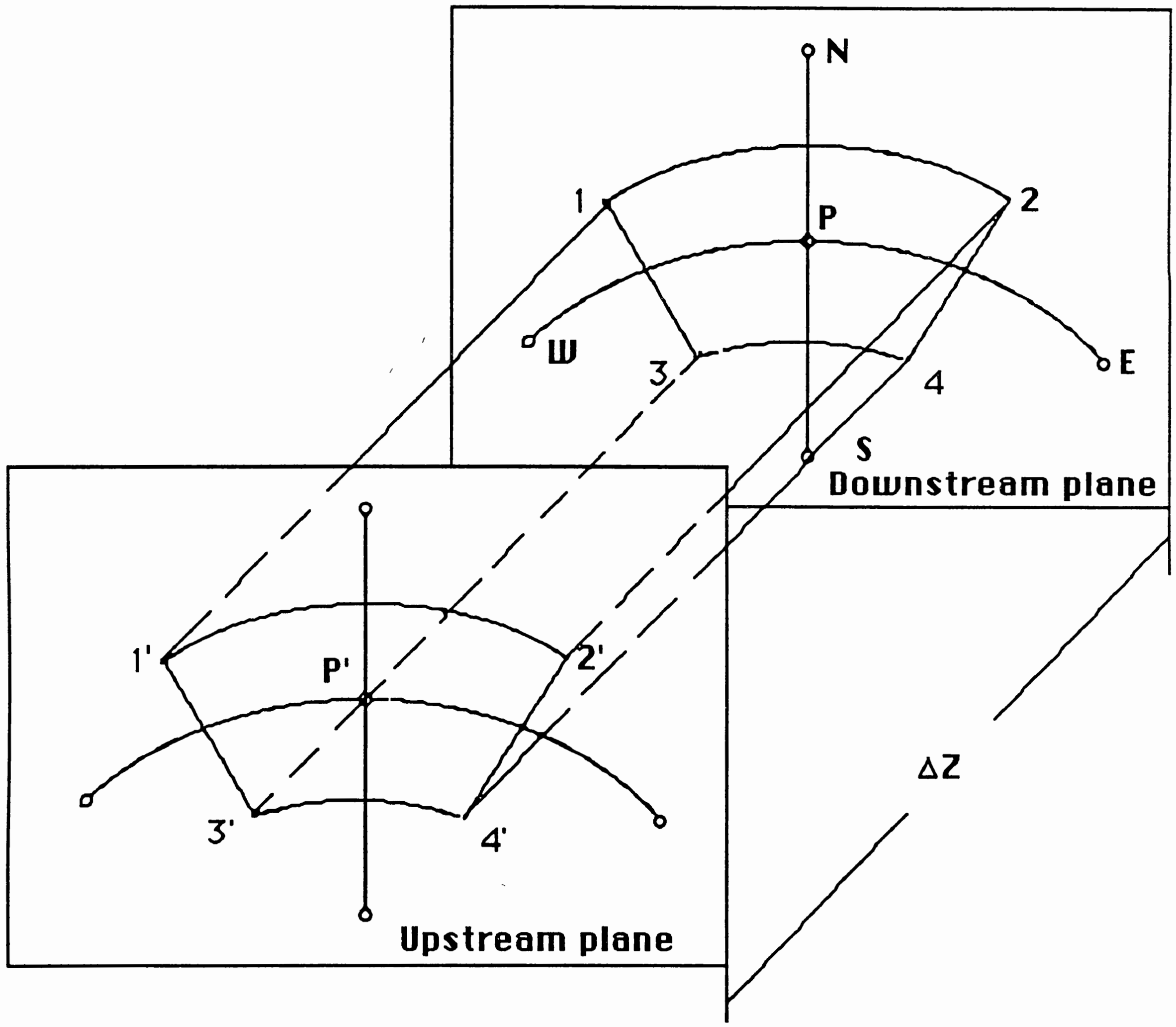

Figure 11. A typical control volume

control volume face.

Power-law Scheme

In order to integrate the general differential equation over the control volume for each grid point, profiles or distributions of variable ϕ, between the grid points, are required. For convenience of analysis, a one-dimensional (x-direction) situation is depicted here; the result will be straightforwardly extended to three dimensions in following sections. For the one-dimensional convection-diffusion problem, the general equation becomes

$$d(\rho u\phi - \Gamma d\phi/dx)/dx = S \tag{4-3}$$

Assuming constant Γ and S, for domain $0 \leq x \leq L$, with the following boundary conditions:

$$x = 0, \qquad \phi = \phi_0$$

$$\text{and} \quad x = L, \qquad \phi = \phi_L,$$

the exact solution for Equation (4-3) is

$$\frac{\phi - \phi_0}{\phi_L - \phi_0} = \frac{\exp(\frac{Px}{L}) - 1}{\exp(P) - 1}\left\{1 - \frac{SL/(\rho u)}{\phi_L - \phi_0}\right\} + \frac{SL/(\rho u)}{\phi_L - \phi_0}\frac{x}{L} \tag{4-4}$$

where P is Peclet number defined by

$$P = \rho uL/\Gamma \tag{4-5}$$

In the present convection problem, it is convenient to combine the convection and diffusion fluxes that appear in Equation (4-3). Let J_j denote the total (i.e., convection plus diffusion) flux in the j direction. Then

$$J_j = \rho u_j \phi - \Gamma \partial\phi/\partial x_j \tag{4-6}$$

Consider the region between grid points P and E in Figure 12. If a one-dimensional convection-diffusion problem without source is solved between points P and E, the exponential solution leads to the following expression for flux J_e, at surface e,

$$J_e = F_e[\phi_p + (\phi_p - \phi_E)/\exp(P_e - 1)] \tag{4-7}$$

where F_e is the mass flow rate $(\rho u)_e A_e$.

Because the exponential function appearing in Equation (4-7) is time-consuming to compute, approximations to the flux expression have been sought. After appraising the previously used upwind scheme and the hybrid scheme, Patankar (1980) proposed a power-law scheme:

$$J_e = F_e\phi_e + \{D_e A(|P_e|) + [-F_e, 0]\}(\phi_p - \phi_E) \tag{4-8}$$

where $$A(|P|) = [0, (1 - 0.1|P|)^5] \tag{4-9}$$

Here the symbol [a,b] is used to denote the greater of a and b. It can be seen that the function A in Equation (4-8)

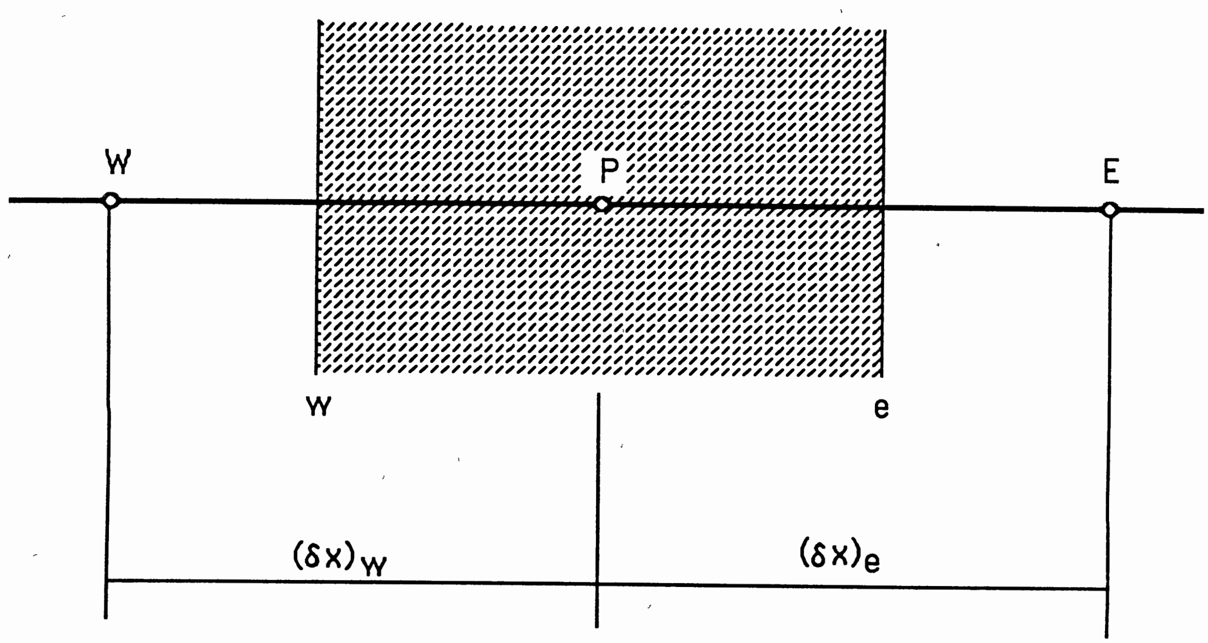

Figure 12. Typical grid point for 1-D problem

is much easier to compute than the exponential function and that Equations (4-8) and (4-9) provide an extremely good approximation to the exact expression given in Equation (4-7).

Discretization Equation

The discretization form of Equation(4-1) is obtained by integrating the equation over a typical control volume. A typical control volume in three-dimensional cylindrical coordinates is depicted in Figure 11 by dotted lines 1'2'3'4'1234. An axial increment Δz is demarcated by two planes, perpendicular to the main stream direction, the upstream plane and downstream plane. Figure 13 gives more details of the cross sectional face of the control volume. The points n, s, e, w setting at the faces of the control volume, are the midpoints of the lines PN, PS, PE, and PW, respectively.

The z-direction convection across the upstream and downstream faces of the control volume is obtained by assuming that in the z-direction ϕ varies in a stepwise manner; i.e., the downstream ($z=z_D$) values of ϕ are supposed to prevail over the interval from z_U to z_D except at z_U. This makes the finite-difference scheme a fully-implicit one. While calculating the z-direction convection and source terms, the variation of ϕ in cross section is also taken to be stepwise. Thus, in the $r\theta$ plane the value of ϕ is assumed to remain uniform and equal to ϕ_P over the shadowed sector (Figure 13) surrounding the point P and to change sharply to ϕ_N, ϕ_S, ϕ_E, or ϕ_W outside the sector.

For the combined function of convection and diffusion in the cross-stream direction, the power-law scheme mentioned previously will be used eventually. However, a separate and simple treatment is preferred here as the first step of the deduction, so that one can follow the integrating process clearly and precisely. For the cross stream convection from the θz and rz faces of the control volume, the value of ϕ convected is taken to be the arithmetic mean of the ϕ values on either side of that face. A linear variation of ϕ between grid points is assumed for diffusion across the θz and rz faces of the control volume.

Based on these assumptions and the principle of mass conservation, the general equation can be integrated term by term over the control volume shown in Figure 11.

Let L^θ, L^r stand for convected mass flow rate in θ, and r direction, respectively, with unit Δz,

$$L^\theta = \Delta r \Delta z (\rho u)_U / \Delta z = \Delta r (\rho u)_U \qquad (4\text{-}10)$$

$$L^r = r\Delta\theta\Delta z (\rho v)_U / \Delta z = r\Delta\theta (\rho v)_U \qquad (4\text{-}11)$$

The subscript U means these values are defined on the upstream plane, therefore, Y-RE

1248E+02

3.45E+0

NU = 0.

3.419E+01

TBULK

1199E-03

6

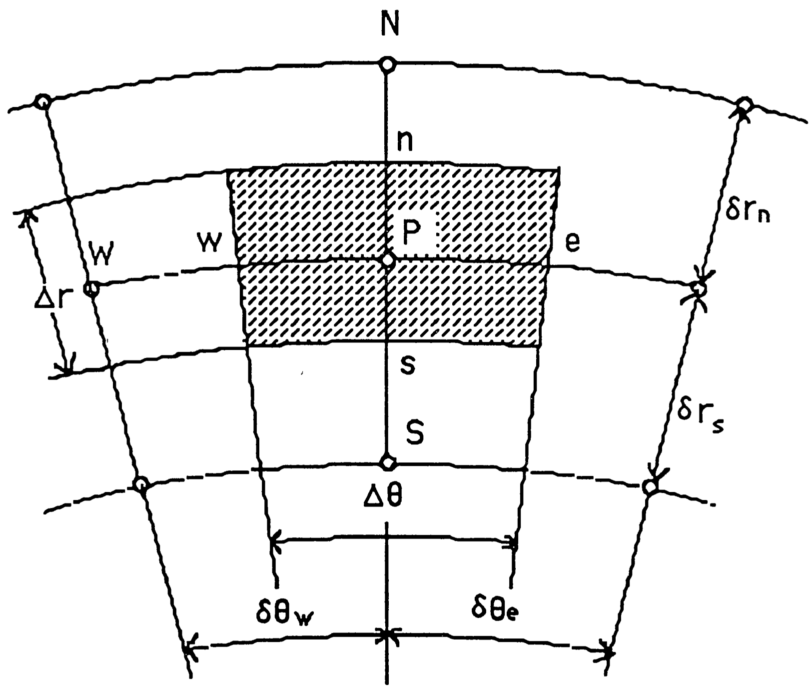

Figure 13. Cross-sectional face of the control volume

$$\int \partial(\rho u\phi)/\partial\theta/r = L^{\theta}_{e}(\phi_E + \phi_P)/2 - L^{\theta}_{w}(\phi_W + \phi_P)/2 \qquad (4\text{-}12)$$

$$\int \partial(\rho r v\phi)/\partial r/r = L^{r}_{n}(\phi_N + \phi_P)/2 - L^{r}_{s}(\phi_S + \phi_P)/2 \qquad (4\text{-}13)$$

Assume F_U and F_D stand for mass flow rate across the upstream face and the downstream face of the control volume, respectively,

$$F_U = r\Delta\theta\Delta y(\rho w)_U/\Delta z \qquad (4\text{-}14)$$

where division by Δz is for consistency with Equations (4-10) and (4-11). By principles of mass balance,

$$F_D - F_U + L^{r}_{n} - L^{r}_{s} + L^{\theta}_{e} - L^{\theta}_{w} = 0$$

then

$$F_D = F_U - L^{r}_{n} + L^{r}_{s} - L^{\theta}_{e} + L^{\theta}_{w} \qquad (4\text{-}15)$$

Therefore,

$$\int \partial(\rho w\phi)/\partial z = F_D\phi_{P,D} - F_U\phi_{P,U} \qquad (4\text{-}16)$$

Suppose T^{θ}, T^{r} represent diffusion in θ and r direction individually,

$$T^{\theta} = \Gamma\Delta r/(r\delta\theta) \qquad (4\text{-}17)$$

$$T^{r} = \Gamma\rho\Delta x/\delta r \qquad (4\text{-}18)$$

then

$$\int \partial(\Gamma\partial\phi/\partial\theta)/\partial\theta/r^2 = T^{\theta}_{e}(\phi_E - \phi_P) - T^{\theta}_{w}(\phi_P - \phi_W) \qquad (4\text{-}19)$$

$$\int \partial(r\Gamma\partial\phi/\partial r)/\partial r/r = T^{r}_{n}(\phi_N - \phi_P) - T^{r}_{s}(\phi_P - \phi_s) \qquad (4\text{-}20)$$

From source linearization

$$\int S_{\phi} = (S_C + S_P\phi_P)\Delta V \qquad (4\text{-}21)$$

where

$$\Delta V = r\Delta\theta\Delta r\Delta z \qquad (4\text{-}22)$$

Substituting Equations (4-12) to (4-21) into Equation (4-1), one gets

$$\begin{aligned}(-L^{r}_{n}/2 + T^{r}_{n})\phi_P + (L^{r}_{s}/2 + T^{r}_{s})\phi_P + (-L^{\theta}_{e}/2 + T^{\theta}_{e})\phi_P + \\ (L^{\theta}_{w}/2 + T^{\theta}_{w})\phi_P + F_U\phi_P - S_P\Delta V\phi_P \\ = (-L^{r}_{n}/2 + T^{r}_{n})\phi_N + (L^{r}_{s}/2 + T^{r}_{s})\phi_S + (-L^{\theta}_{e}/2 + T^{\theta}_{e})\phi_E + \\ (L^{\theta}_{w}/2 + T^{\theta}_{w})\phi_W + F_U\phi_{P,U} + S_C\Delta V \qquad (4\text{-}23)\end{aligned}$$

where the terms within parentheses are the sums of convection and diffusion across each face of the control volume. The factor 1/2 arises from the assumption of the interfaces being midway. However, one prefers a more accurate scheme here, e.g., the power-law scheme mentioned in Section 3. Finally the discretization equation becomes the following simple form:

$$a_P\phi_P = a_N\phi_N + a_S\phi_S + a_E\phi_E + a_W\phi_W + F_U\phi_{P,U} + S_C\Delta V \qquad (4\text{-}24)$$

where

$$a_P = a_N + a_S + a_E + a_W + F_U - S_P\Delta V \qquad (4\text{-}25)$$

$$a_N = D_n A(|P_n|) + [-F_n, 0] \tag{4-26}$$

$$a_S = D_s A(|P_s|) + [\ F_s, 0] \tag{4-27}$$

$$a_E = D_e A(|P_e|) + [-F_e, 0] \tag{4-28}$$

$$a_W = D_w A(|P_w|) + [F_w, 0] \tag{4-29}$$

At this stage, it is useful to write Equation(4-24) in a generalized form

$$a_P \phi_P = \Sigma a_{nb} \phi_{nb} + b \tag{4-30}$$

where the subscript nb denotes the neighbor grid points of P; the summation is to be taken over all the neighbors.

Treatment of UHF Boundary Condition

In this investigation, a uniform heat flux (UHF) boundary condition is provided by electrical heating. Figure 14 shows one of the control volumes involving boundary grid point. In most engineering calculations, a simple one-side formula was employed for the boundary flux J_w,

$$J_{w,i} = \Gamma_{i,M2}(T_{i,M1} - T_{i,M2})/\Delta r_{i,M1} \tag{4-31}$$

Since

$$\Gamma_{i,M2} = k_{i,M2}/Cp_{i,M2} \tag{4-32}$$

Then

$$J_{w,i} = q''_{w,i}/Cp_{i,M2} \tag{4-33}$$

Thus, the boundary temperature, $T_{i,M1}$, was simply obtained

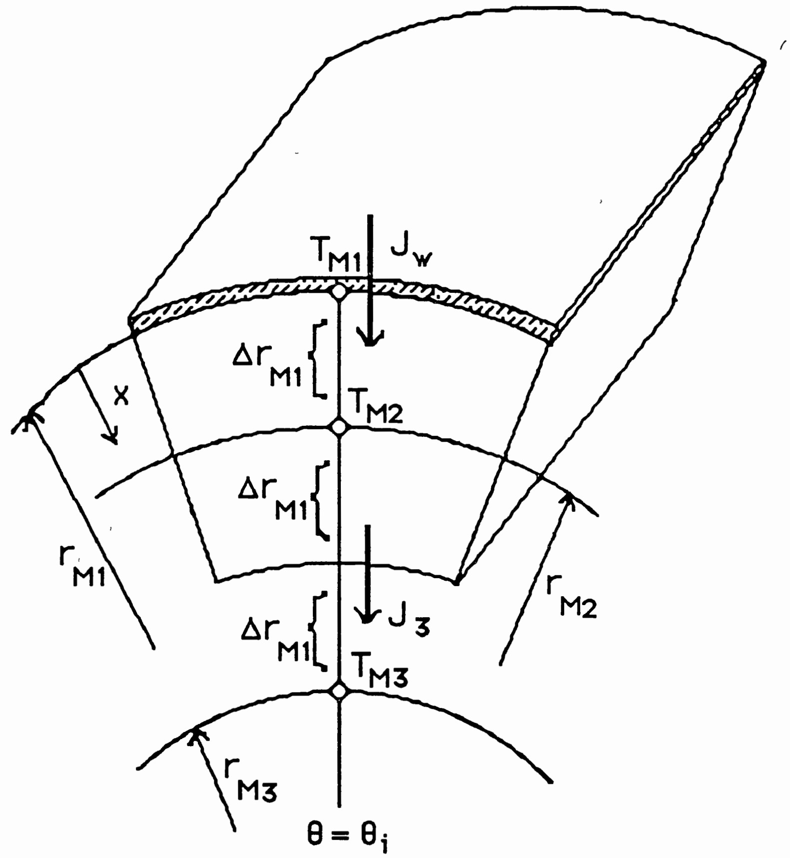

Figure 14. A control volume near the tube wall

by

$$T_{i,M1} = q''_{w,i}\Delta r_{i,M1}/k_{i,M2} + T_{i,M2} \qquad (4\text{-}34)$$

However, this simple formula would not give a converged solution; no matter how many iterations were taken, values of $T_{i,M2}$ kept linearly increasing. It seems that the treatment of the UHF boundary condition is so critical to the success of the numerical method that a higher-order formula is required. Over the control volume near the tube wall described in Figure 14, by neglecting tangential flux variation in this volume, the radial flux J is assumed to be linear in the r-direction. Then

$$J = \Gamma_{M2}(\partial T/\partial r) = J_w + (J_3 - J_w)[(r_{M1} - r)/(2\Delta r_{M1})] \qquad (4\text{-}35)$$

where the flux J is considered to be positive if it enters the calculation domain. For convenience of analysis, variable substitution is used here. Let

$$x = r_{M1} - r \qquad (4\text{-}36)$$

then

$$\partial x = -\partial r \qquad (4\text{-}37)$$

In the calculation domain

r: $r_{M3} + \Delta r_{M3}$ to r_{M1}

x: 0 to $2\Delta r_{M1}$

Then Equation (4-35) becomes

$$J = -\Gamma_2(\partial\phi/\partial x) = J_w + (J_3 - J_w)[x/(2\Delta r_{M1})] \qquad (4\text{-}38)$$

Integration gives

$$\Gamma_{M2}(T_{M1} - T) = J_w x + (J_3 - J_w)x^2/(4\Delta r_{M1})$$

When $x = \Delta r_{M1}$, $T = T_{M2}$. So,

$$\Gamma_{M2}(T_{M1} - T_{M2}) = J_w \Delta r_{M1} + (J_3 - J_w)\Delta r_{M1}/4$$

Therefore

$$J_w = (4/3)\Gamma_{M2}(T_{M1} - T_{M2})/\Delta r_{M1} - (1/3)J_3 \qquad (4\text{-}39)$$

or

$$T_{M1} = [(3/4)\Delta r_{M1}J_w + (1/4)\Delta r_{M1}J_3]/\Gamma_{M2} + T_{M2} \qquad (4\text{-}40)$$

where J_3 is the energy flux crossing through the bottom surface of the volume, which is created by diffusion as well as convection and can be computed by a power-law scheme.

It has been established that Equation (4-40) is a better expression for boundary temperature under UHF condition. This treatment has brought about satisfactory results.

Solving the Nonlinear Equations with a Linear Method

When one has constructed algebraic equations like Equation (4-24) for all internal grid points in the calculation domain, and solved the boundary grid by the boundary treatment just mentioned, the next task is to solve this set of equations. If these equations are truly linear, a straightforward solution would yield the final answer. However, it must be recognized at this stage that these equations are only nominally linear. The coefficients in Equation (4-24) may themselves depend on the value of ϕ (see Equations (3-2) to (3-5)). Further, since ϕ can stand for a number of physical quantities, such as velocity and temperature, the coefficients for one meaning of ϕ may be influenced by some of the other ϕ's. For example, when ϕ stands for temperature, its discretization coefficients depend on velocity u, v, and w as shown in Equation (3-6). These velocity components, on the other hand, depend on temperature while calculating the variable property solution.

Because of these interlinkages and nonlinearities, the final solution is to be obtained by iteration. At any given stage, the discretization coefficients can be calculated from the current estimates of all the ϕ values. Then the algebraic equations like Equation (4-24) are solved by line-by-line TDMA (TriDiagonal Matrix Algorithm) technique with block-correction procedure (Patankar, 1980). To avoid divergence of the strongly nonlinear equations, underrelaxation is employed. When, after many repetitions of this process, all the ϕ values cease to change, the final converged solution is reached.

Thus, the solution to a set of nonlinear and interlinked equations is obtained via many intermediate solutions of nominally linear and decoupled algebraic equations.

Pressure-Velocity Coupling in the Main Stream Direction

In the parabolic direction, the value of pressure drop dp/dz must be chosen such that, when it is used in z-momentum equation, values of w will reflect the correct cross sectional mass flow rate m:

$$m = \Sigma \rho \Delta A w_p \qquad (4\text{-}41)$$

Based on a method proposed by Raithby and Schneider (1979), the following procedures are executed

Guess (dp/dz)*, then solve w*. The corresponding mass flow rate is

$$m^* = \Sigma \rho \Delta A w_p^* \qquad (4\text{-}42)$$

Motivated by the linear relation between w and dp/dz, for a given set of coefficients, an equation for the rate of change of w with dp/dz is sought. Defining

$$Q = -dp/dz, \qquad f_p = \partial w/\partial Q \qquad (4\text{-}43)$$

if the f_p's were known, the correct velocities would be related to the w*'s by

$$w_p = w_p^* + f_p \Delta Q \qquad (4\text{-}44)$$

$$\Delta Q = -[dp/dz - (dp/dz)^*] \tag{4-45}$$

The ΔQ value is chosen to make the total mass flow rate correct; i.e.,

$$\Delta Q = (m - m^*)/(\Sigma\rho\Delta A f_p) \tag{4-46}$$

The equation for f_p is

$$a_p f_p = a_N f_N + a_S f_S + a_E f_E + a_W f_W + \Delta V \tag{4-47}$$

where the coefficients are the same as those in the z-momentum equation. Therefore, f_p can be solved by the general procedure, then ΔQ is found by Equation (4-46), at last, w_p and dp/dz are solved by Equations (4-44) and (4-45).

Pressure-Velocity Coupling at Cross Section

At any cross section, momentum equations for u and v contain the pressure gradient $(-\partial p/\partial\theta)/r$ and $(-\partial p/\partial r)$, respectively, as important source terms, which are not expressible in terms of u, v, or other ϕ's. If the velocity components and the pressure are calculated for the same grid points, some physically unrealistic results, such as zig-zag pressure field and velocity distributions, arise. A remedy for this ailment is the staggered grid (Patankar, 1980).

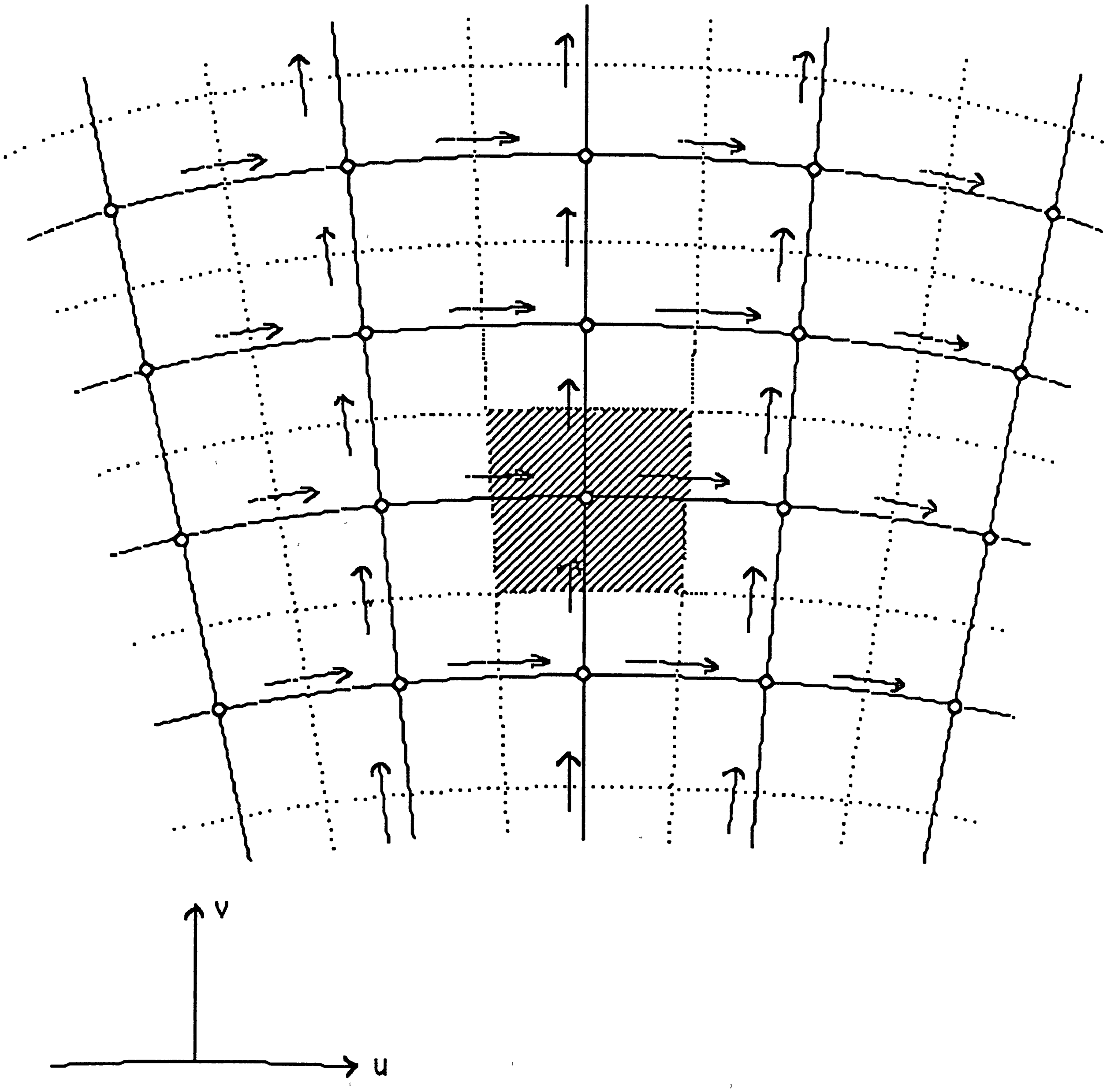

Figure 15. Staggered grid

Figure 15 shows a portion of grid at the cross section. In the staggered grid system, only variables other than cross section velocities are calculated at the grid points shown by dots, while the velocities u and v are evaluated at the corresponding control volume faces marked by short arrows. As a result, one can obtain an accurate mass flow rate at each face and the pressure difference between two grid points can play a real role of "driving force" to the velocity component located between them.

Figure 16 illustrates the appropriate control volumes for u and v. For the θ-momentum equation, the final discretization form is

$$a_e u_e = \Sigma a_{nb} u_{nb} + b + A_e (p_P - p_E) \qquad (4\text{-}48)$$

For the r-momentum equation

$$a_n v_n = \Sigma a_{nb} v_{nb} + b + A_n (p_P - p_N) \qquad (4\text{-}49)$$

where the coefficient expressions for a_{nb}, a_e, and a_n are identical to those given in Equations (4-25) to (4-29), the term b includes the source terms other than pressure gradient, and A_e and A_n stand for the areas over which the pressure force acts.

At this step, if the pressure field is given, the velocity fields would be figured out by Equations (4-48) and (4-49), However, since the pressure field is unknown, one needs to estimate the pressure field first. Let p* stand for the estimated pressure field; then the

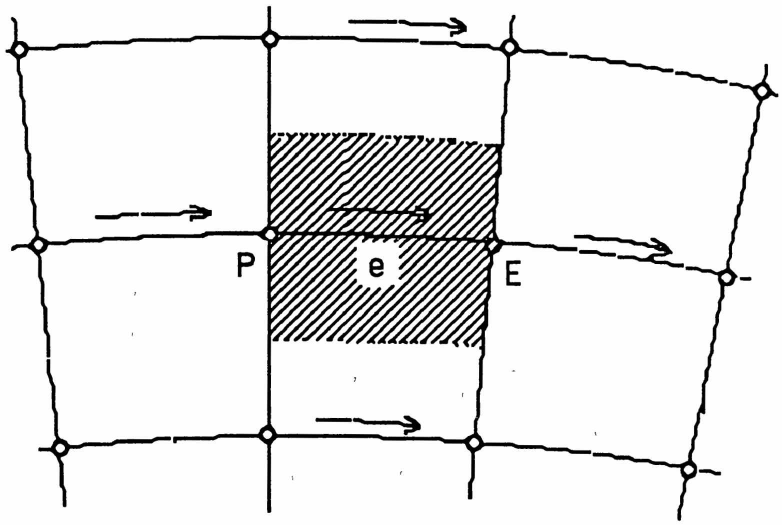

a). C. V. for u

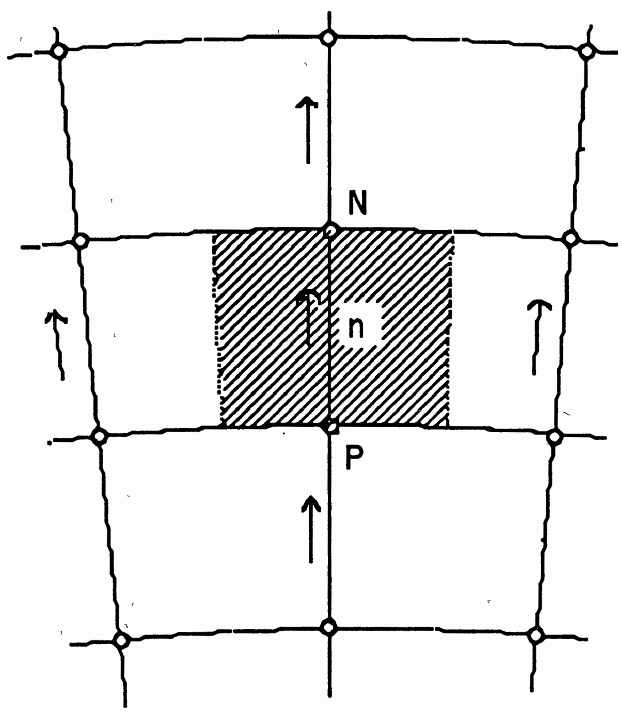

b). C. V. for v

Figure 16. Control volume for u and v

provisional velocities are expressed by u* and v*.

$$a_e u^*_e = \Sigma a_{nb} u^*_{nb} + b + A_e(p^*_P - p^*_E) \qquad (4\text{-}50)$$

Introducing pressure correction p' and velocity corrections u' and v'

$$p = p^* + p'$$

$$u = u^* + u'$$

$$v = v^* + v'$$

Subtracting Equation (4-50) from (4-48)

$$a_e u'_e = \Sigma a_{nb} u'_{nb} + A_e(p'_P - p'_E) \qquad (4\text{-}51)$$

Neglecting $Sa_{nb}u'_{nb}$, Equation (4-51) simply becomes,

$$u'_e = d_e(p'_P - p'_E) \qquad (4\text{-}52)$$

where

$$d_e = A_e/a_e$$

Similarly,

$$v'_n = d_n(p'_P - p'_N) \qquad (4\text{-}53)$$

Substituting the above expressions for u and v into the continuity equation at a given cross section, a discretization equation for the pressure correction can be obtained:

$$a_P p'_P = a_N p'_N + a_S\, p'_S + a_E p'_E + a_W p'_W + b \qquad (4\text{-}54)$$

W → vel
ΔA → small ar[illegible]
σ → vol flow rate [illegible]

where

$$a_N = \rho_n d_n A_n \tag{4-55}$$

$$a_S = \rho_s d_s A_s \tag{4-56}$$

$$a_W = \rho_w d_w A_w \tag{4-57}$$

$$a_E = \rho_e d_e A_e \tag{4-58}$$

$$a_P = a_N + a_S + a_W + a_E \tag{4-59}$$

$$b = (\rho v^* A)_s - (\rho v^* A)_n + (\rho u^* A)_w - (\rho u^* A)_e \tag{4-60}$$

Patankar (1980) called this strategy as the SIMPLE (Semi-Implicit Method for Pressure-Linked Equations) procedure, which is summarized as follows:

1). Guess the pressure field p^*.

2). Solve the momentum equations to get u^* and v^*.

3). Solve the pressure correction equation for p'.

4). Correct the pressure, $p = p^* + p'$

5). Correct velocities, $u = u^* + u'$, and $v = v^* + v'$

6). Return to step 2) with the corrected pressure as the new p^* field. Repeat until convergence.

The Overall Solution Procedure

The complete solution of a three-dimensional tube flow is obtained by repeating the solution for one forward step in the z direction. For the first forward step, the values of ϕ at the inlet plane are known. For subsequent forward steps, the ϕ values obtained on the downstream plane of the previous step become available as the upstream plane values for the current step. With this general framework, the various steps in the calculation sequence are outlined here.

1). Start with the initial guess for the ϕ values for the downstream plane. The known ϕ values on the upstream plane can serve as satisfactory guesses.

2). Solve z-momentum equation for w, obtain dp/dz by the technique mentioned in Section 7.

3). Solve θ-momentum, r-momentum, and pressure correction equations for u and v by SIMPLE procedure.

4) Solve energy equation for T, using the method in Section 5 for UHF boundary treatment.

5). Take the downstream ϕ values as the upstream values for the next forward step and return to 1) to begin the calculation sequence for the next Δz.

CHAPTER V

PROGRAMMING AND COMPUTATIONS

The Computer Program

A three-dimensional computer program for the solving strategy mentioned previously has been created. This program is based on a fundamental teaching program for two-dimensional conduction-type problems of Patankar (1984).

Programming, modifying, and testing of the program took about one year. Major programming work includes mixed convection, pressure-velocity decoupling, variable properties, UHF boundary treatment, and extension to the 3-D situation. Tests of the 2-D program were carried out for all example problems in Patankar (1984), and the examples also served as the limiting cases for testing the 3-D program.

The program in FORTRAN consists of four major parts: MAIN, SETUP, SOLVE, and TUBE. Each part includes several subprograms. Function of the subprograms are briefly described as follows:

MAIN controls the sequence of operations.

SETUP1 calculates geometrical quantities.

SETUP2 calculates the discretization coefficients.

SOLVE obtains the solution of the discretization equations.

DIFLOW uses the power-law scheme for total flux.

START gives operating conditions and initial values.

GRID assigns the grid points and control volumes.

DENSE computes the density at each grid point.

VISCO computes the viscosity.

SPHT is for specific heat of the fluid.

CONDY is for thermal conductivity of the fluid.

BOUND gives boundary conditions each iteration.

GAMSOR specifies Γ and S for each individual variable.

Figure 17 is the flow chart of the program. The MAIN monitors the whole routine, TUBE specifies operating conditions and furnishes subroutines for physical properties. Mathematical models for properties of the sample fluids are given in Appendix A. SETUP computes the coefficients, and SOLVE gets the solution for the equations. MAIN visits GRID, START, and SETUP1 only once for a case, INPUT once for a marching station, and other subprograms once per iteration.

A brief guide to the computer program is furnished in Appendix B.

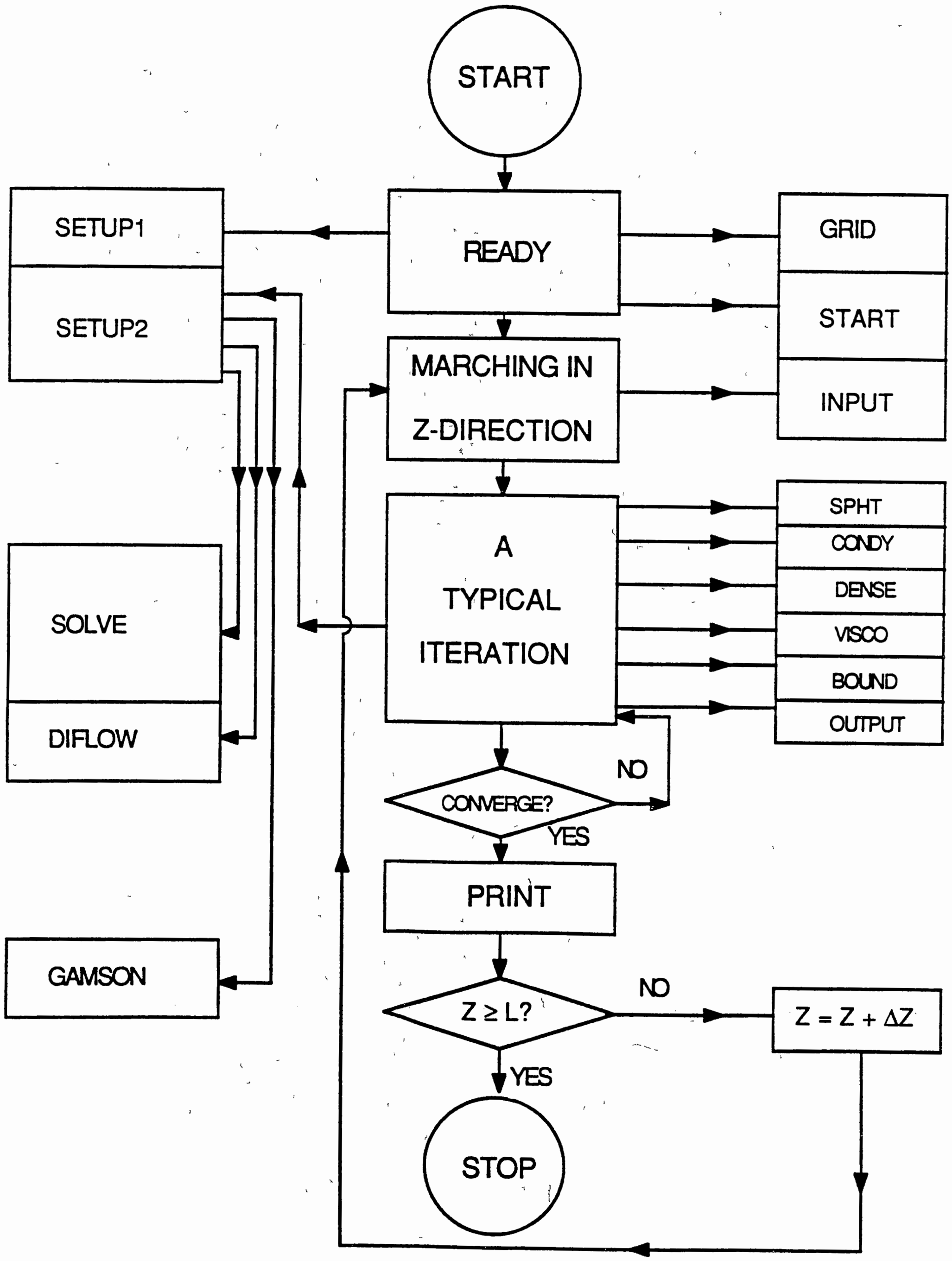

Figure 17. Flow chart of the 3-D program

Computational Runs

The 3-D program was executed on the VAX 6320 at the Computer Center of Oklahoma State University. Computations were carried out for a number of runs of Chen's (1988) experimental work. Table III lists conditions for these computations corresponding to Chen's work.

For the early runs, a 15x15x44 (θxrxz) grid was used and a uniform grid spacing was chosen in the θ and r directions. The axial step size Δz was varied from 0.02 m at the entrance to about 0.1 m towards the end of the tube. The value of Δz was adjusted so that the 12 experimental stations along the length of the tube would coincide with appropriate computational steps. Then a denser grid system, 21x21x44, was used. Grid spacing was still uniform in the θ direction, while a nonuniform spacing was chosen in the r direction, with grid lines being more closely packed near the tube wall. For most runs, a 19x19x44 grid, with nonuniform spacing in r direction, system was used. CPU time is approximately 7 minutes for the 15x15x44 system, 17 minutes for 19x19x44, and 25 minutes for 21x21x44. For the same operating conditions, the results of the denser grid system did not show significant difference from the coarser one.

The convergence criterion for ending iterations is

TABLE III

CONDITIONS FOR COMPUTATIONAL RUNS

Run No.	$q''_w (w/m^2)$	m (kg/s)	x	Re_{in}	Re_{out}	Pr_{in}	Pr_{out}
1103	14100	0.02798	0.	2474	3941	6.2	3.7
2105	12200	0.0785	0.9987	354	585	209	128
2107	11600	0.0521	0.9987	222	452	221	111
2110	20300	0.167	0.9305	1361	1809	116	88
2121	9010	0.09985	0.6584	1580	1833	53	46
2135	5110	0.04002	0.283	514	749	28	19
2137	11300	0.0655	0.283	1769	2284	26	20
2139	3050	0.0341	0.283	1104	1249	22	19

$$\Sigma \frac{| \phi_{ij}^{(n+1)} - \phi_{ij}^{(n)} |}{|\phi_{ij}^{(n+1)}|} \le \varepsilon \qquad (5-1)$$

.0001

.0005

The output for each marching station consists of key values for each iteration and converged solutions for distributions of three velocity components, stream function at cross section, and temperature. Appendix C illustrates a typical printout for one station.

CHAPTER VI

RESULTS AND DISCUSSIONS

Peripheral Variation of Wall Temperature

Figures 18 to 24 show comparisons of computed inside tube wall temperature at the top, T_{top} and at the bottom, T_{bottom}, with Chen's (1988) experimental data for Runs listed in Table III, using the nominally uniform heat flux. It can be seen that agreement between the numerical results and experimental data is quite good, except Figure 22 (the experimental data for Run#2135 are questionable). However, the measured T_{bottom}'s are generally several degrees higher than computed ones, while the measured T_{top}'s are lower than the computed. This inconsistency may be explained by the following.

As mentioned in Chapter IV, the boundary temperatures, i. e., the inside wall temperatures, were obtained by only considering the communication between the boundary grid point (grid point on the inside tube wall) at which the wall heat flux exerts, and its inner neighboring point, e. g., points 1 and 3 in Figure 25. The peripheral interaction between boundary grid points, e.g., points 1 and 2 in Figure 25, mainly the tube wall conduction, was not taken into

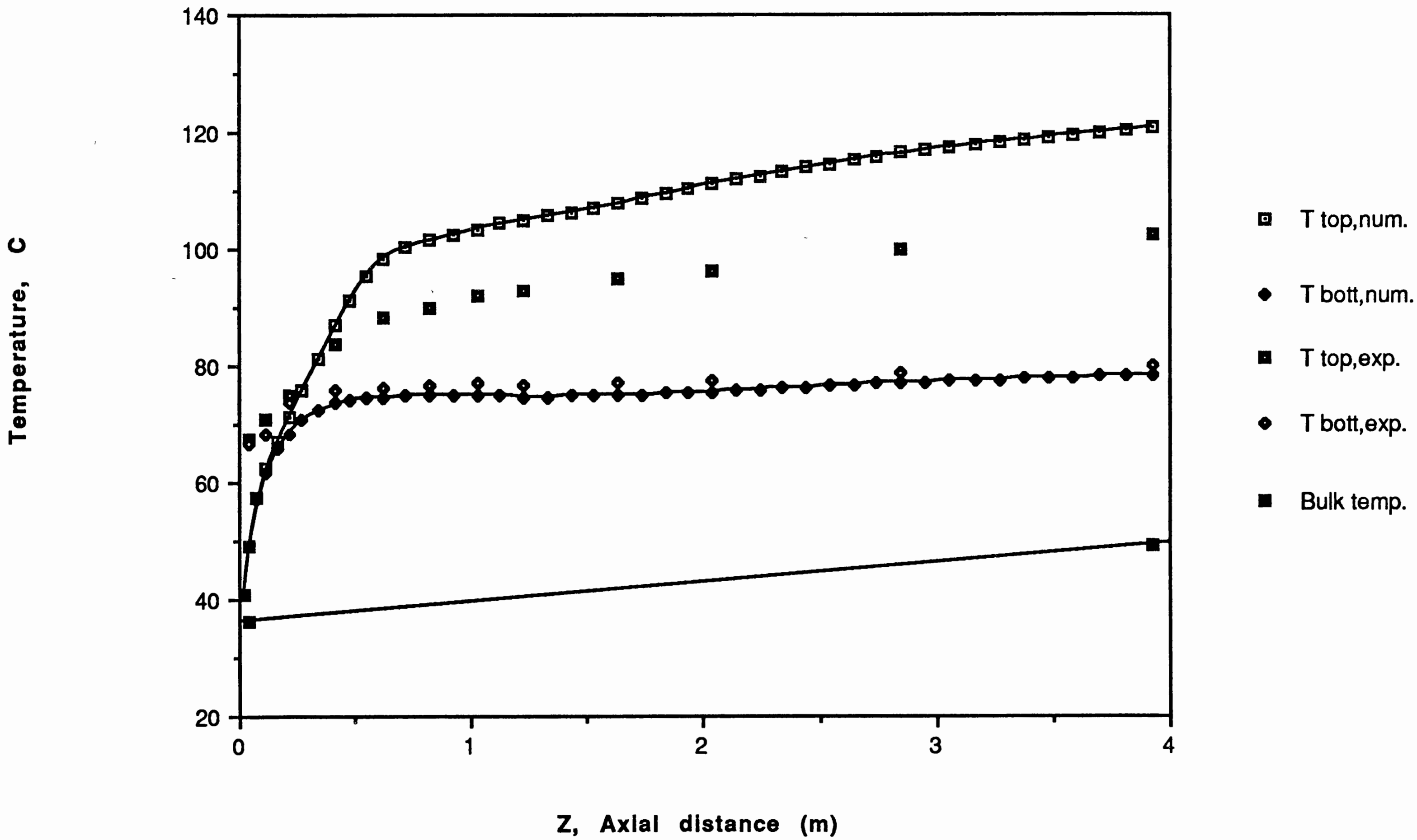

Figure 18. Peripheral wall temperature variation (Run#2105)
[Re: 354-585, Gr: 3480-12600, Pr: 209-128]

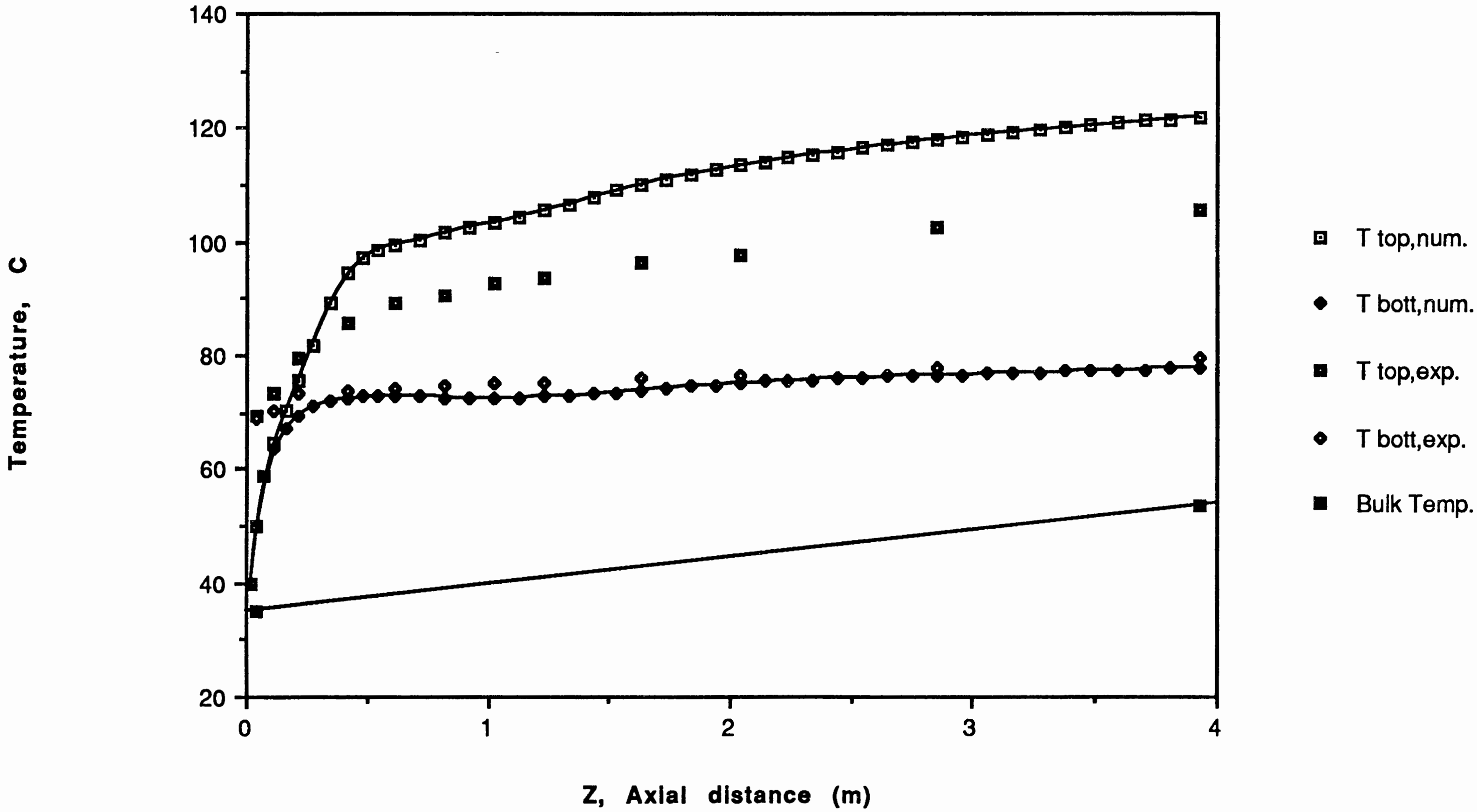

Figure 19. Peripheral wall temperature variation (Run#2107)
[Re: 222-452, Gr: 3450-15700, Pr: 221-111]

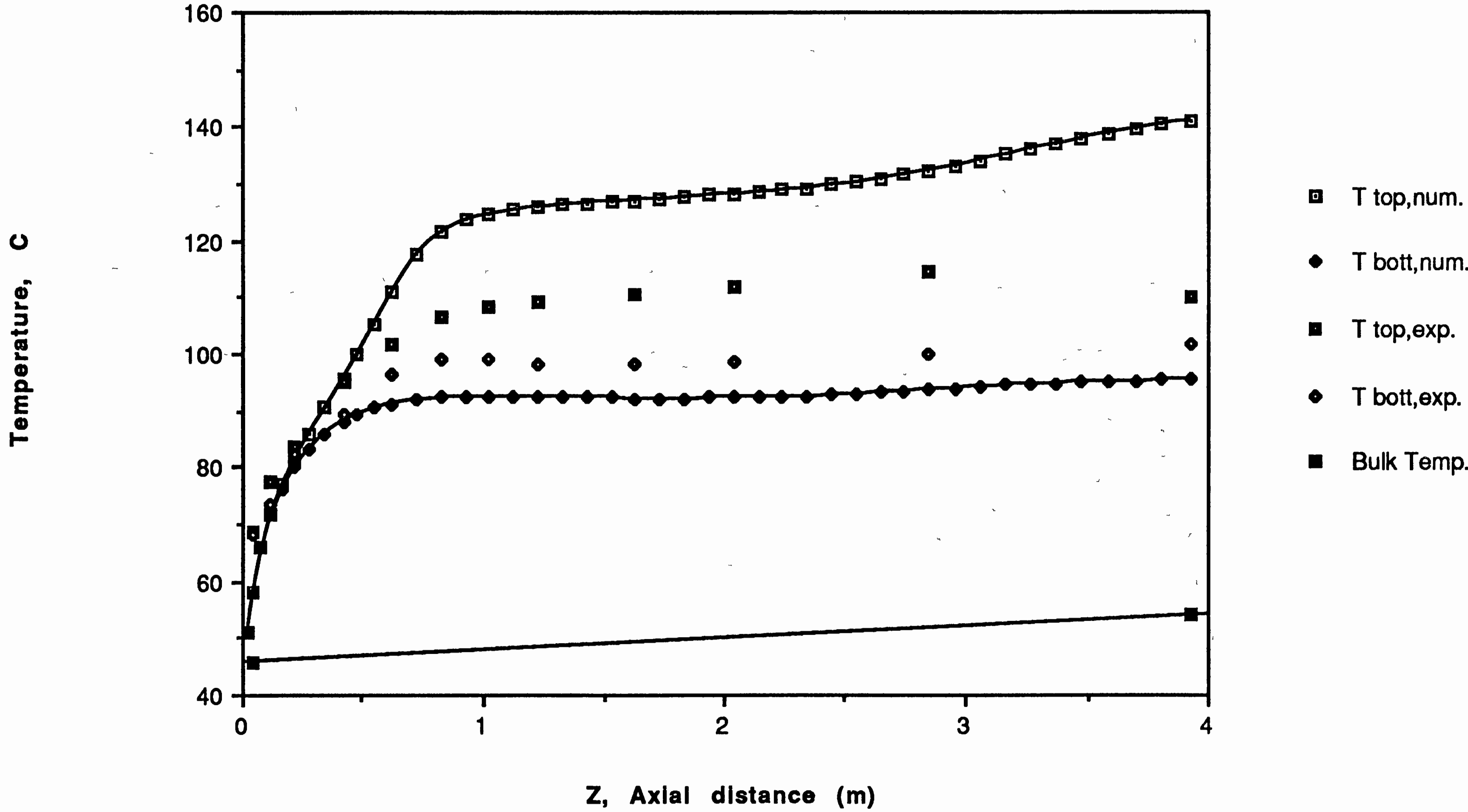

Figure 20. Peripheral wall temperature variation (Run#2110)
[Re: 1360-1810, Gr: 8840-34000, Pr: 116-88]

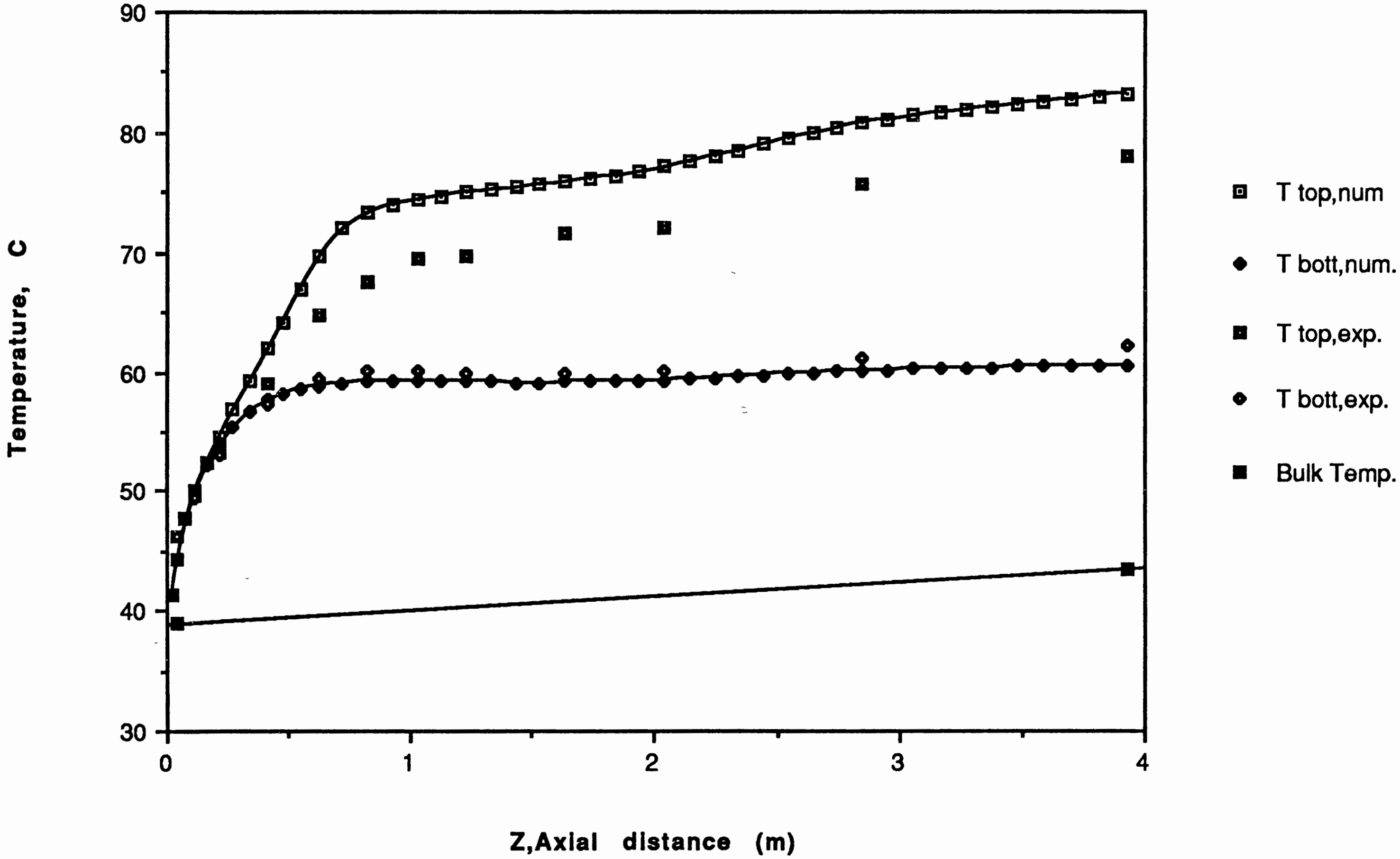

Figure 21. Peripheral wall temperature variation (Run#2121)
[Re: 1580-1830, Gr: 8580-39900, Pr: 53-46]

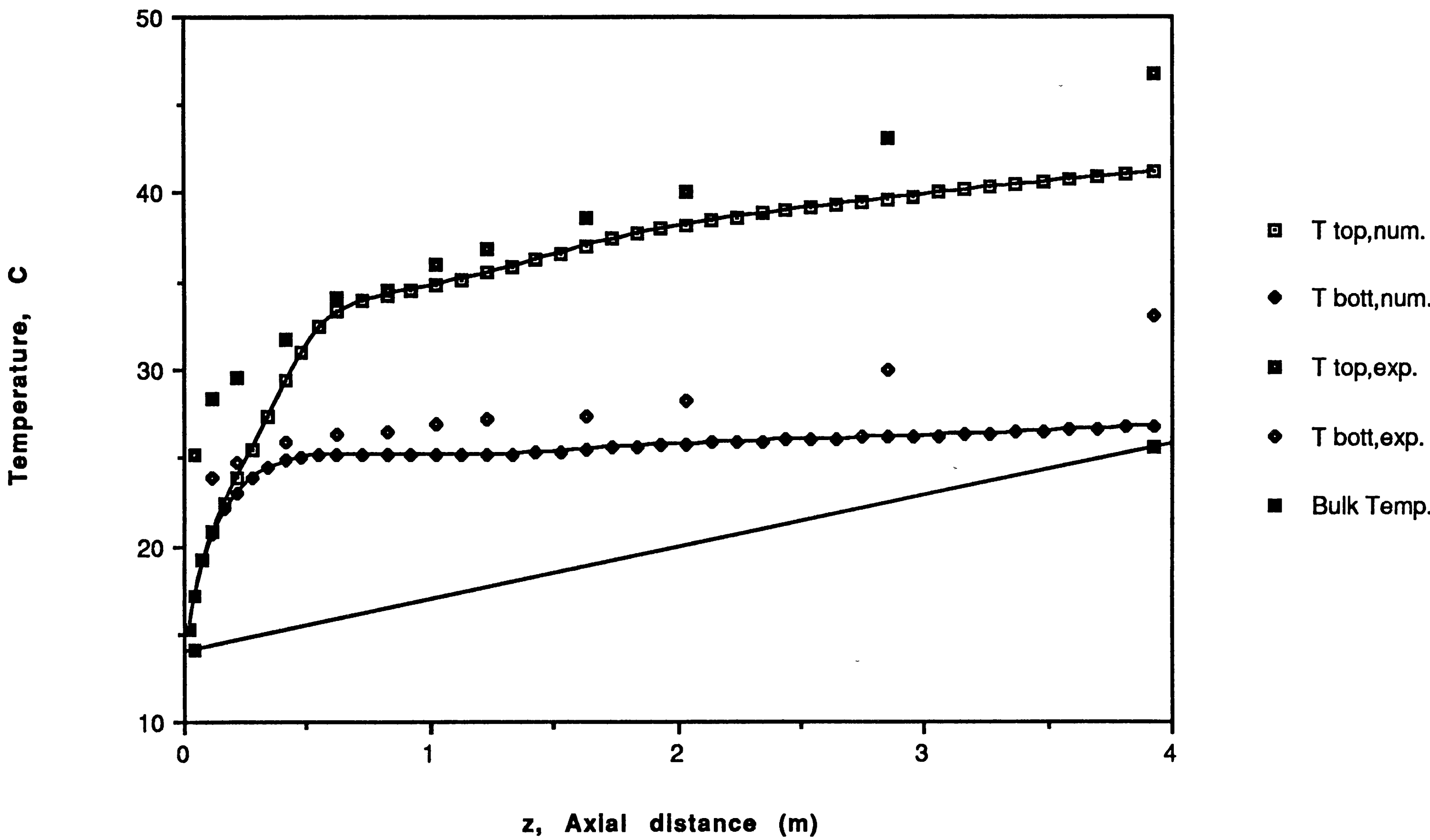

Figure 22. Peripheral wall temperature variation (Run#2135)
[Re: 514-749, Gr: 16800-47300, Pr: 28-19]

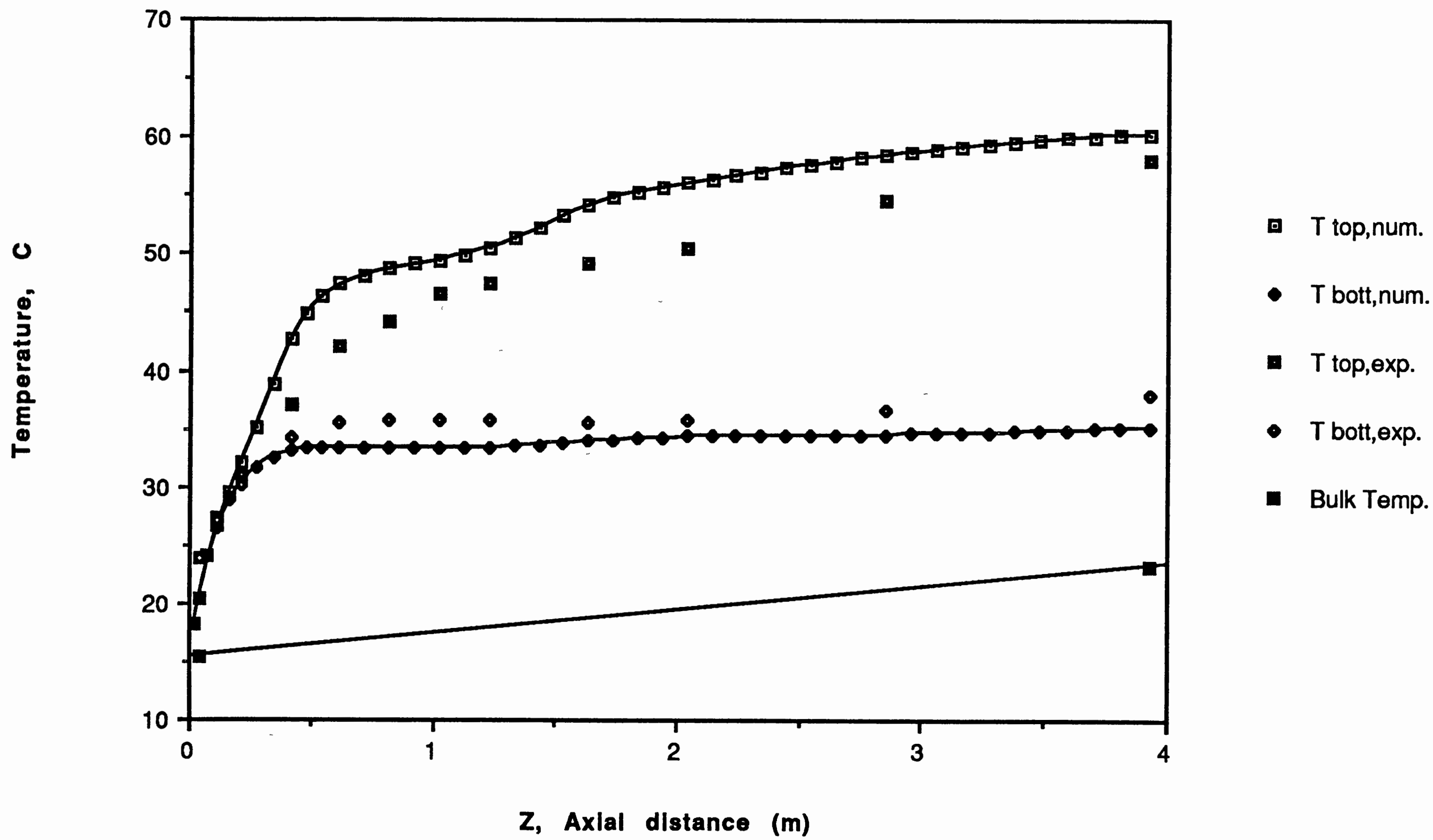

Figure 23. Peripheral wall temperature variation (Run#2137)
[Re: 1770-2284, Gr: 14100-67300, Pr: 26-20]

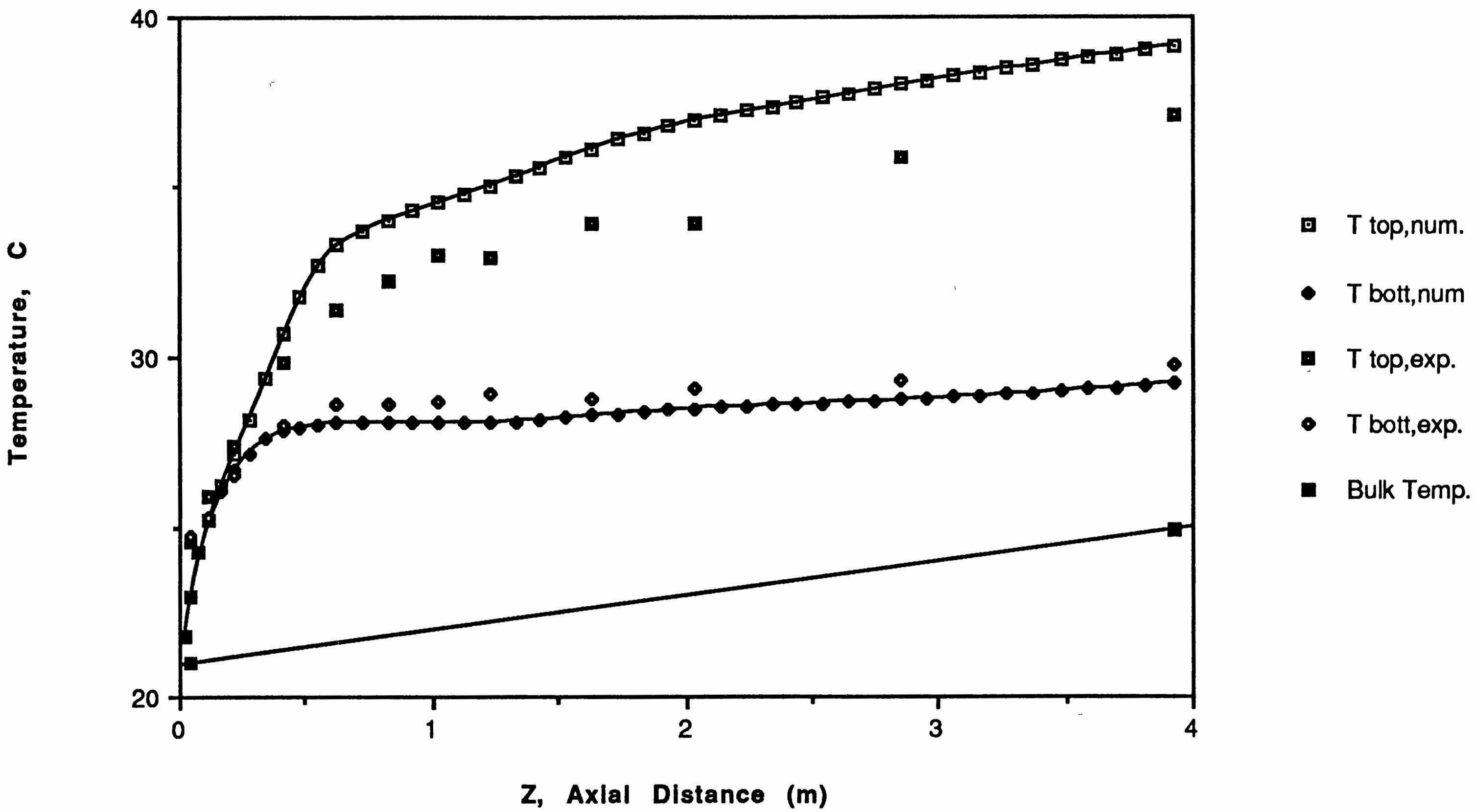

Figure 24. Peripheral wall temperature variation (Run#2139)
[Re: 1100-1250, Gr: 9280-26900, Pr: 22-19]

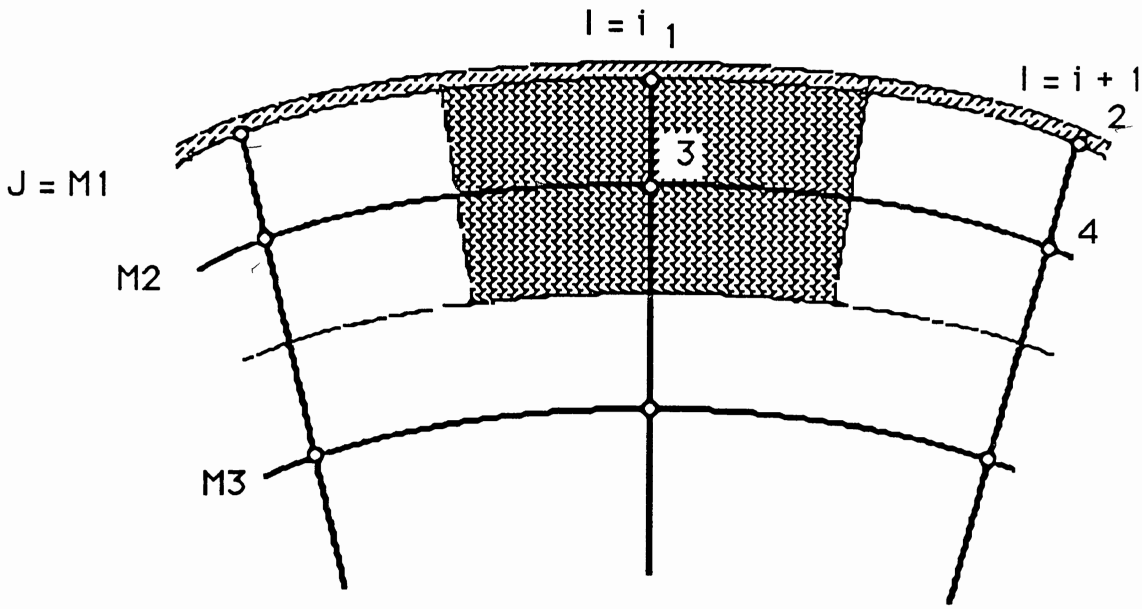

Figure 25. Near-wall control volume

account. However, usually the thermal conductivity of the wall is much higher than the fluid; therefore, the highly conductive wall would suppress the sharp peripheral temperature variation originated by the flowing field. Qualitatively, the extent of the suppression depends on the magnitude of the peripheral wall temperature difference which measures the effect of the natural convection, the temperature level of the wall relative to the local fluid or ambient temperature which measures the heat flux and reflects the heat loss to the surroundings, and the material of the tube. The effect of the suppression can be observed by comparison of Figure 20 (Run #2110) and Figure 24 (Run #2139). For the former, the computed peripheral wall temperature difference is as high as $45^{\circ}C$, and the average wall temperature is around $100^{\circ}C$. For the latter, the corresponding temperatures are $10^{\circ}C$ and $30^{\circ}C$.

The basic agreement between numerical results and experimental data reveals that the flowing field with secondary flow still controls the temperature distribution, even at the inside wall---the interface between the fluid and the tube. The finding is contrary to the conclusion of Faris and Viskanta (1969), in which they claimed that for all liquids excepting liquid metals, the assumption that inside tube wall temperature was uniform circumferentially was justifiable for ordinary tube thicknesses. Hence, the validity and the necessity of the infinite wall conductivity model may be suspected because it conceals a major consequence of mixed convection---the peripheral wall temperature variation---while assuming a circumferentially constant wall temperature.

Figure 26 is an exploration of flow in transition region. Although the Reynolds number of this run is as high as 3941, numerical results still show the same trends as the experiments.

Distribution of the Inside Wall Heat Flux

As shown in Figure 25, the metal tube wall provides heat to the computation domain by passing D. C. current through it, which serves as a surface source at the interface of the near-boundary control volume. If temperature of the tube wall were uniform circumferentially and the material of the tube wall were homogeneous, the electric current would produce a peripherally uniform heat flux. However, buoyancy-induced secondary flow results in peripheral wall temperature variation, which affects considerably the distribution of the heat flux at the inside tube wall. For instance, if the temperature at the top of the tube is higher than that at the bottom, (during heating), part of the heat produced within the top region of the tube wall would not go directly into the fluid at the top location, but instead it would go towards the bottom region of the tube wall by peripheral wall conduction driven

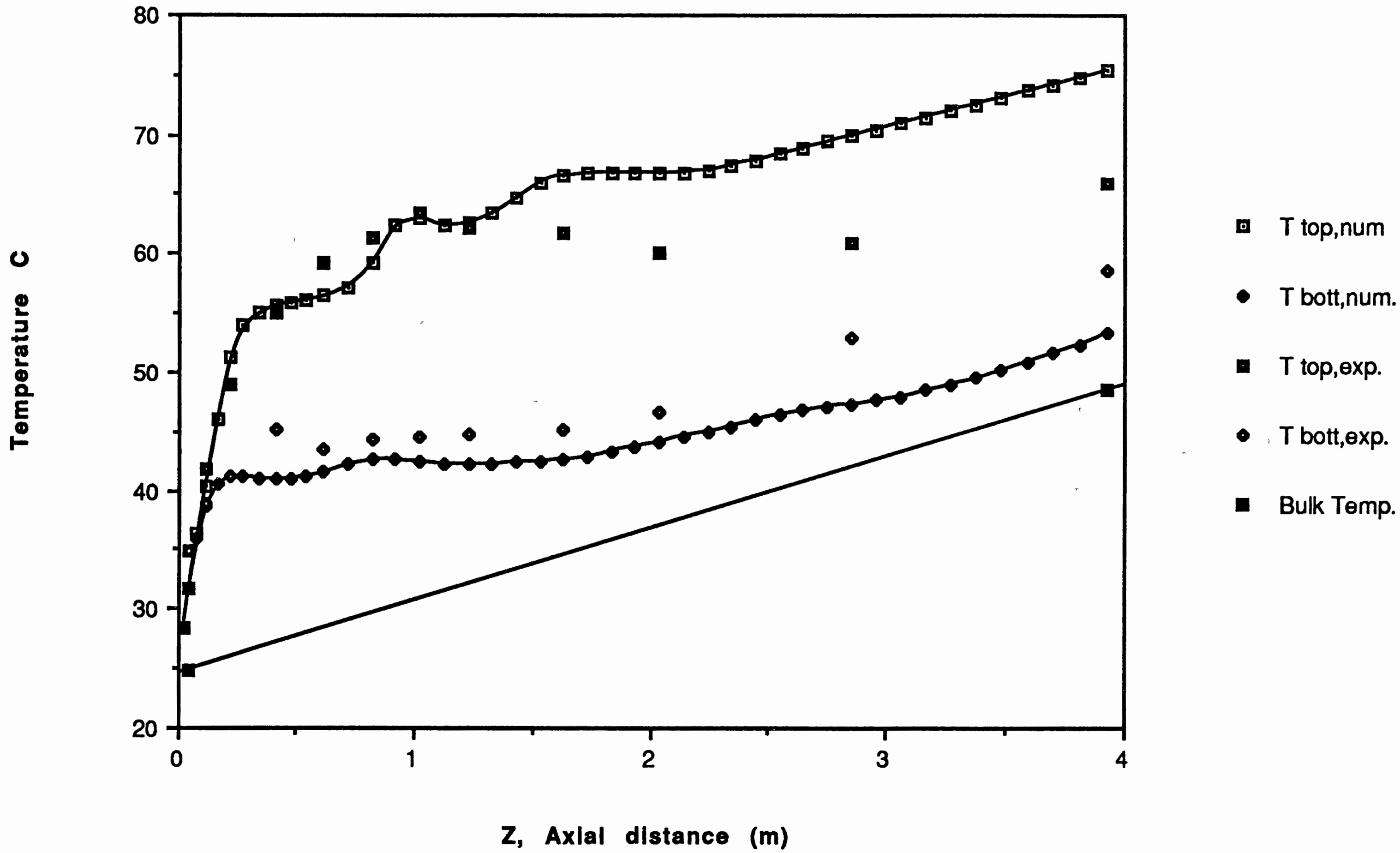

Figure 26. Peripheral wall temperature variation (Run#1103)
[Re: 2470-3940, Gr: 131000-747000, Pr: 6.2-3.7]

by the circumferential temperature gradient. This portion of the heat produced at the top of the tube would finally transfer into the fluid near the bottom of the tube. As a consequence, a peripherally nonuniform heat flux distribution results. Therefore, the term "nominally uniform heat flux" has been employed in this thesis.

From the measured outside wall temperature, Chen (1988) calculated the inside wall temperature and the inside wall heat flux using a two-dimensional relaxation method. The method accounted for the peripheral and radial wall conduction, while neglecting axial conduction. His results demonstrated a considerable nonuniformity of the wall heat flux. For example, for Run #2137, the computed heat flux at the bottom of the tube is as as high as 11,865 W/m^2, while at the top of the tube, the heat flux is as low as 7,043 W/m^2.

With linearly interpolating Chen's heat flux data, computations for Runs #2121 and #2137 were conducted using variable heat flux. Figures 27 and 28 give the results. The better agreement between computations and experiments revealed the importance of the wall peripheral conduction.

Effect of Secondary Flow on Axial Velocity Profile

For pure forced convection, the axial velocity profiles are symmetric about the axis of the tube. With the addition of buoyancy induced secondary flow, the symmetric velocity

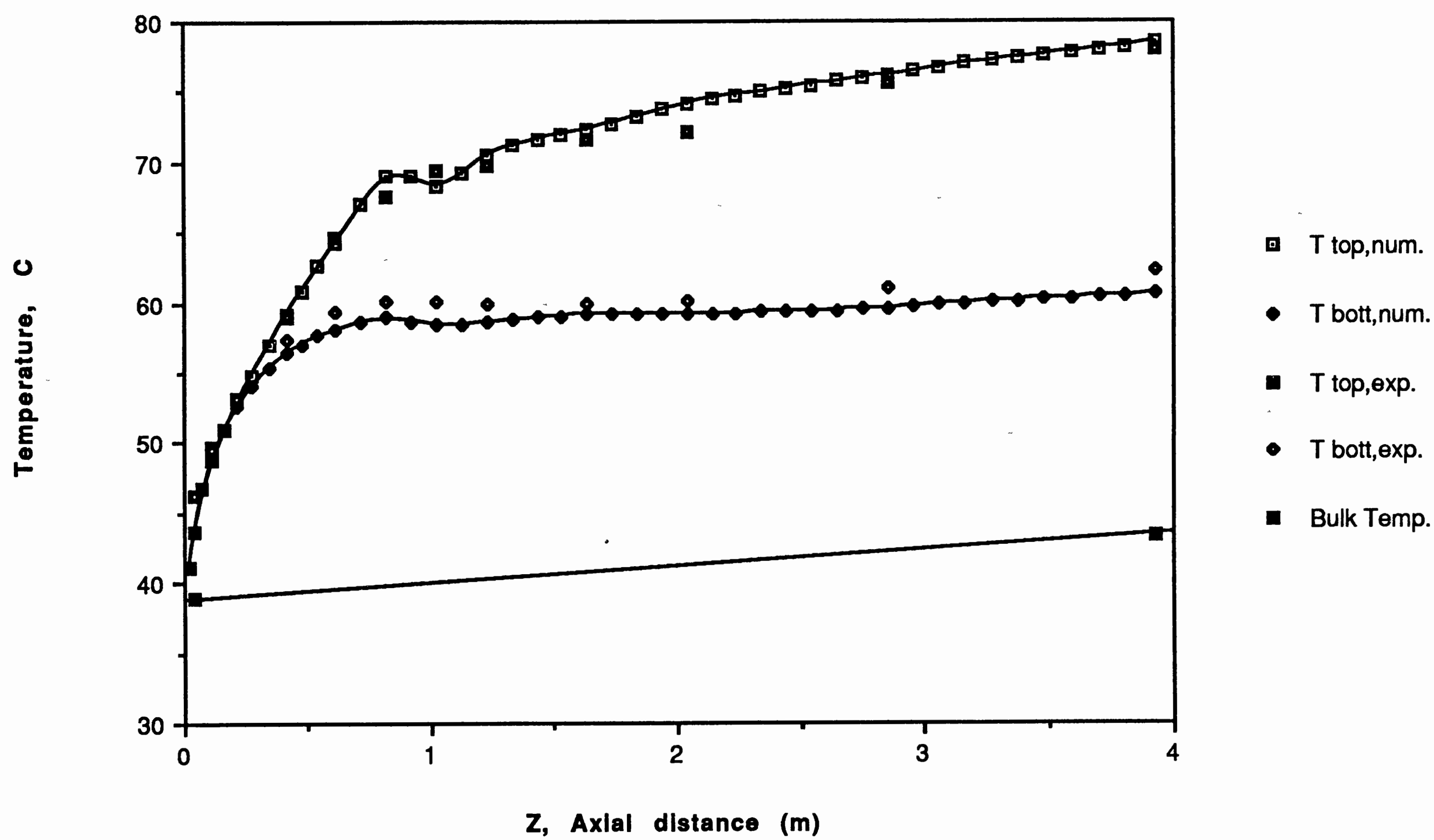

Figure 27. Peripheral wall temperature variation

with variable heat flux (Run#2121)

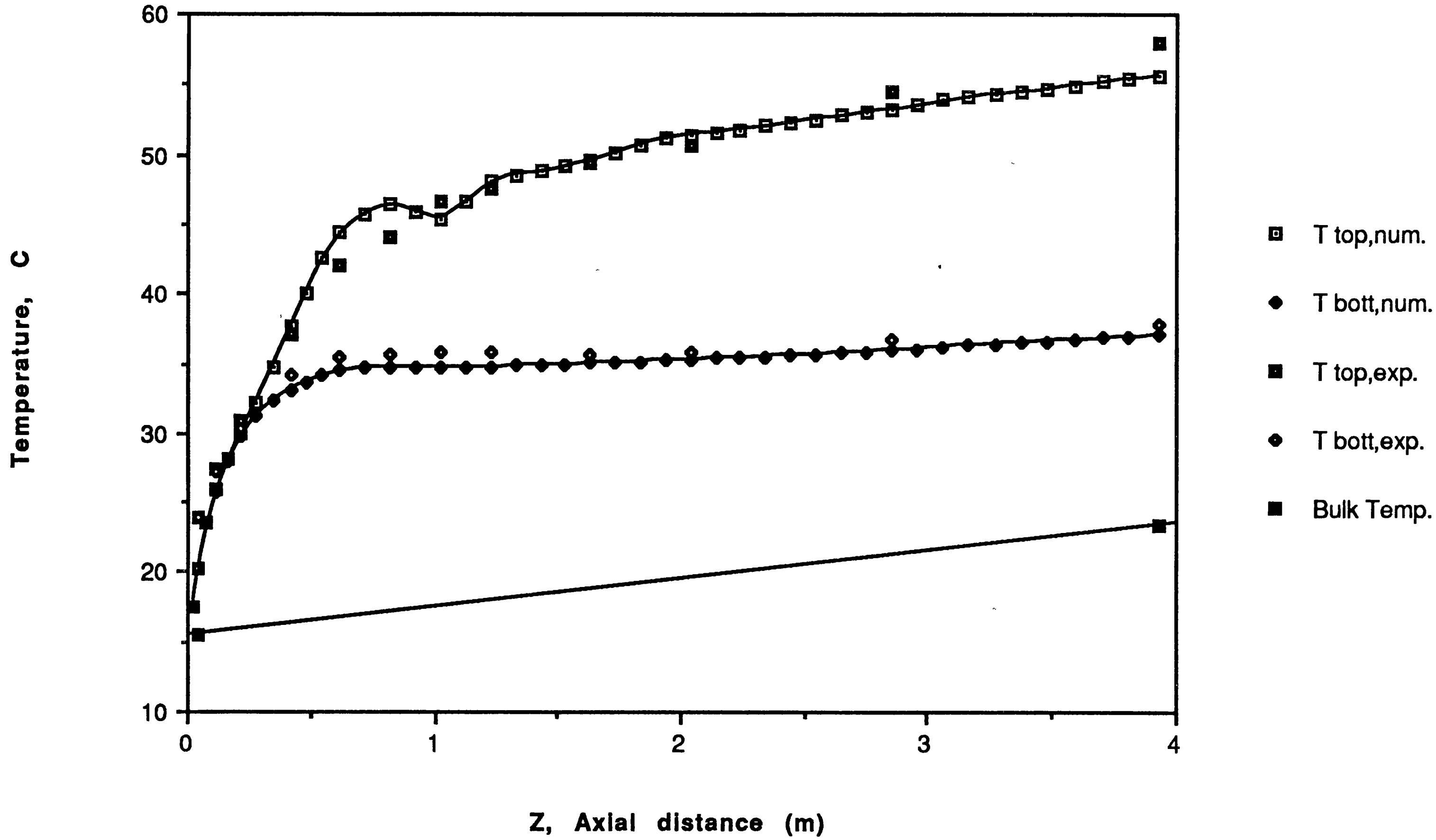

Figure 28. Peripheral wall temperature variation
with variable heat flux (Run#2137)

profile is still retained in the horizontal central plane ($\theta=\pi/2$). However, this symmetry is lost along the vertical central plane ($\theta=0$ and $\theta=\pi$). Figures 29 to 31 illustrate the developing profiles of dimensionless axial velocity w/w_b along the vertical central plane for the typical runs. For each run, profiles at four axial locations: z=0.114m, z=0.418m, z=1.634m, and z=3.926m (the end of the testing tube), were plotted.

Figure 29 shows profiles for Run#2137, near the entrance (z=0.114m), the velocity profile is nearly uniform over the cross section. But further downstream, the curves are distorted due to buoyancy effects. The distortion for this run is displacement of maximum velocity from the central axis towards the bottom wall of the tube. This feature is consistent with those reported by Hishida et al. (1982) for Pr=0.7, and Choudhury and Patankar (1988) for Pr=0.72. However, both of those works are for isothermally heated horizontal tubes in which effect of free convection reaches a peak along the length of the tube, then decreases gradually with the decrease of temperature difference between the wall and bulk flow, and finally vanishes far downstream; therefore, a fully developed parabolic profile for Poiseuille flow is eventually attained. For UHF condition, the temperature difference always exists, and as a result, secondary flow would not vanish downstream. Figures 29 to 31 support this assertion.

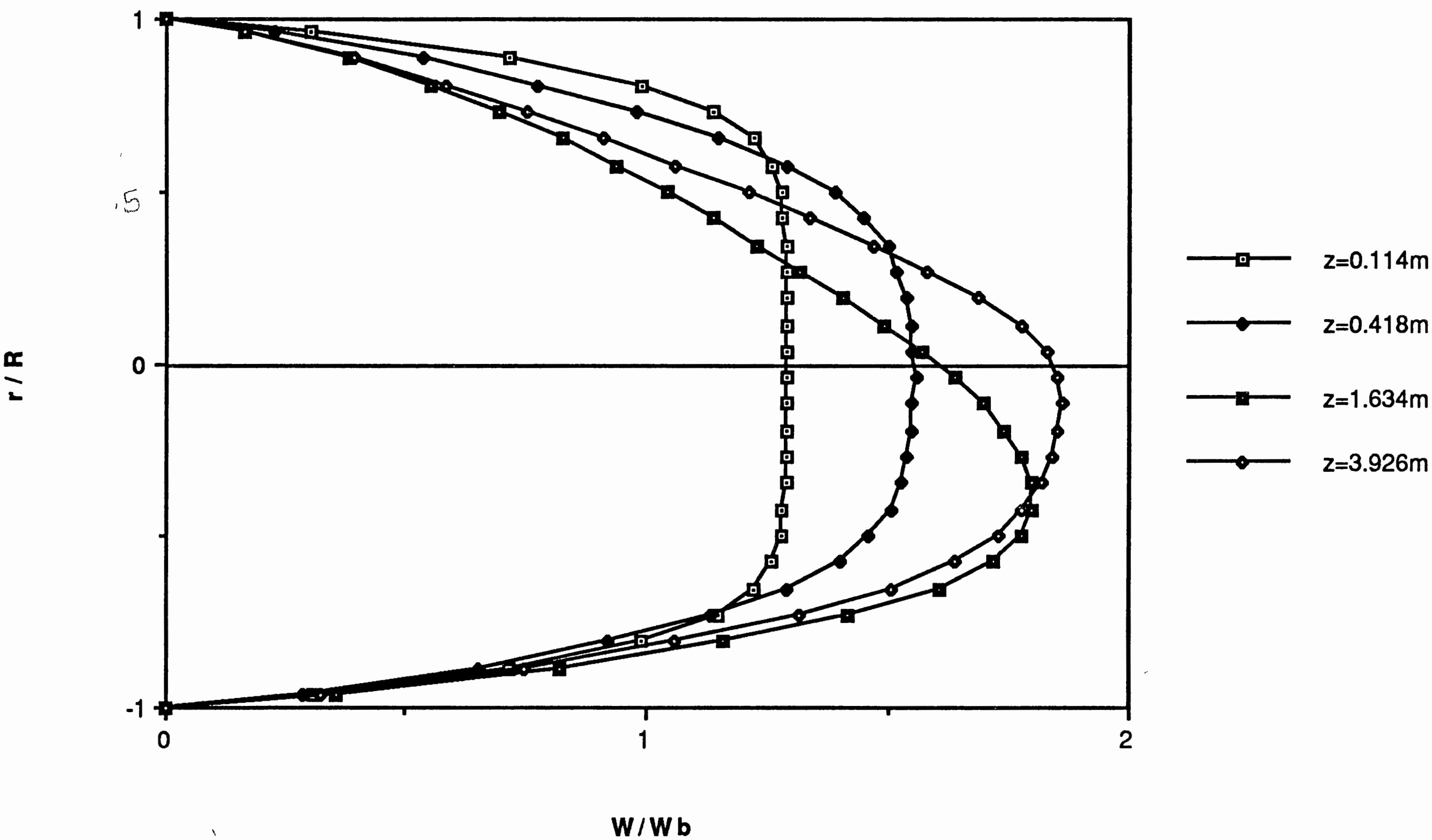

Figure 29. Axial velocity profiles (Run#2137)

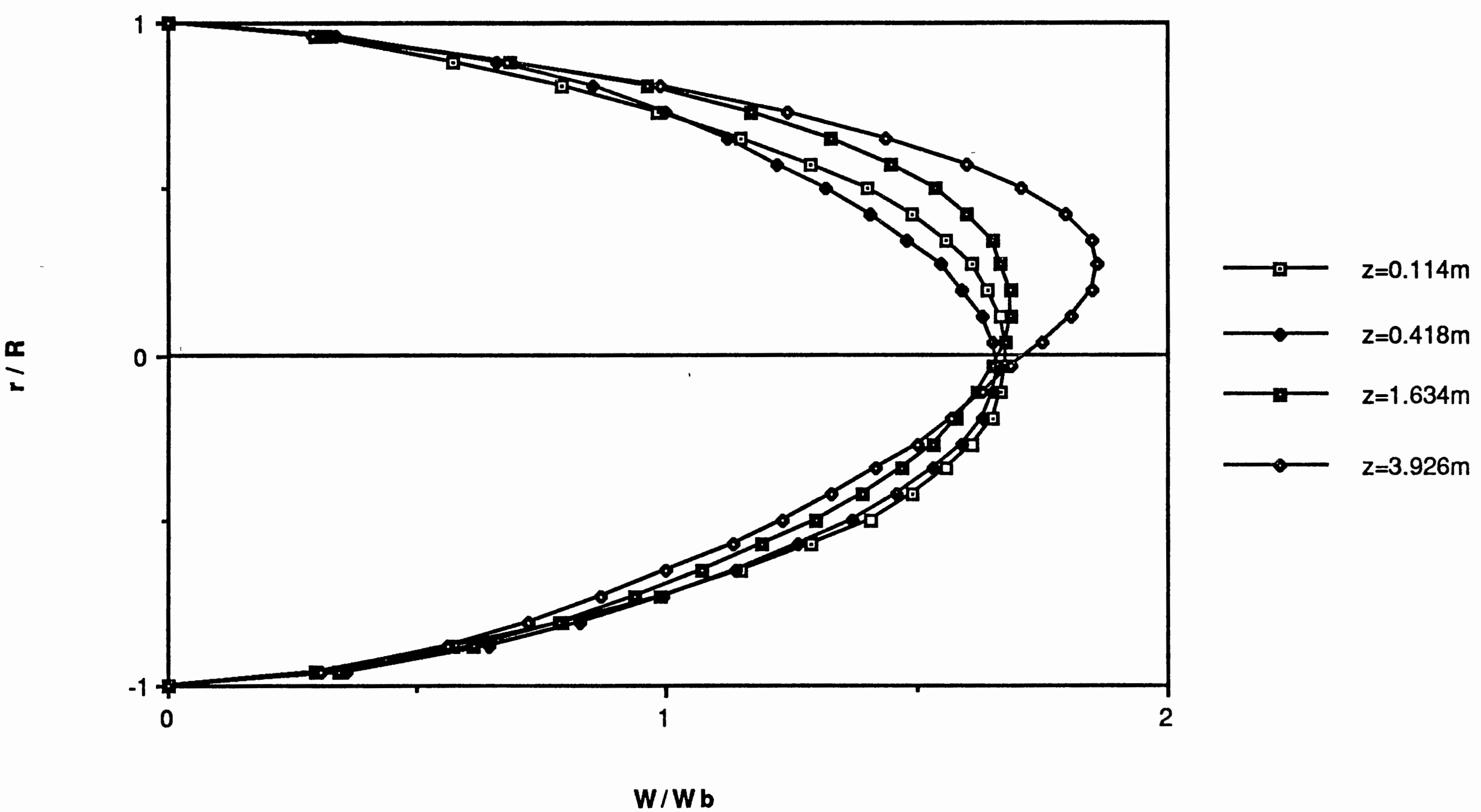

Figure 30. Axial velocity profiles (Run#2107)

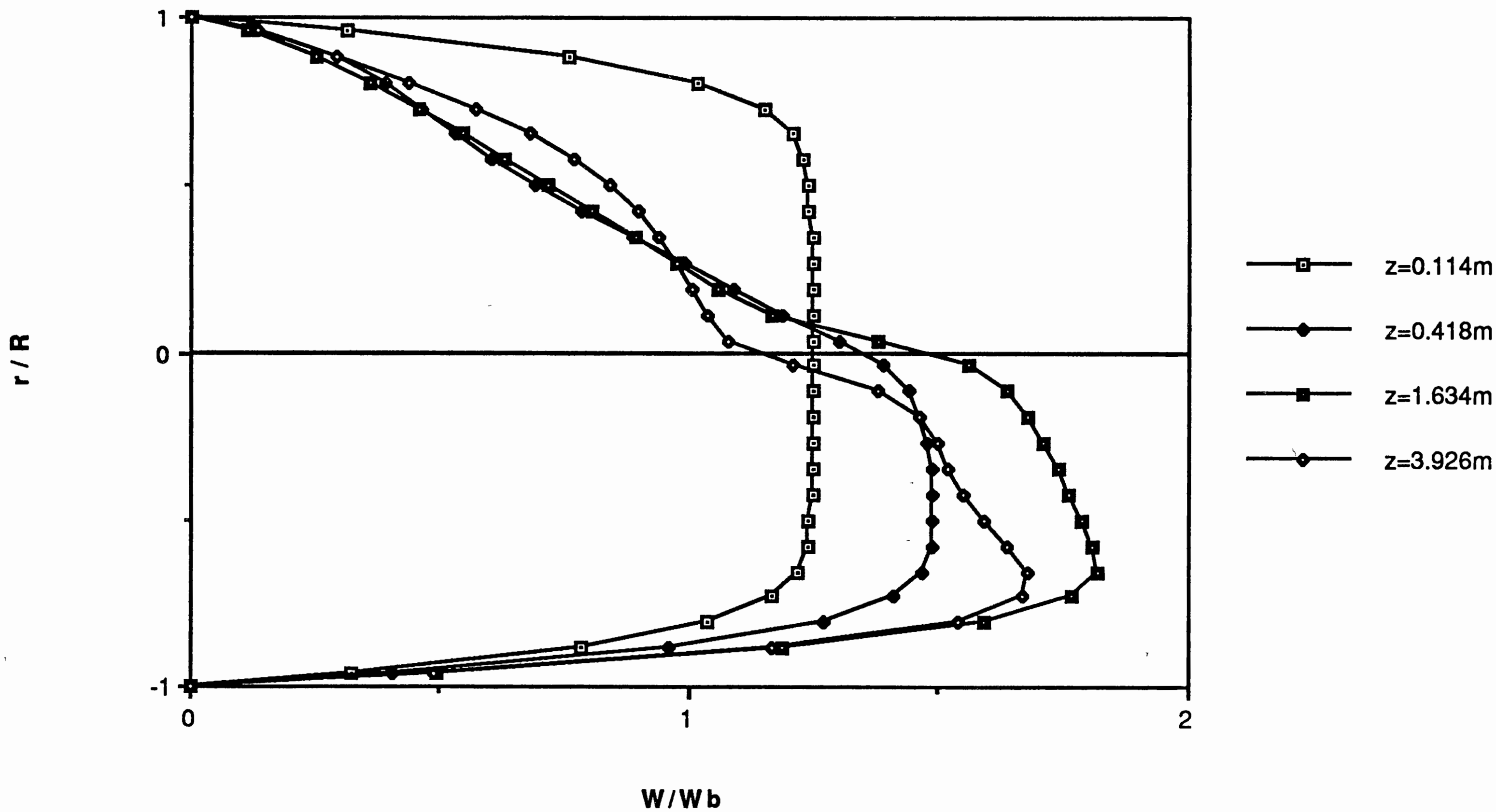

Figure 31. Axial velocity profiles (Run#1103)

For Run#2107, Figure 30 demonstrates an opposite tendency to Run#2137 (Figure 29). The maximum shifts towards the top wall of the tube and the curves reveal considerable asymmetry. This kind of velocity profile agrees with Palen and Taborek's prediction (1985). It results mainly from the highly temperature-dependent viscosity of the fluid. Figure 32 is a viscosity chart for diethylene glycol-water mixtures from Obermeier et al. (1985). From this chart, one can see that viscosity of 100% DEG (close to the fluid in Run#2107) is much more sensitive to temperature than that of 25% mixture (close to Run#2137).

Therefore, it can be explained that, for Run#2107, the high temperature sensitivity of the fluid dominates the flow process. Because temperature of the fluid near the top of the tube is higher than that near the bottom of the tube, viscosity of the fluid near the top is lower, hence the maximum velocity would shift towards the top of the tube. For Run#2137, the small temperature-dependence of viscosity is overweighed by the buoyancy effect, and therefore the maximum shifts towards the bottom of the tube.

Considering Run#1103 is in the transition region, the unusual velocity profile curves at downstream locations shown in Figure 31 are not surprising.

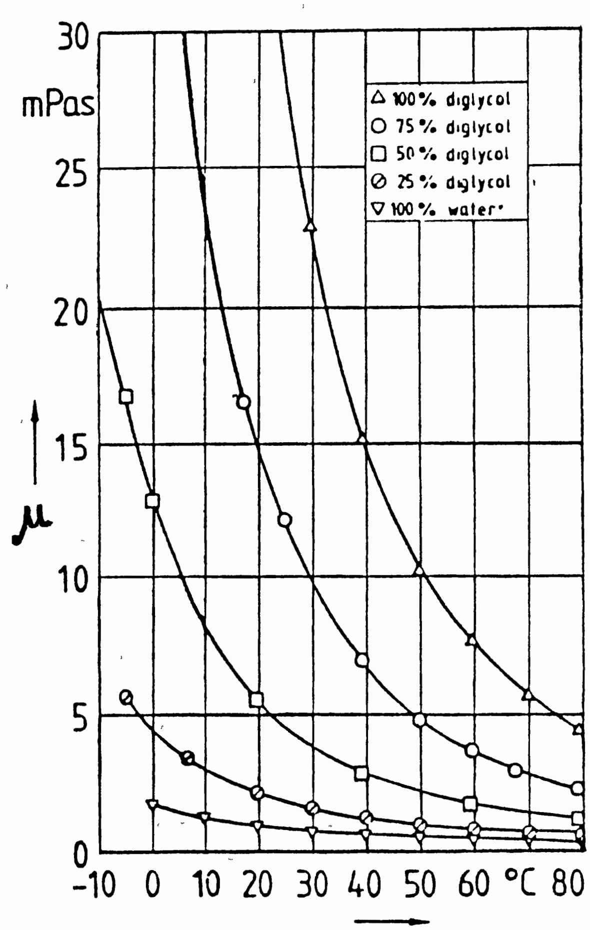

Figure 32. Viscosity of diethylene glycol-water mixtures (Obermeier et al., 1985)

About Fully Developed Flow

Shah and London (1978) defined so-called hydrodynamically fully developed flow as "when the fluid velocity distribution at a cross section is of an invariant form, i.e., independent of the axial distance x, i. e., $w = w(r,\theta)$ only and $u, v = 0$".

Kays and Crawford (1980) described fully developed flow as the boundary layer meeting itself at the tube centerline, and the velocity distribution establishing a fixed pattern that was invariant thereafter. They emphasized their assumption for the discussion that the fluid properties, including density, were not changing along the length of the tube.

It is apparent that neither of the definitions can be applicable to the current situation of mixed convection in which secondary flow, i.e., velocities normal to the duct axis, and property variation play very important roles. Therefore, it is suggested that the argument of "fully developed flow" with mixed convection in horizontal tube is not a valid concept, at least not in the simple terms used for the constant property case.

As mentioned in the Literature Survey, however, most researchers used the concept of fully developed flow while dealing with mixed convection, but they relaxed the academic definitions cited above by focusing only on the "invariant velocity profile" and neglecting other restraints. Hishida et al., and Choudhury and Patankar, indeed, found fully developed velocity profiles by the relaxed definition for isothermally heated tubes.

Even comparing the relaxed definition with the presented figures, one can not find an invariant velocity profile within the tube length (4m) of the present study. As a result, it may be doubted that there exists fully developed flow inside the horizontal tubes of a typical size of shell-and-tube heat exchanger if laminar mixed convection exists.

Effect of Secondary Flow on Heat Transfer

With neglecting secondary flow and employing constant properties and nominal uniform heat flux for Run #2137, Figure 33 illustrates the computed profiles of the inside tube wall temperature and bulk temperature versus the axial distance of the tube. In order to evaluate the effect resulted from the assumption of fully developed velocity profile at the inlet of the tube (used in most literature), a wall temperature curve, computed on condition of fully developed velocity profile and developing temperature profile (so-called Graetz-Nusselt problem), is also depicted on the figure. The significant influence of this assumption on heat transfer can be understood clearly. It can be seen that at the outlet of the tube, the temperature difference

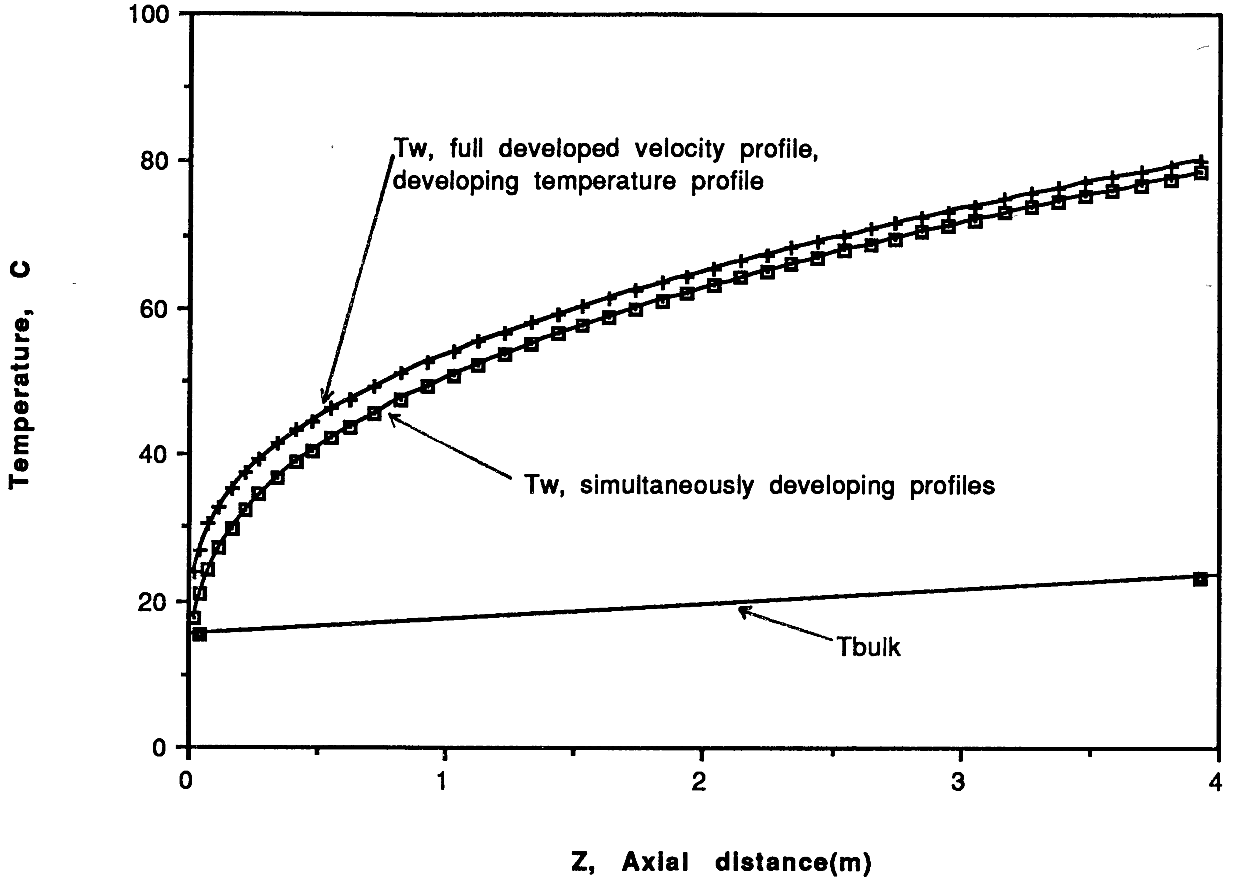

Re: 1770-2280
Gr: 14100-67300
Pr: 26-20

Figure 33. Variation of wall temperature for pure forced convection (Run#2137)

has not reached a constant, which means the temperature profile is still developing at that location. The result agrees with the traditional pure forced convection prediction of Kays and Crawford (1980).

However, with considering the buoyancy induced secondary flow for the same run, Run #2137, the profile of the average inside wall temperature shows considerable difference from the traditional prediction (Figure 34).

Comparing Figure 34 with Figure 33 suggests that the effect of the buoyancy-induced secondary flow is so strong that it reduces the effect of the thermal entrance length predicted by the standard pure forced convection method, to a great extent.

Figures 34 to 40 show the computed circumferential mean inside wall temperature using the nominally uniform heat flux, compared with experimental data which were obtained by simply taking arithmetic mean of the measured local data (4 or 8) around the circumference, for the computational runs. It can be seen that the entrance effect dominates for only a short length from the inlet; after that length, the secondary flow dominates for the rest of the tube.

For pure forced convection, after the thermal entrance length, the profile of the increasing wall temperature parallels the profile of the bulk temperature, so that a constant temperature difference between the two exists, and hence a fully developed temperature profile is obtained.

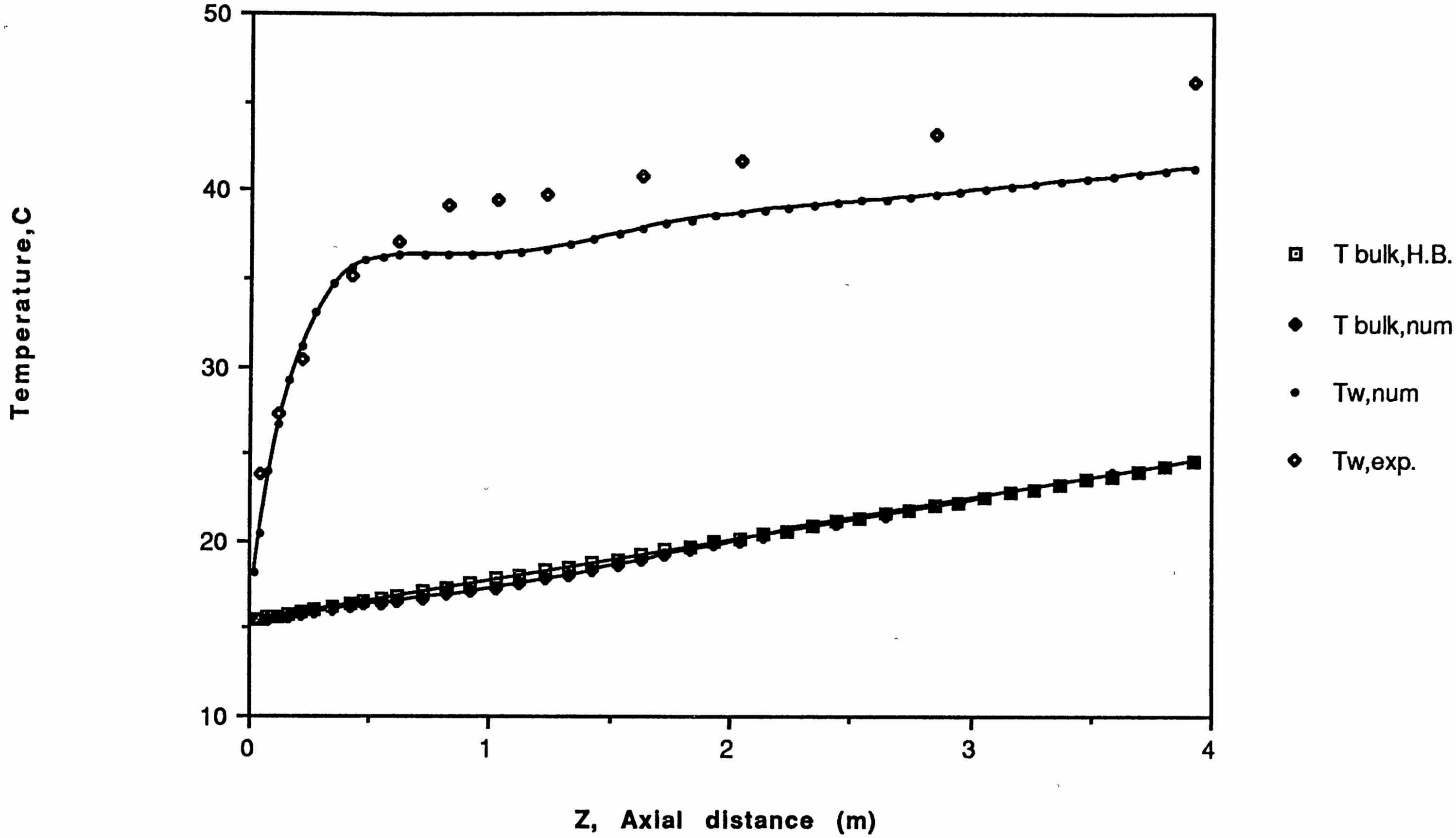

Figure 34. Variation of mean wall temperature and bulk temperature (Run#2137)

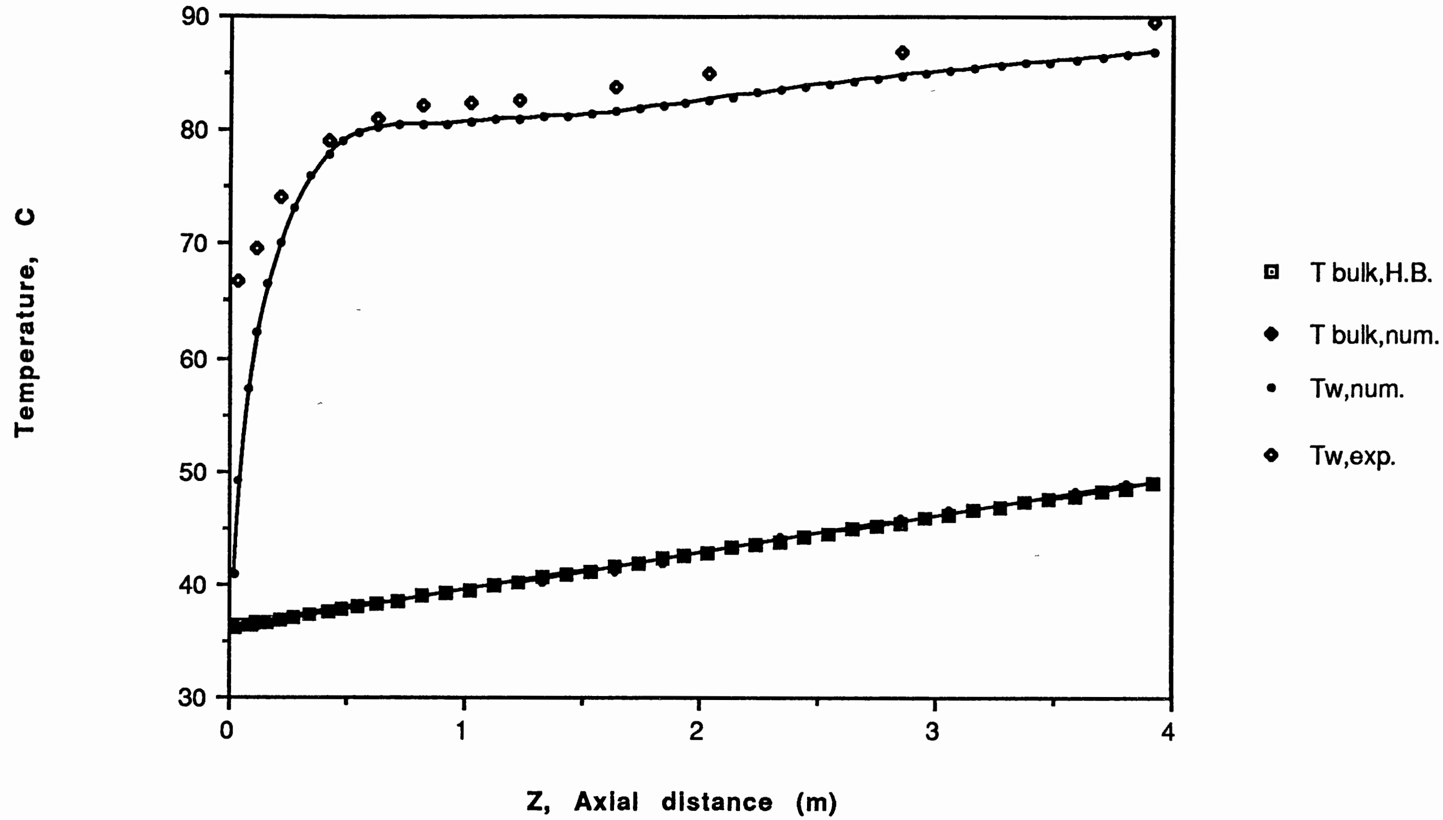

Figure 35. Variation of mean wall temperature and bulk temperature (Run#2105)

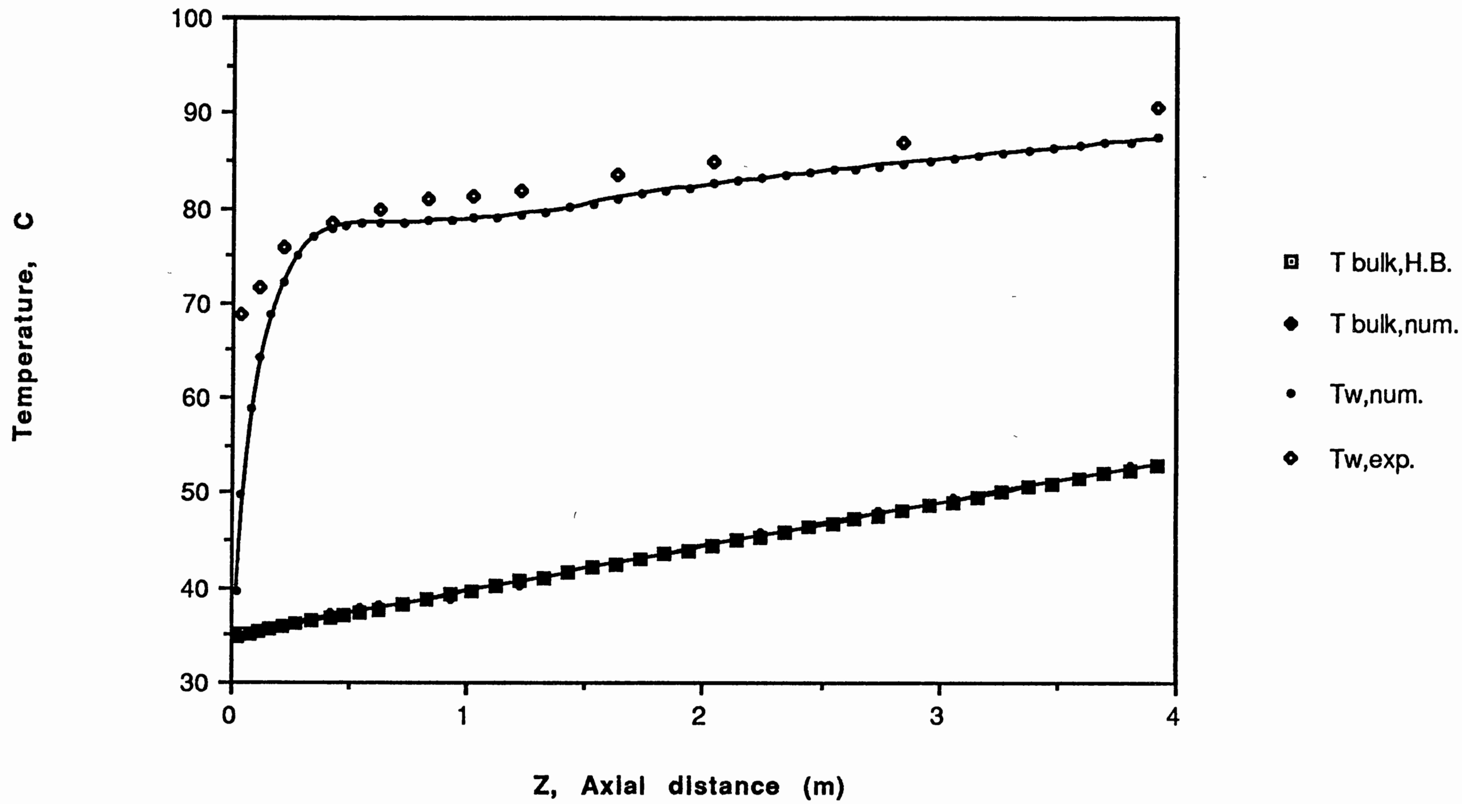

Figure 36. Variation of mean wall temperature and bulk temperature (Run#2107)

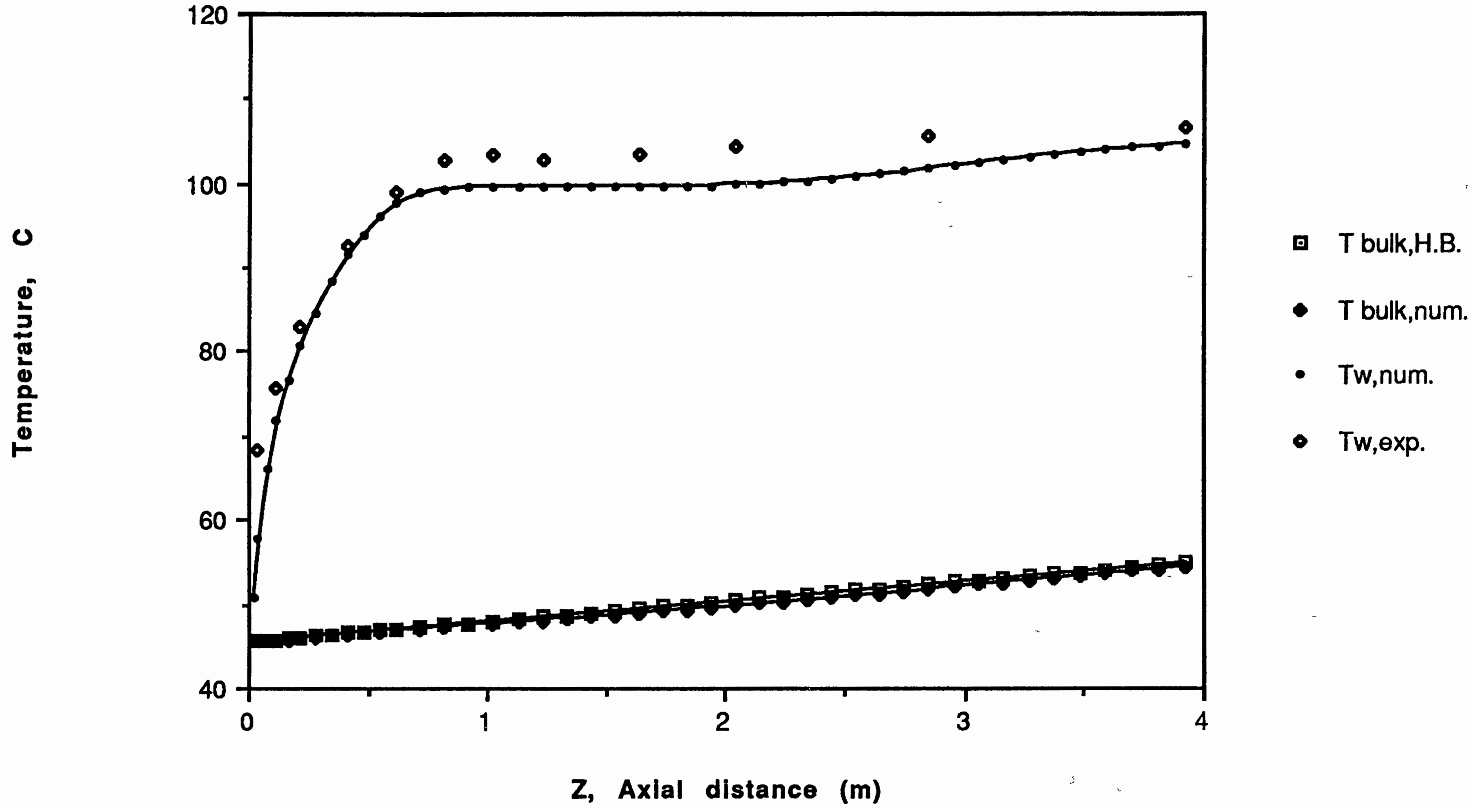

Figure 37. Variation of mean wall temperature
and bulk temperature (Run#2110)

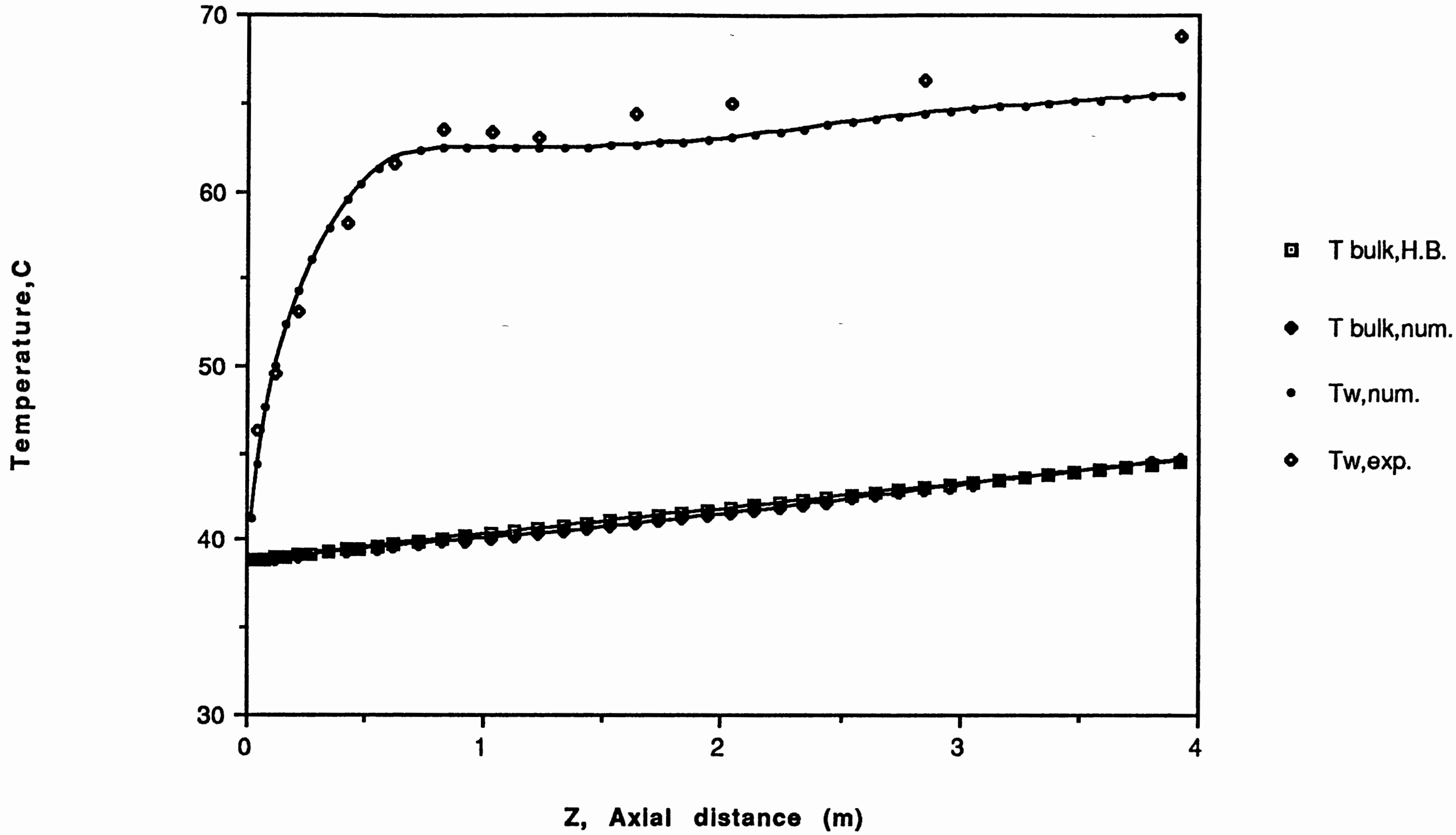

Figure 38. Variation of mean wall temperature and bulk temperature (Run#2121)

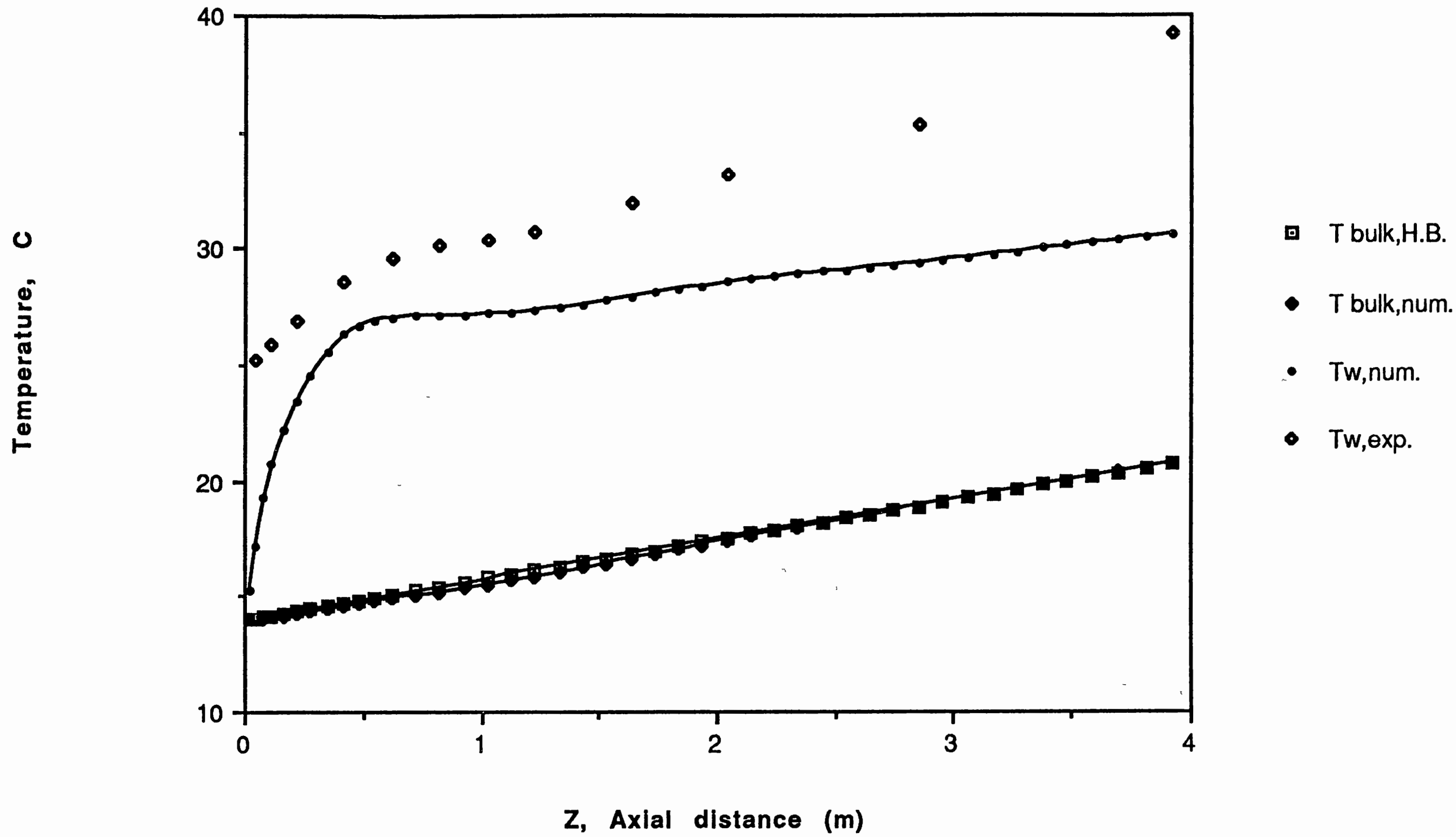

Figure 39. Variation of mean wall temperature and bulk temperature (Run#2135)

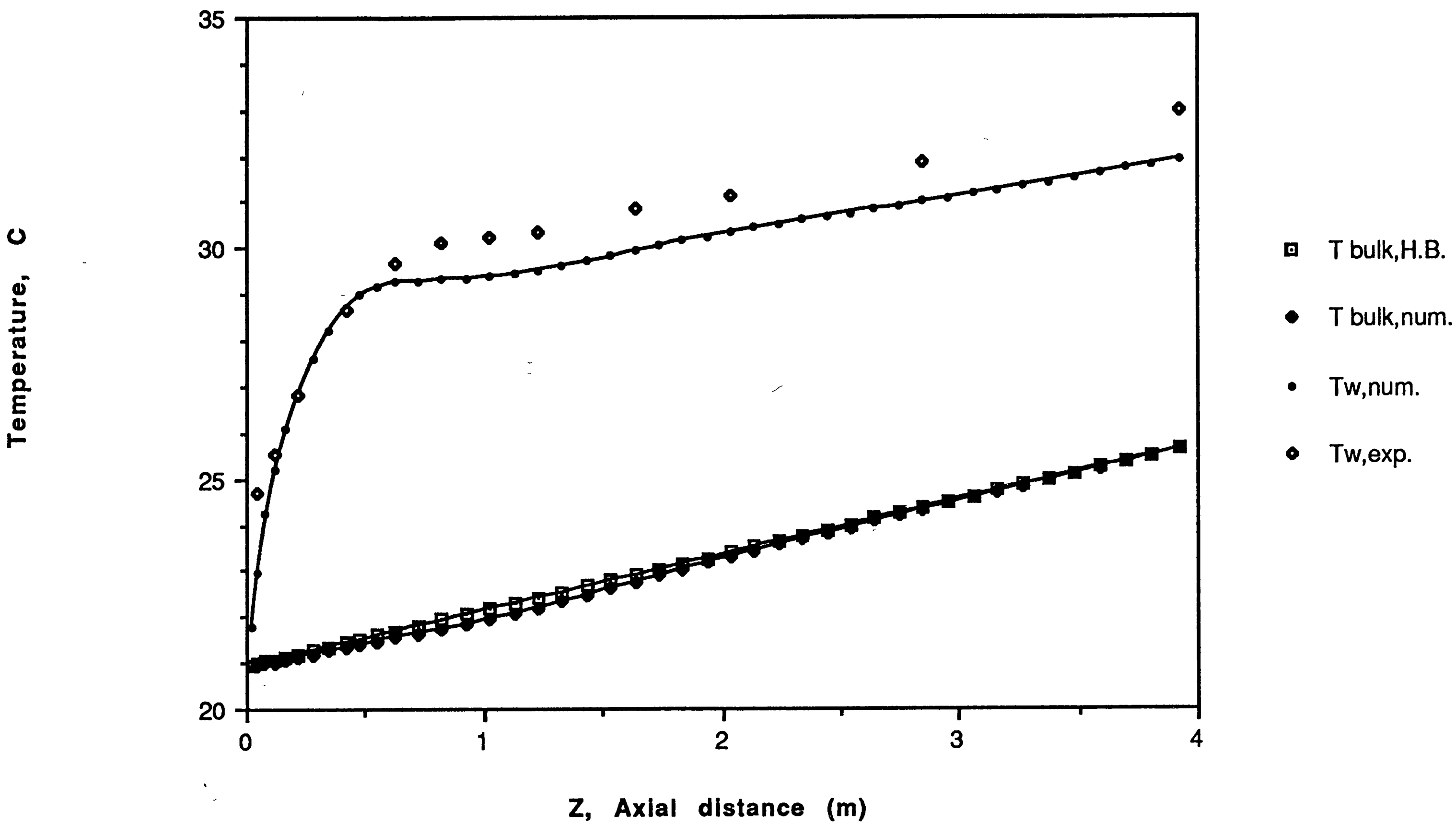

Figure 40. Variation of mean wall temperature and bulk temperature (Run#2139)

However, including the buoyancy effect changes the situation and the temperature difference between the wall and the bulk flow decreases monotonically, and therefore, a fully developed temperature profile cannot be found along the test tube.

This is because heat transfer is based on the flow field under the circumstance of the complex mixed convection. From the discussion in Section 4 of this chapter, it is realized that with mixed convection and nominally uniform heat flux, a fully developed velocity profile could not have been obtained for the runs currently considered; needless to say, a fully developed temperature profile can not be reached either.

Figures 41 to 47 shows the axial variation of the Nusselt number for the typical runs. The local peripheral average Nusselt number, Nu_z, is defined as

$$Nu_z = q''_w d_i / (k(T_{w,avg} - T_b)) \qquad (6-1)$$

where q''_w is the nominal uniform heat flux, d_i is the inside diameter of the tube, k is thermal conductivity of the fluid defined at the local bulk temperature and $T_{w,avg}$ is the peripheral mean inside wall temperature of the tube.

The local Nusselt numbers from Chen's work (1988) are also depicted on the figures. It can be seen that the difference between numerical results and experiments

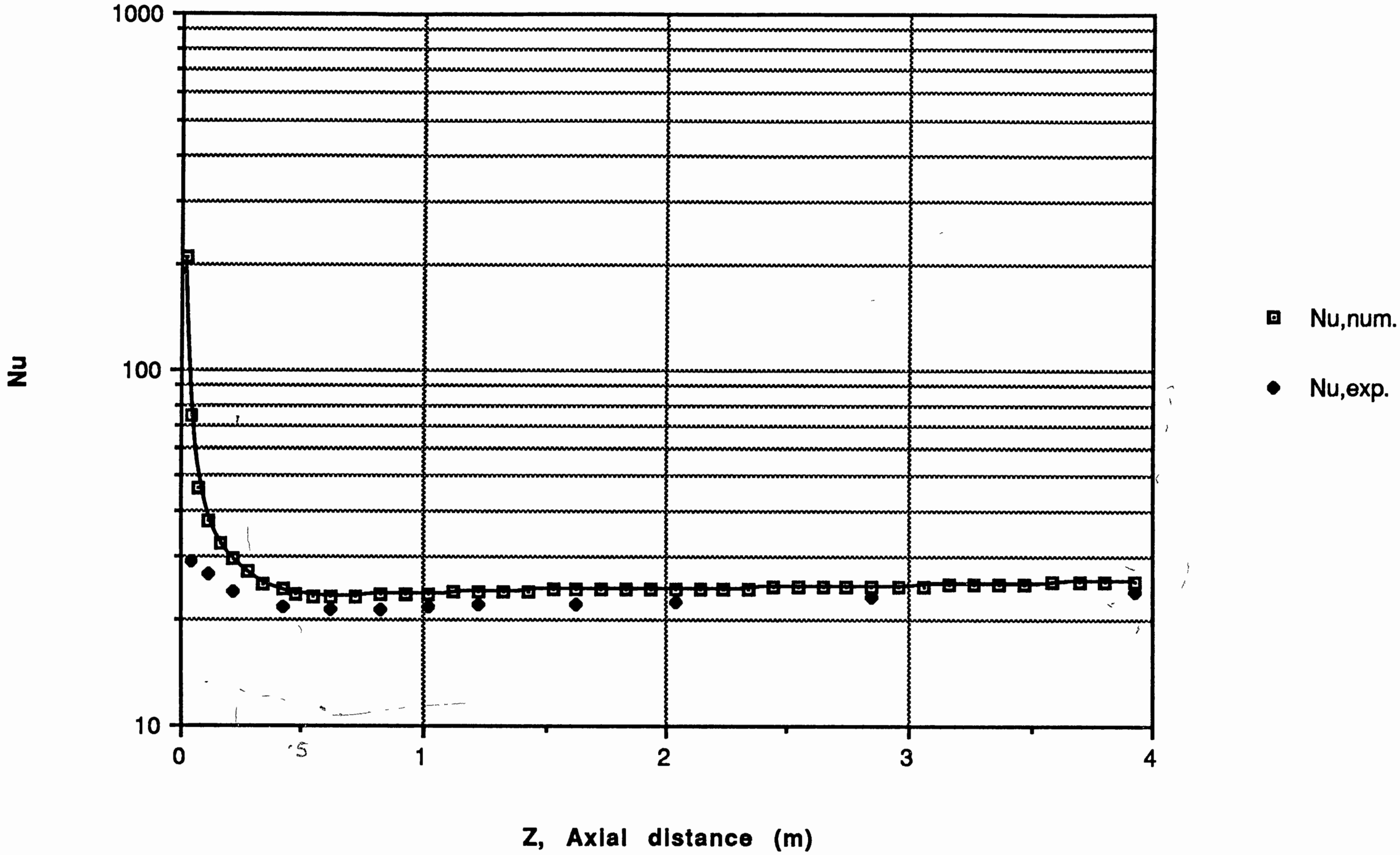

Figure 41. Variation of Nusselt number (Run#2105)
[Re: 354-585, Gr: 3480-12600. Pr: 209-128]

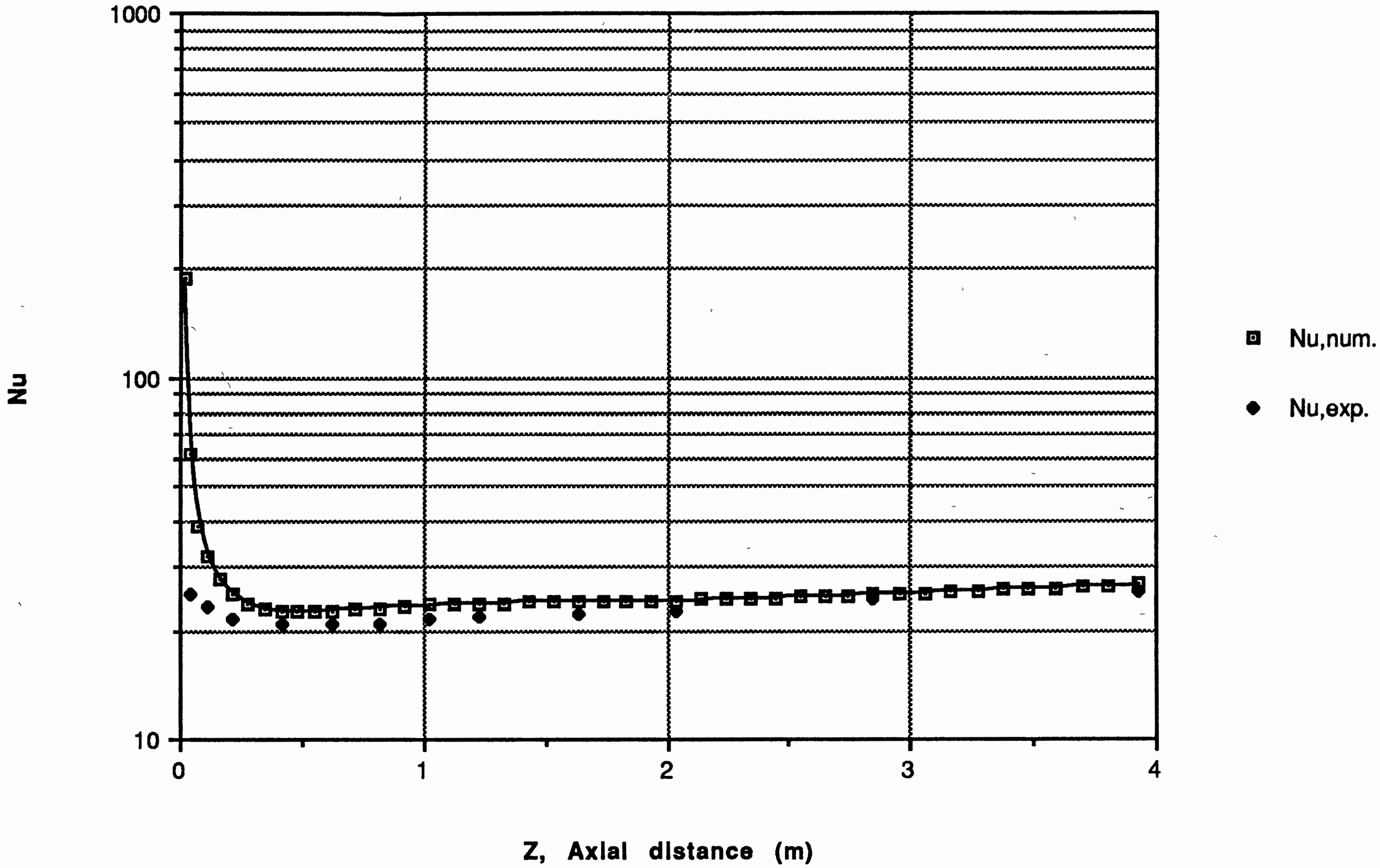

Figure 42. Variation of Nusselt number (Run#2107)
[Re: 222-452, Gr: 3450-15700, Pr: 221-111]

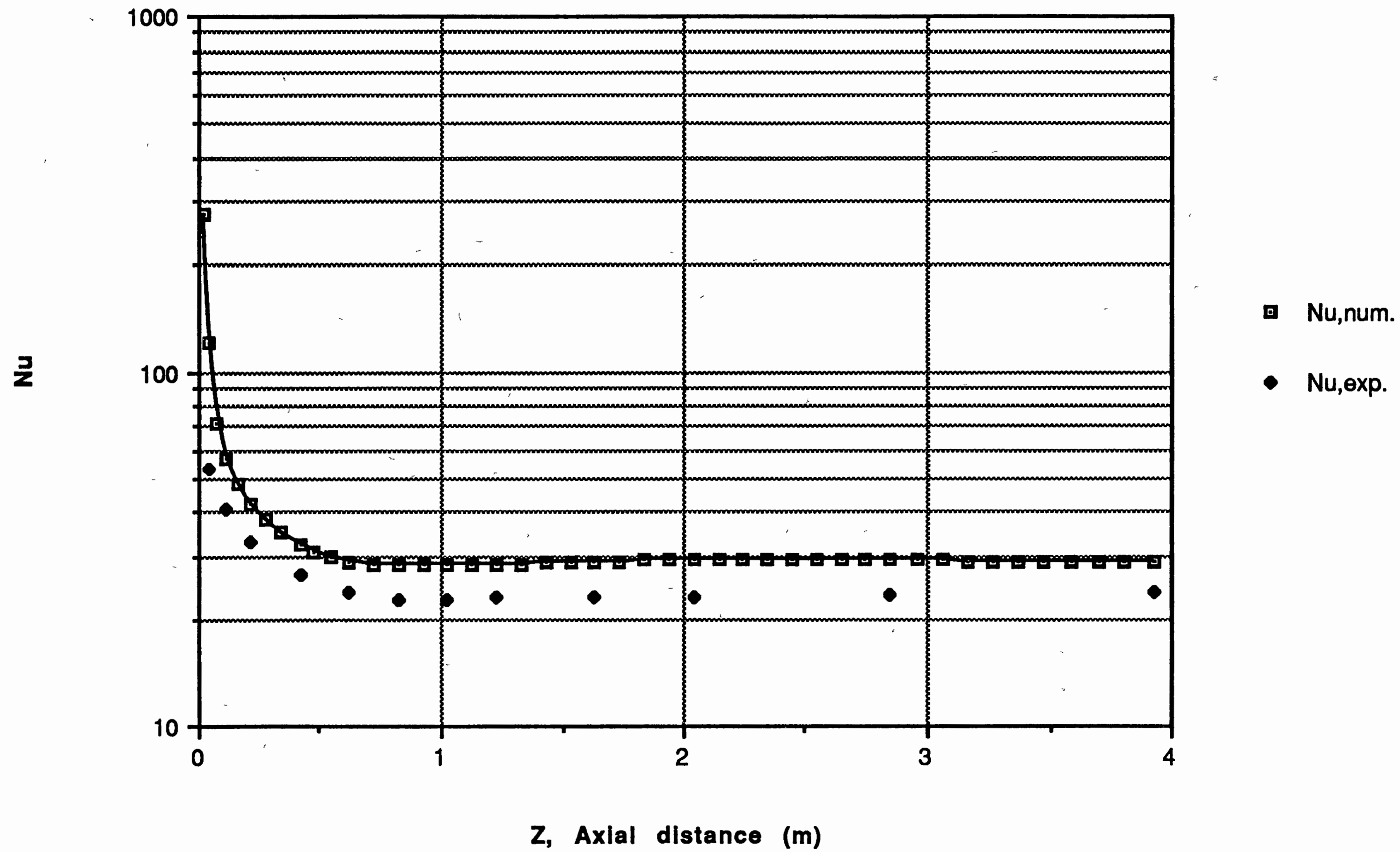

Figure 43. Variation of Nusselt number (Run#2110)
[Re: 1360-1810, Gr: 8840-34000, Pr: 116-88]

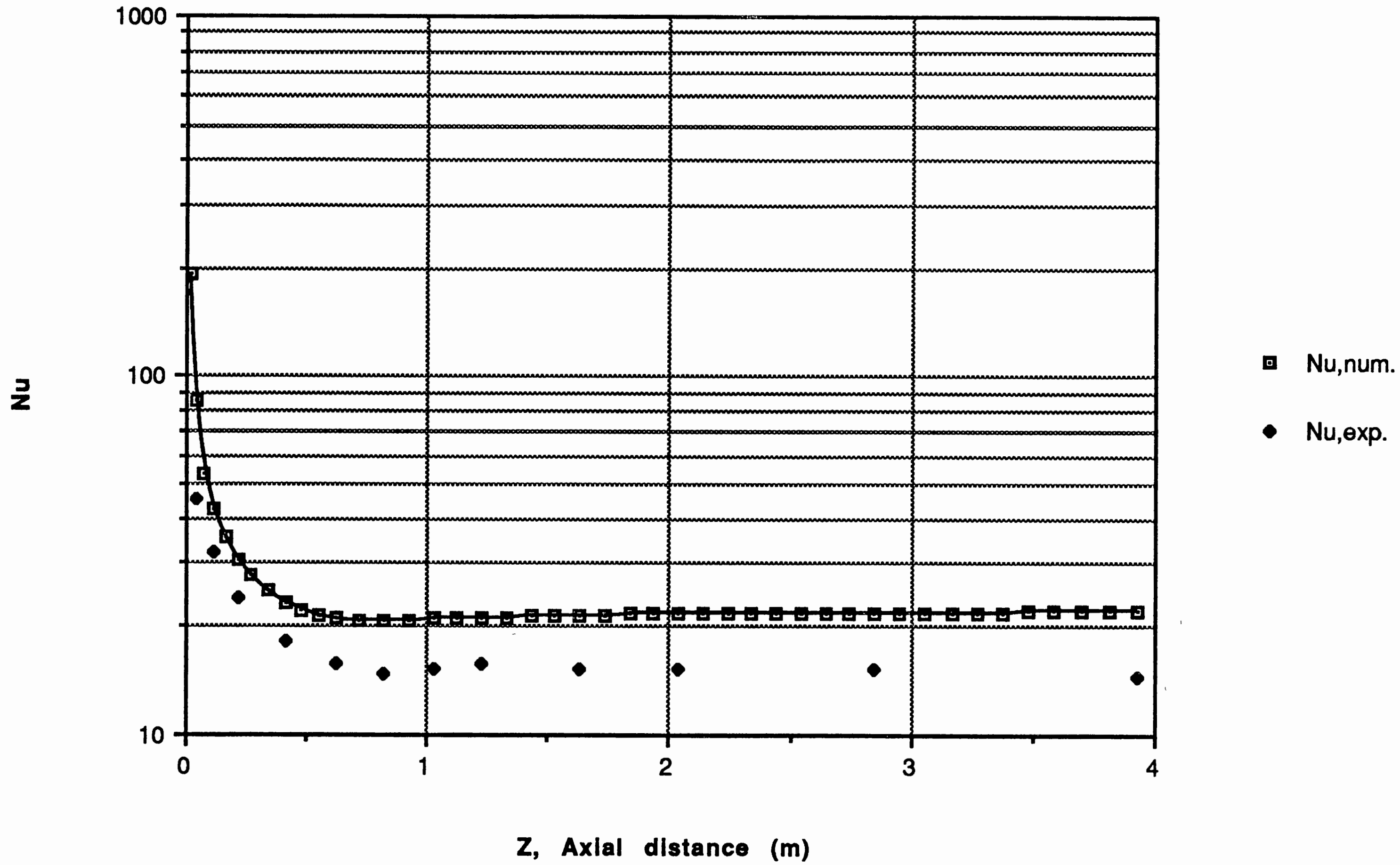

Figure 44. Variation of Nusselt number (Run#2121)
[Re; 1580-1830, Gr: 8580-39900, Pr: 53-46]

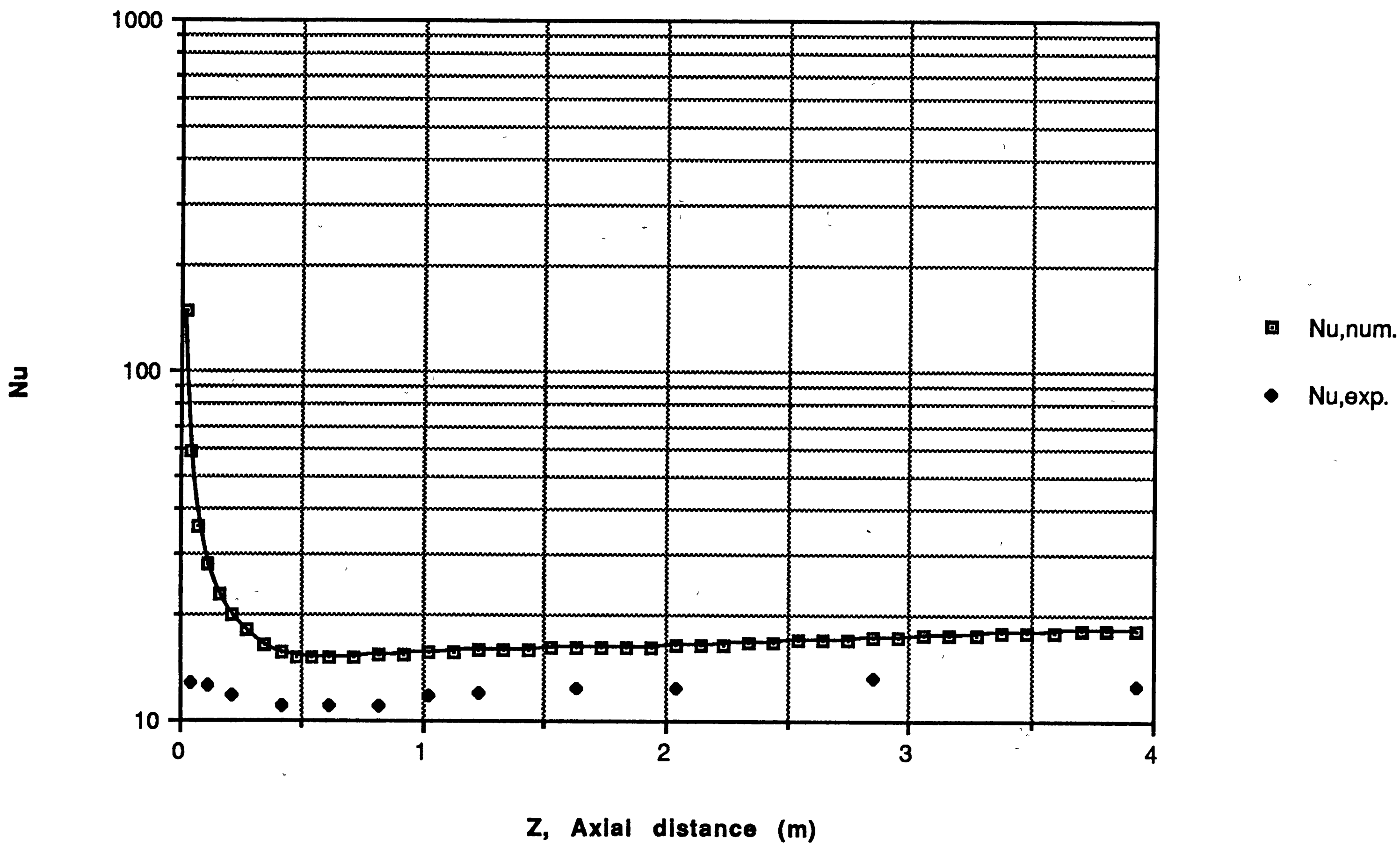

Figure 45. Variation of Nusselt number (Run#2135)
[Re: 514-749, Gr: 16800-47300, Pr: 28-19]

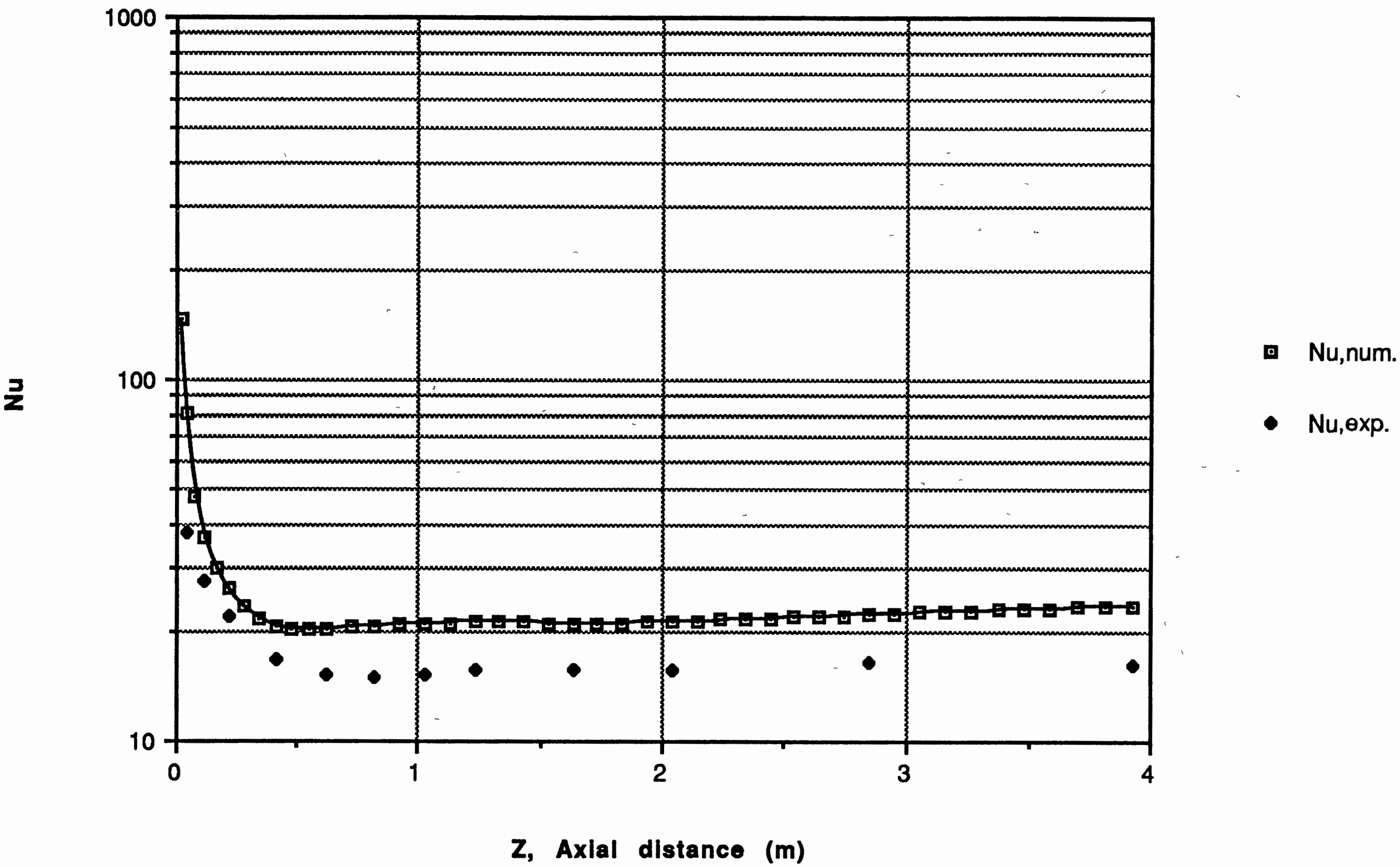

Figure 46. Variation of Nusselt number (Run#2137)
[Re:1770-2280, Gr:14100-67300, Pr: 26-20]

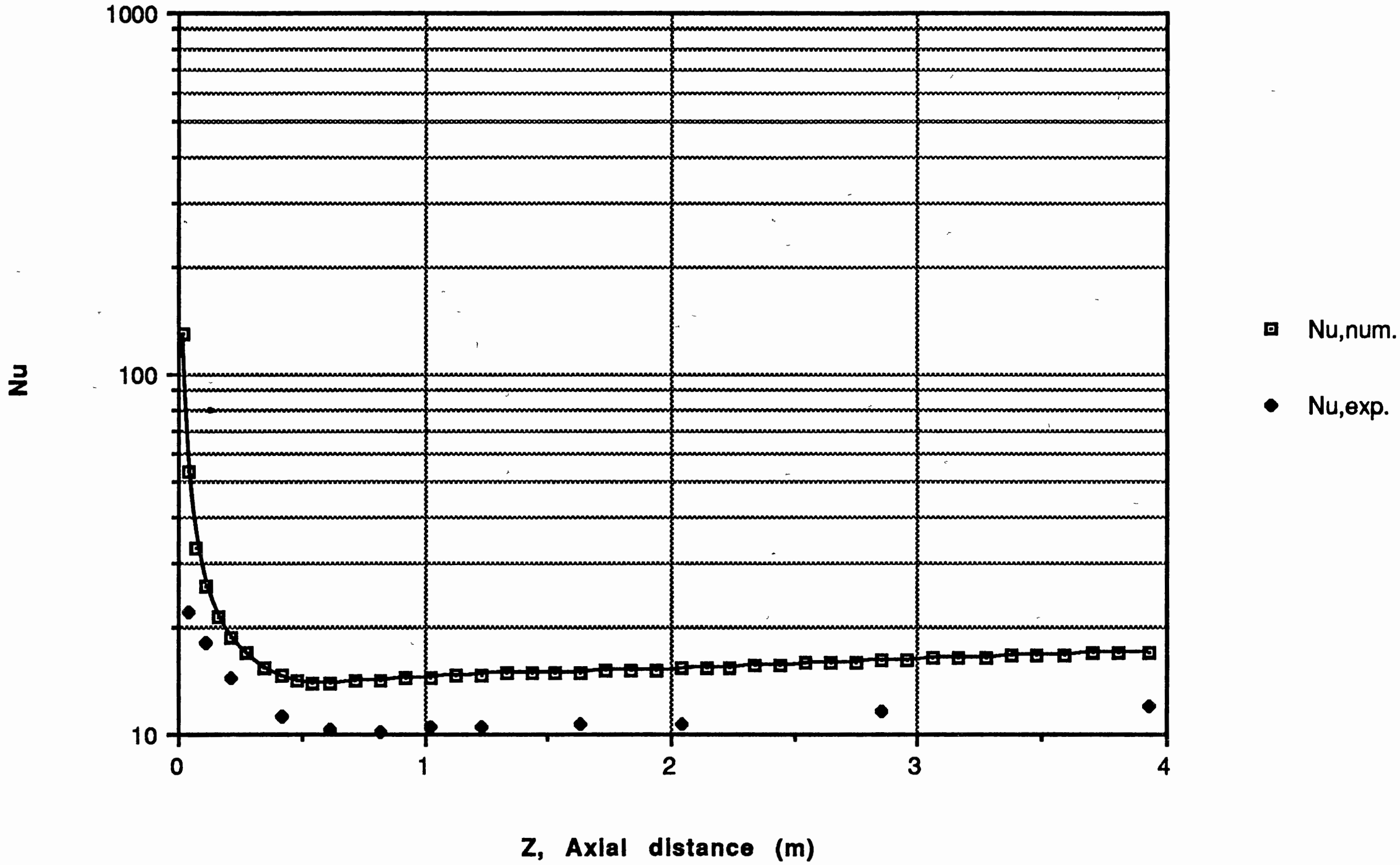

Figure 47. Variation of Nusselt number (Run#2139)
[Re: 1100-1250, Gr: 9280-26900, Pr: 22-19]

increases with increase of the Grashof number. The major reason for this may be that a larger Grashof number would bring about a stronger secondary flow, hence a considerable peripheral variation of wall heat flux, therefore, the assumption of uniform heat flux used in numerical solution (Equation 6-1) would have less reliability.

About the Local Bulk Mean Temperature

For heat transfer study, the local bulk mean temperature is a very important parameter, it indicates the heat absorbed by the fluid upto the axial location z where the bulk mean temperature is calculated. The bulk temperature can be obtained by the following integration over the cross section of the tube at a certain axial location z.

$$T_b = \iint wTr\,dr\,d\theta / \left(\iint wr\,dr\,d\theta\right) \tag{6-2}$$

where w and T are the computed local values.

On the other hand, for the case of heating with uniform heat flux, the local bulk temperature can be obtained by heat balance,

$$T_{b,HB} = T_{in} + \pi d_i q''_w z/(mc_p) \tag{6-3}$$

where q''_w is the nominal constant heat flux, and c_p is constant.

Figures 34 to 40 also show bulk temperature for the corresponding runs, using Equations (6-2) and (6-3), respectively. The basic agreement of the two methods supports the validity of the numerical method.

Axial Variation of Pressure Gradient

The local pressure gradient was determined by the pressure-velocity decoupling technique mentioned in Chapter IV. In order to compare with the pure forced convection situation, the pressure gradient may be expressed by the Fanning friction factor,

$$f = (-dp/dz)d_i/((1/2)\rho w_b^2) \qquad (6\text{-}4)$$

where w_b is the local mean velocity.

From the conventional prediction (Kays and Crawford, 1980), the product of f and Re is 64 for fully developed laminar flow. Figure 48 illustrates the variation of the product of f and Re with tube length for Run#2137, with considering only pure forced convection and constant properties. The agreement with the conventional prediction supports the validity of the analytical approach.

Considering the buoyancy effect and variable properties, Figure 49 presents the variation for the same run, Run#2137. And Figures 50 and 51 show results for

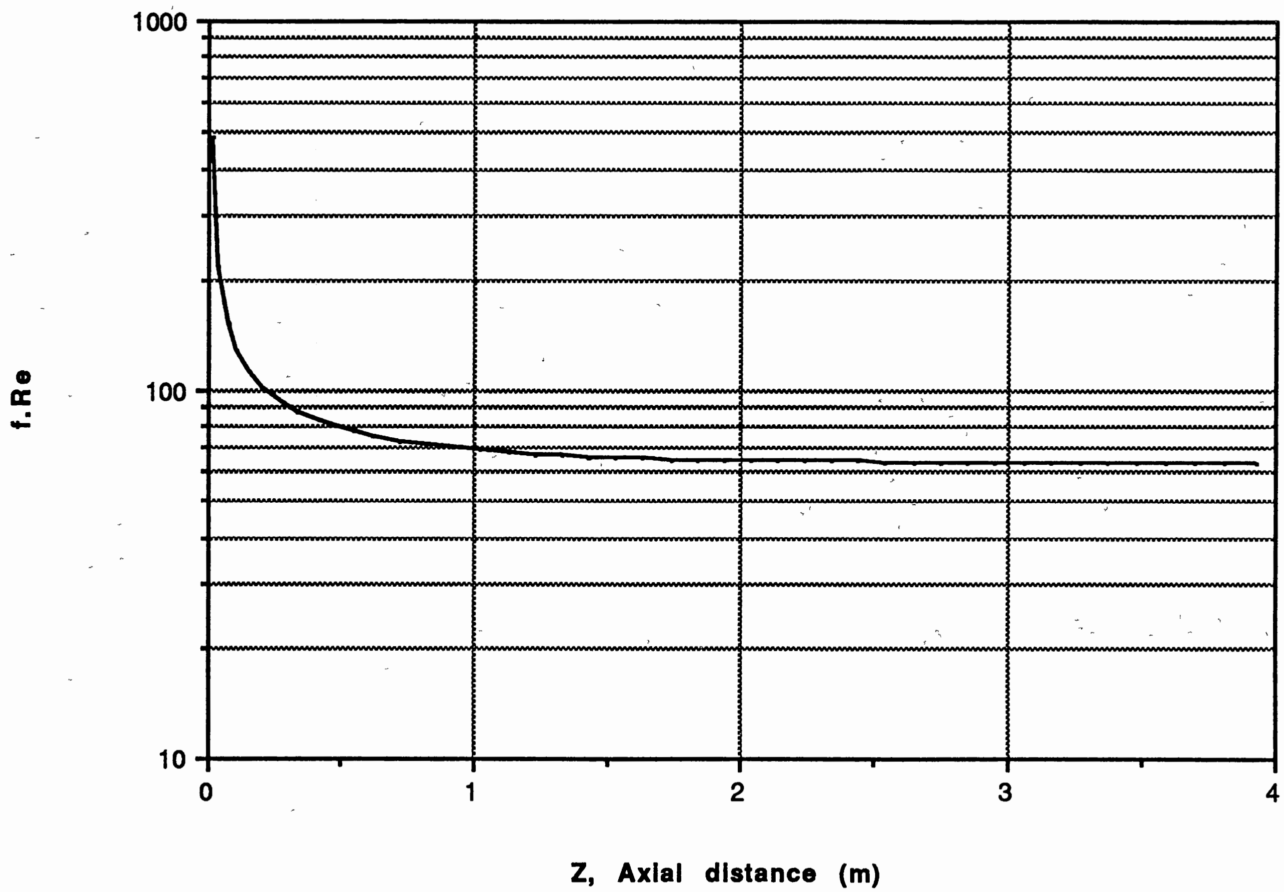

Figure 48. Variation of f.Re for pure forced
convection (Run#2137)

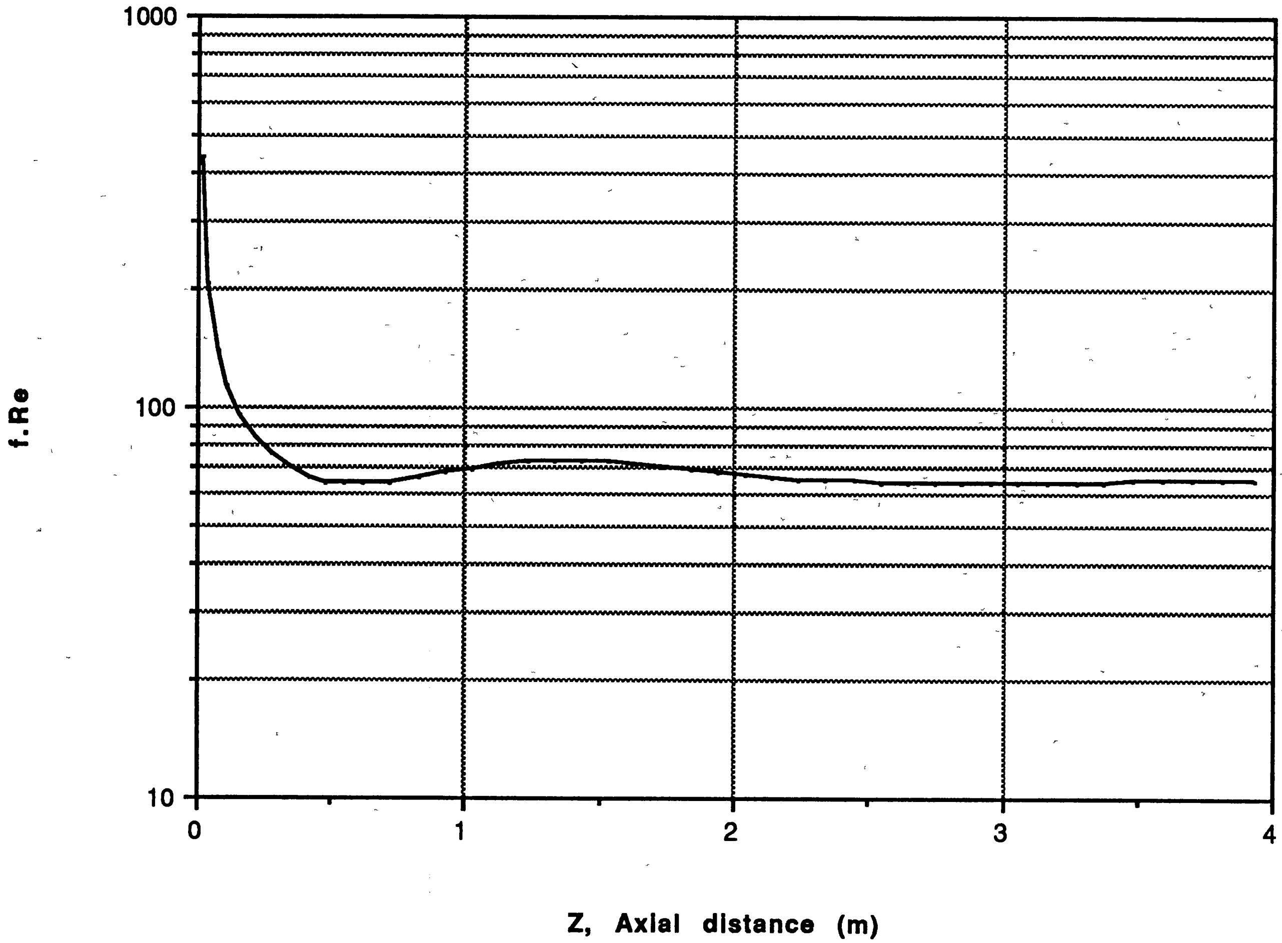

Figure 49. Variation of f.Re (Run#2137)

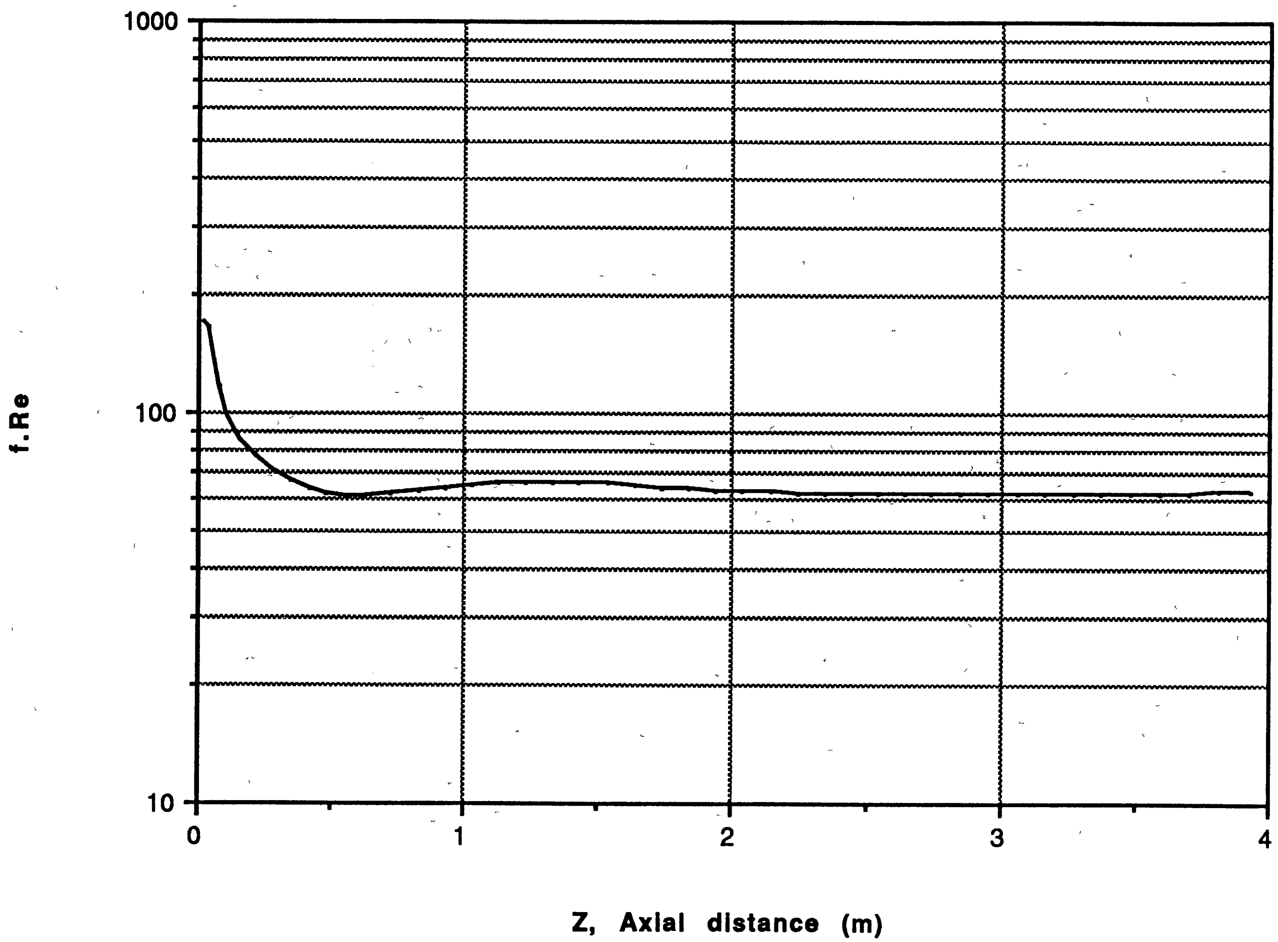

Figure 50. Variation of f.Re (Run#2135)

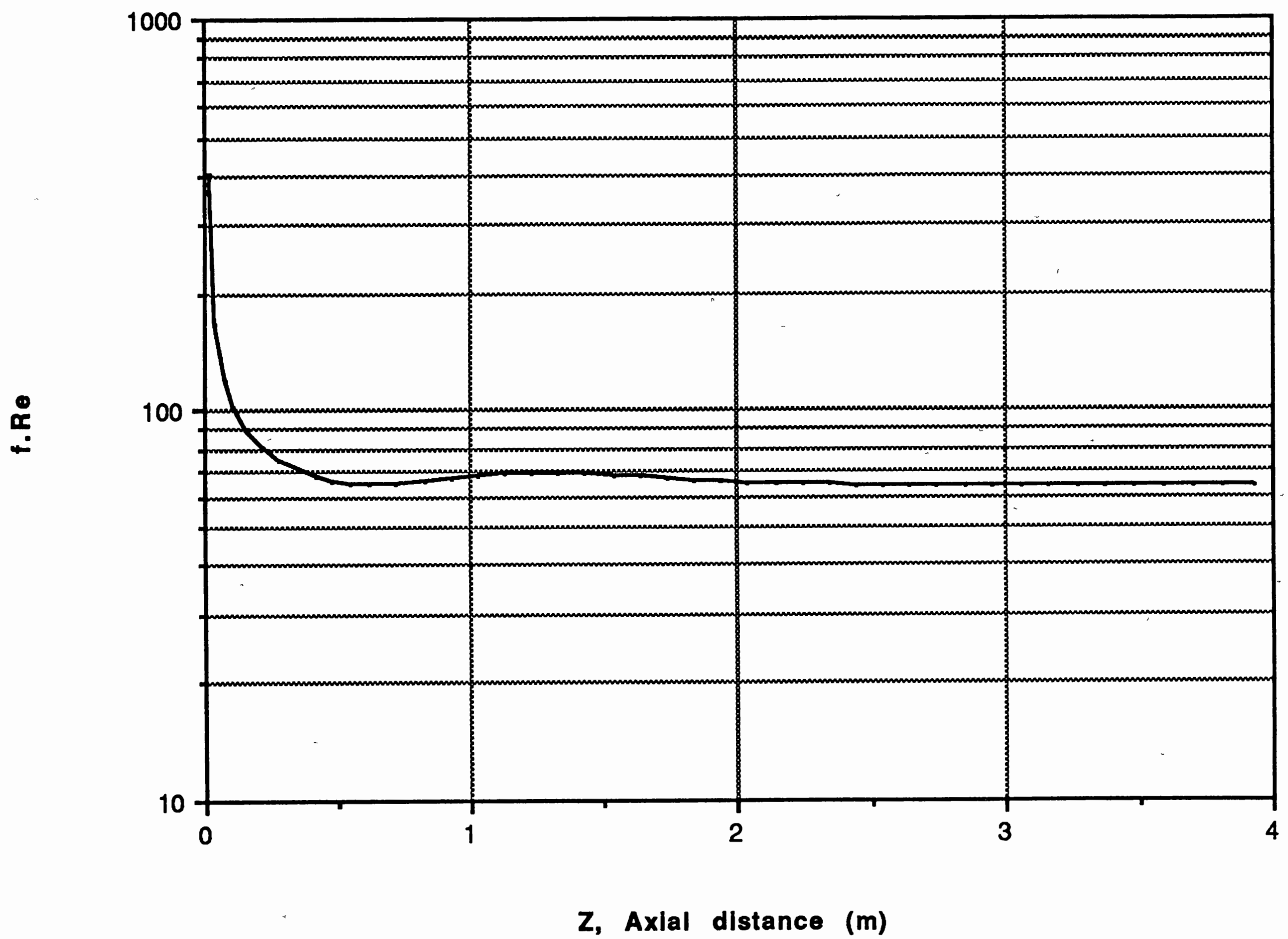

Figure 51. Variation of f.Re (Run#2139)

Runs#2135 and #2139. It seems that the secondary flow has little effect on the hydraulic entrance length. After the entrance length, a peak value of f.Re marks onset of the secondary flow.

It should be pointed out here that, on the one hand, the secondary flow would increase the pressure drop. On the other hand, considering variable properties, the decreasing viscosity of the fluid would decrease the pressure drop. The net result is a compromise between these two processes.

CHAPTER VII

EXPLORATION OF FLOW REGIMES

In 1964, Metais and Eckert presented the flow regime maps (e. g., Figure 6), which were based on correlations and data available at that time. Concerning horizontal tubes, for example, they employed Oliver's correlation (1962) to account for laminar mixed convection, while Sieder and Tate's (1936) equation was used for laminar pure forced convection. The demarcations of the pure forced convection and mixed convection regimes were established at the conditions under which the actual heat flux deviated by lass than ten percent from the value predicted for either forced or mixed convection acting singly. A very few experimental data, all of them using a nominally uniform wall temperature boundary condition, were marked on the figure (Figure 6). Because those data represented the average properties for the entire tube, it is difficult for the data to show clearly the significance of the natural convection.

In order to judge the magnitude of natural convection effect and verify the flow regime map for horizontal tubes, more experimental data and new characteristic parameter(s) should be pursued. Chen's experimental work (1988) provides a good data base for this purpose. Since it gives local heat transfer coefficients both axially and circumeferentially, one is able to use a new dimensionless parameter, h_t/h_b, the ratio of the heat transfer coefficient at the top of the tube to that at the bottom, as a measure of the significance of natural convection. As mentioned previously, the buoyancy-induced secondary flow would result in considerable peripheral temperature variation and nonuniform distribution of heat flux at the tube wall, and hence, the peripheral variation of the heat transfer coefficient. Therefore, the stronger the natural convection, the smaller the ratio. Without natural convection, the ratio should always be unity. As a consequence, the ratio is always less than unity (with heating) if mixed convection exists.

After introducing the new parameter and classifying it into four categories,

$$0.8 \le h_t/h_b \le 1.0$$

$$0.6 \le h_t/h_b < 0.8$$

$$0.4 \le h_t/h_b < 0.6$$

$$0.0 \le h_t/h_b < 0.4$$

Figure 52 correlates all of Chen's data with log(Re) - log(Pr) coordinates, at axial stations 6, 8, 10, and 12. These plots demonstrate different classes of the effect of natural convection with apparent flow regime pattern,

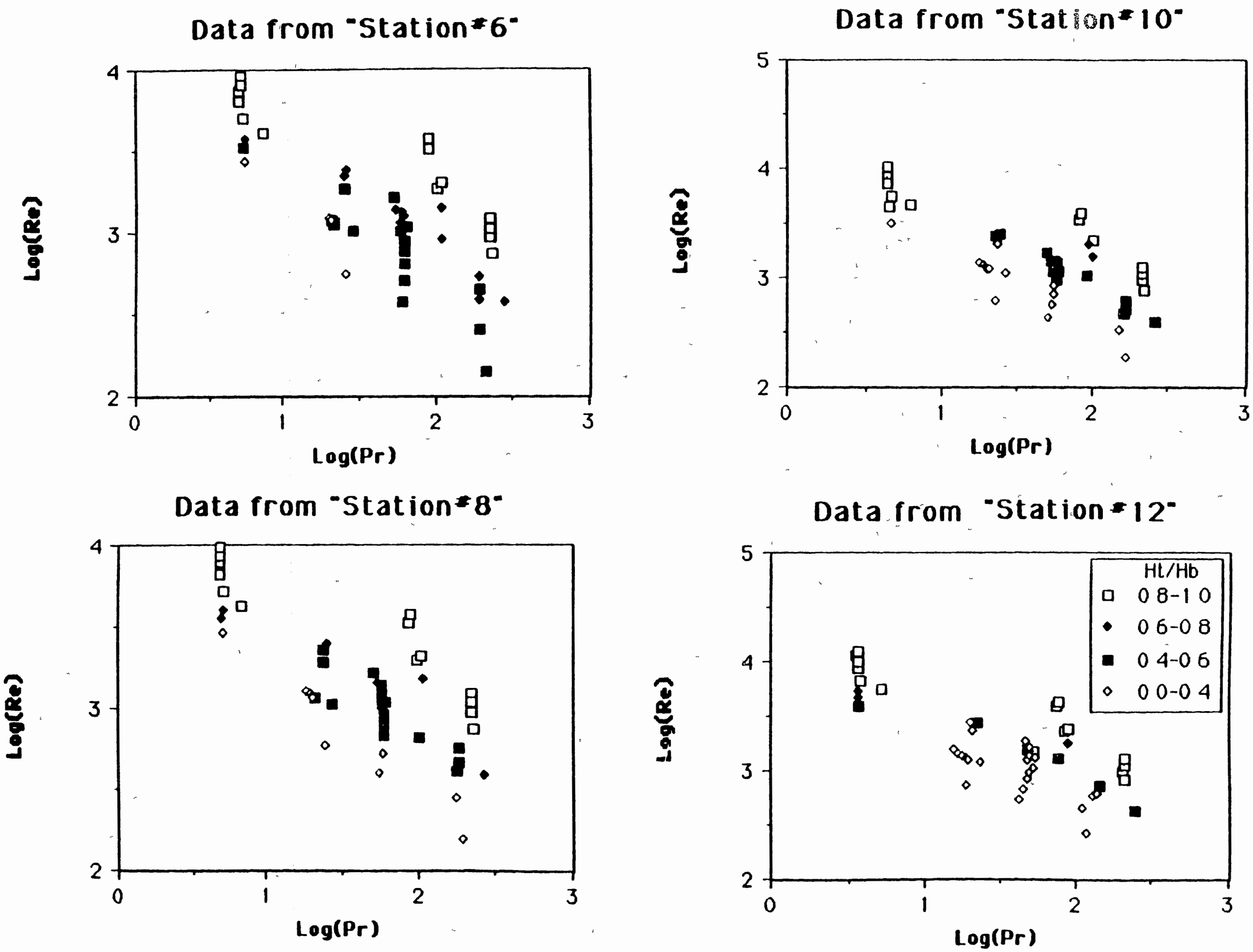

Figure 52. Re vs. Pr for different values of h_t/h_b

including laminar, turbulent and transition flow regions. If a critical value, $h_t/h_b = 0.8$, for the demarcation of mixed and forced convection, is assumed, the influence of Pr on the demarcation would be obvious; with increase of Pr, the demarcating Re decreases, and therefore, the natural convection effect decreases.

Figure 53 plots the data on log(Re) - log(Gr) coordinates. The larger the Gr, the higher the demarcating Re, and the effect of natural convection increases.

That the four subplots of Figures 52 and 53 show almost the same pattern reveals that the axial distance has minor influence on natural convection, and suggests it is possible to expand the correlation to more data using different tubes.

Abdelmessih (1986) conducted an experimental study on horizontal U-tubes. She used four different sizes of U-tubes with electrically heated straight tube sections. For each test section, local axial and peripheral wall temperatures were measured and the local peripheral heat transfer coefficients at the various locations were calculated. Her experimental data for straight tube sections upstream of the bends can be incorporated into the data bank of the present study. Specifications of the four test tubes are shown in Table IV.

With the four test tubes, Abdelmessih carried out 84 runs. Distilled water and almost pure ethylene glycol were

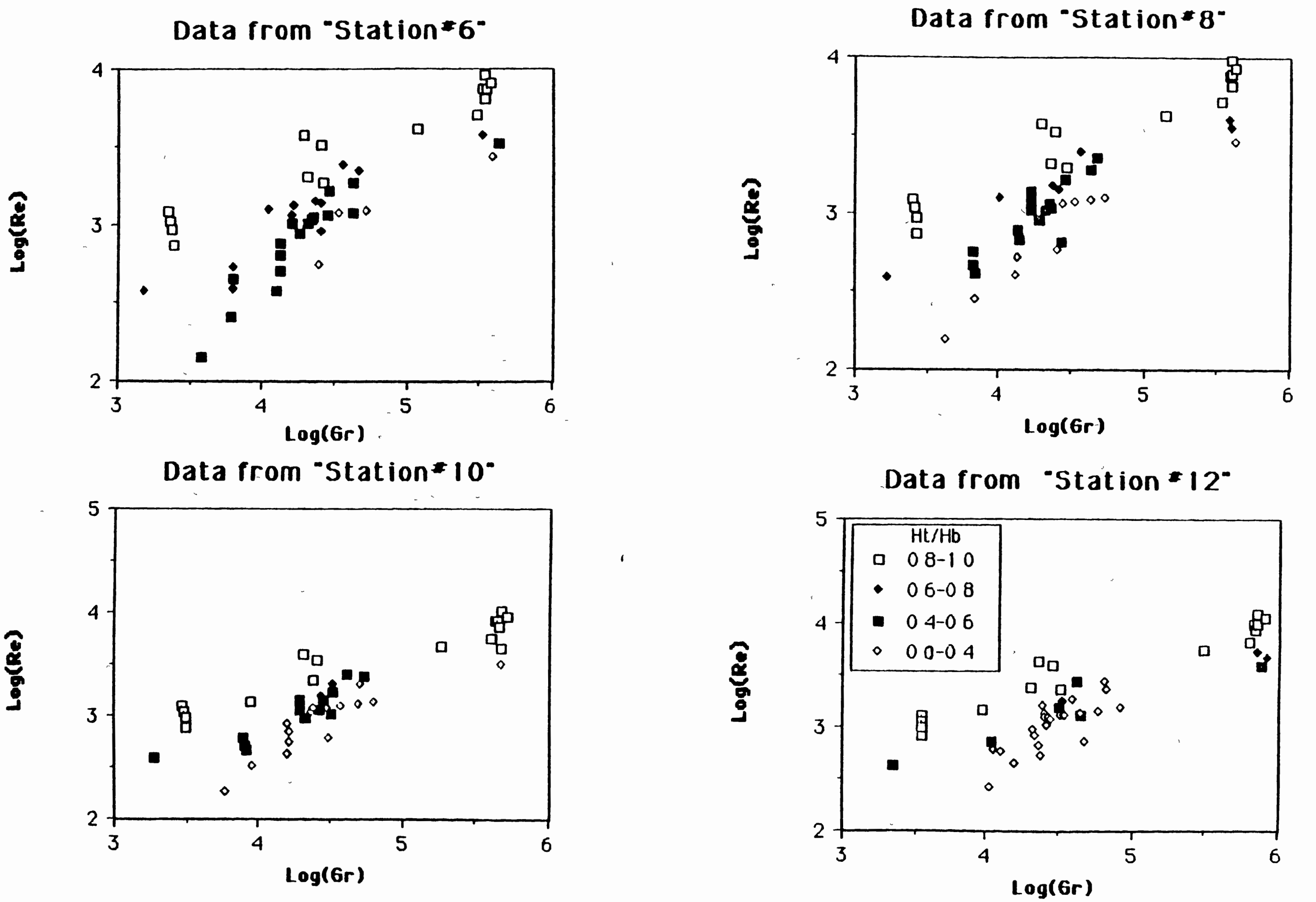

Figure 53. Re vs. Gr for different values of h_t/h_b

TABLE IV

ABDELMESSIH'S TEST SECTIONS UPSTREAM FROM THE U-BENDS

Section	L*(m)	d_o(m)	d_i(m)	Material
A	1.492	0.0222	0.0195	Inconel 600
B	1.175	0.0222	0.0195	Inconel 600
C	2.753	0.0191	0.0157	SS 304
D	2.740	0.0191	0.0157	SS 304

* heated length

TABLE V

ABDELMESSIH'S DATA INCLUDED IN FIGURES 54 AND 55

Section	Run Number
A	22, 23, 24, 25, 27, 29, 30, 31, 32, 49, 55, 56, 58, 59, 60
B	102, 103, 105, 106, 107
C	201, 202, 203, 204, 205
D	302, 303, 304, 305, 306

the test fluids. The experiments covered the local bulk Re range of 120 to 2500, Pr from 4 to 110, and Gr from 2500 to 1,130,000. Thirty representative runs have been selected to combine with Chen's data for flow regime investigation. Table V shows the run number of each test section.

Figures 54 and 55 show patterns of the parameter, h_t/h_b, at log(Re) - log(Pr), and log(Re) - log(Gr) coordinates, respectively, with addition of Abdelmessih's data. In these figures, Chen's data at the station 10 (close to geometrical mid-point of the tube), and Abdelmessih's data at the station 2 were selected.

While the above two figures show reasonably good separation among the flow regimes, attempts to correlate the data by the product of Gr and Pr, i. e., the Rayleigh number, Ra, failed. The Metais-Eckert regime map for horizontal tubes (Figure 6) thus must be regarded as questionable, and further study in this area is required.

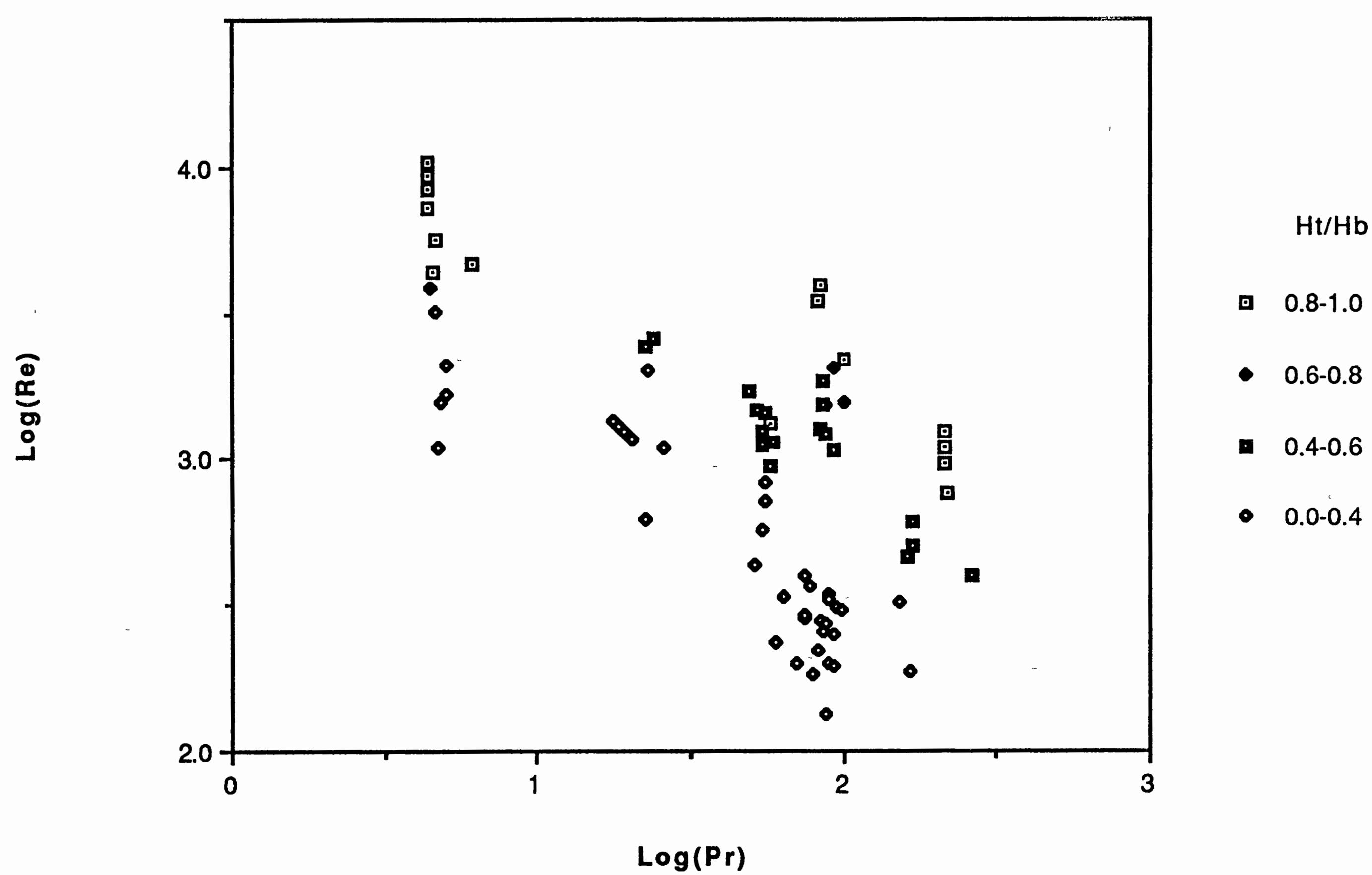

Figure 54. Flow regimes for Chen and Abdelmessih's data, Re vs. Pr.

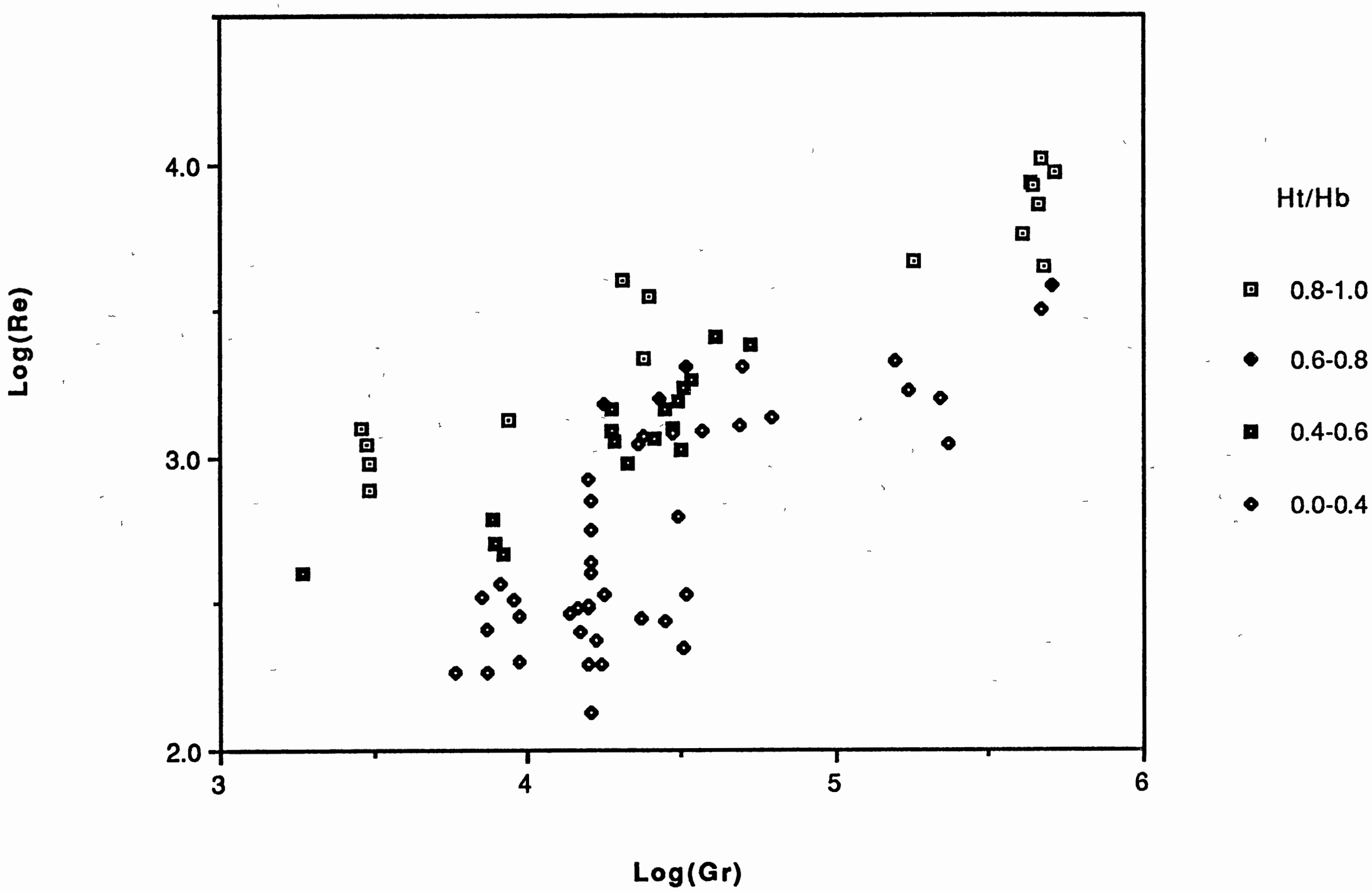

Figure 55. Flow regimes for Chen and Abdelmessih's data, Re vs. Gr.

CHAPTER VIII

AN IMPROVED HEAT TRANSFER CORRELATION

As mentioned in the Literature Survey, there are few correlations dealing with simultaneously developing velocity profile and temperature profile mixed convection heat transfer inside horizontal tubes with uniform heat flux. Based on his experimental data in laminar flow region, Chen (1988) derived a correlation for local peripheral average Nusselt numbers:

$$Nu_z = \{4.364+0.00106Re^{0.81}Pr^{0.45}[1+14.0\exp(0.063z/d_i)] +0.268(GrPr)^{1/4}[1 - \exp(-0.042z/d_i)]\}(\mu_b/\mu_w)^{0.14} \quad (8\text{-}1)$$

Abdelmessih (1986) correlated her local experimental data for straight tubes upstream of a U-bend with the following equation,

$$Nu_z = 4.364 + 0.3271Gr^{0.25}Pr^{0.25}(\mu_b/\mu_w)^{0.14} \quad (8\text{-}2)$$

This equation does not include any dependency upon local axial position.

For practical design of heat exchangers, however, a correlation giving an axial average value, instead of local values, of the inside heat transfer coefficient of the tube is more convenient. Recently, Palen and Taborek (1985) investigated over 600 horizontal tube data points on hydrocarbon oils, and developed the following correlation:

$$Nu = 2.5 + 4.55(Re^*)^{0.37}(d_i/L)^{0.37}Pr^{0.17}(\mu_b/\mu_w)^{0.14} \qquad (8\text{-}3)$$

where

$$Re^* = Re + 0.8Gr^{0.5}$$

Equation (8-3) is based on arithmetic average bulk physical properties and gives axial average Nusselt number. The following general limitations are imposed upon Equation (8-3)

$$0 < \mu_b/\mu_w < 55$$

$$20 < Pr < 10000$$

$$0.1 < Re < 2000$$

$$0 < Gr < 3 \times 10^7$$

$$40 < L/d_i < \infty$$

Since most of the data they used were for conditions approximating uniform wall temperature, instead of uniform heat flux, Palen and Taborek claimed the correlation (Equation 8-3) should be better suited to UWT than to UHF cases.

As a consequence of this, an improved heat transfer correlation for uniform heat flux condition, including entrance effect and mixed convection, will be developed in this chapter.

Chen and Abdelmessih's data were employed. Data reduction involved calculations of the axial average Nusselt number by the length-weighted method and of physical properties based on arithmetic mean bulk temperature. Since Abdelmessih's data did not provide values of the Sieder and Tate viscosity ratio term, a viscosity chart for ethylene glycol by Gallant (1968) was used to supply this term. Data for the correlation are listed in Appendix D.

As for pure forced convection, the correlating approach to use dimensionless parameters and empirically determined constants has been successfully practiced in the past, for both laminar and turbulent heat transfer with or without entrance effect. Since, as mentioned previously, mixed convection incorporates a buoyancy-induced secondary flow, the new heat transfer correlation should reflect the following contributions: the forced convection (primary flow), the natural convection (secondary flow), the entrance effect, and the variable properties (especially the temperature-dependent viscosity). Assuming that the forced convection and natural convection terms are additive, the basic format of the correlation would be

$$Nu = [4.364 + C_1 Re^{C2} Pr^{C3} (d_i/L)^{C4} + C_5 (GrPr)^{C6}] (\mu_b/\mu_w)^{0.14} \tag{8-4}$$

The first term in the brackets of Equation (8-4) is the predicted constant value for hydraulically and thermally fully developed pure forced convection. The second term stands for the developing convective conduction effect in which besides the Reynolds and Prandtl numbers, the ratio of the tube diameter to the tube length is also incorporated, so that this term will go to zero as $L \to \infty$. The natural convection expression, the third term, is expected to be a function of the Grashof number and the Prandtl number, probably a function of their product which is the Rayleigh number. According to the analysis in Chapter VII, the axial location has less influence on natural convection, therefore, the entrance effect was neglected in the natural convection term. For convenience of design applications, the conventional Sieder-Tate viscosity correction factor was employed to account for the major effect of temperature dependence of physical properties.

Regression analyses were conducted using models based on Equation (8-4), over the experimental data. The following correlation was finally selected.

$$Nu = [4.364 + 0.1Re^{0.387}Pr^{0.415}(d_i/L)^{0.147} + 0.11(GrPr)^{0.3}](\mu_b/\mu_w)^{0.14} \quad (8\text{-}5)$$

Equation (8-5) is valid for

$1 < \mu_b/\mu_w < 5$

$4 < Pr < 270$

$100 < Re < 2500$

$1500 < Gr < 2 \times 10^5$

$50 < L/d_i < 300$

Equation (8-5) has a root-mean-square deviation of 10% when compared with the experimental data as shown in Figure 56. Figure 57 gives the relative deviation as a function of Reynolds number. It can be seen that relative errors of all data (except one peculiar point) fall into a domain of ±23%.

By assuming that the physical properties remain the same for the entire tube, Chen (1988) integrated the correlation for local Nusselt number of laminar mixed convection, Equation (8-1), with respect to z from 0 to L, and obtained an expression for axial average Nusselt number as follows:

$$Nu = \{4.364 + 0.00106Re^{0.81}Pr^{0.45}[1 + 222d_i/L - 222d_i/L \exp(-0.063L/d_i)] + 0.268(GrPr)^{0.25}[1 - 23.8d_i/L + 23.8d_i/L \exp(-0.042L/d_i)]\}(\mu_b/\mu_w)^{0.14} \qquad (8-6)$$

Figure 58 presents comparison between experimental data and Chen's prediction, Equation (8-6). It can be seen that Equation (8-6) has a little higher deviation than Equation(8-5). Furthermore, Equation (8-6) is too complicated to be used in engineering applications. Even Chen himself did not recommend this equation.

Figure 59 shows comparison of Palen and Taborek's prediction, Equation(8-3), with the experimental data. For most data points, Equation (8-3) is overpredicted. The maximum relative error is as high as 96%.

Compared to the most recent correlations, Equation (8-

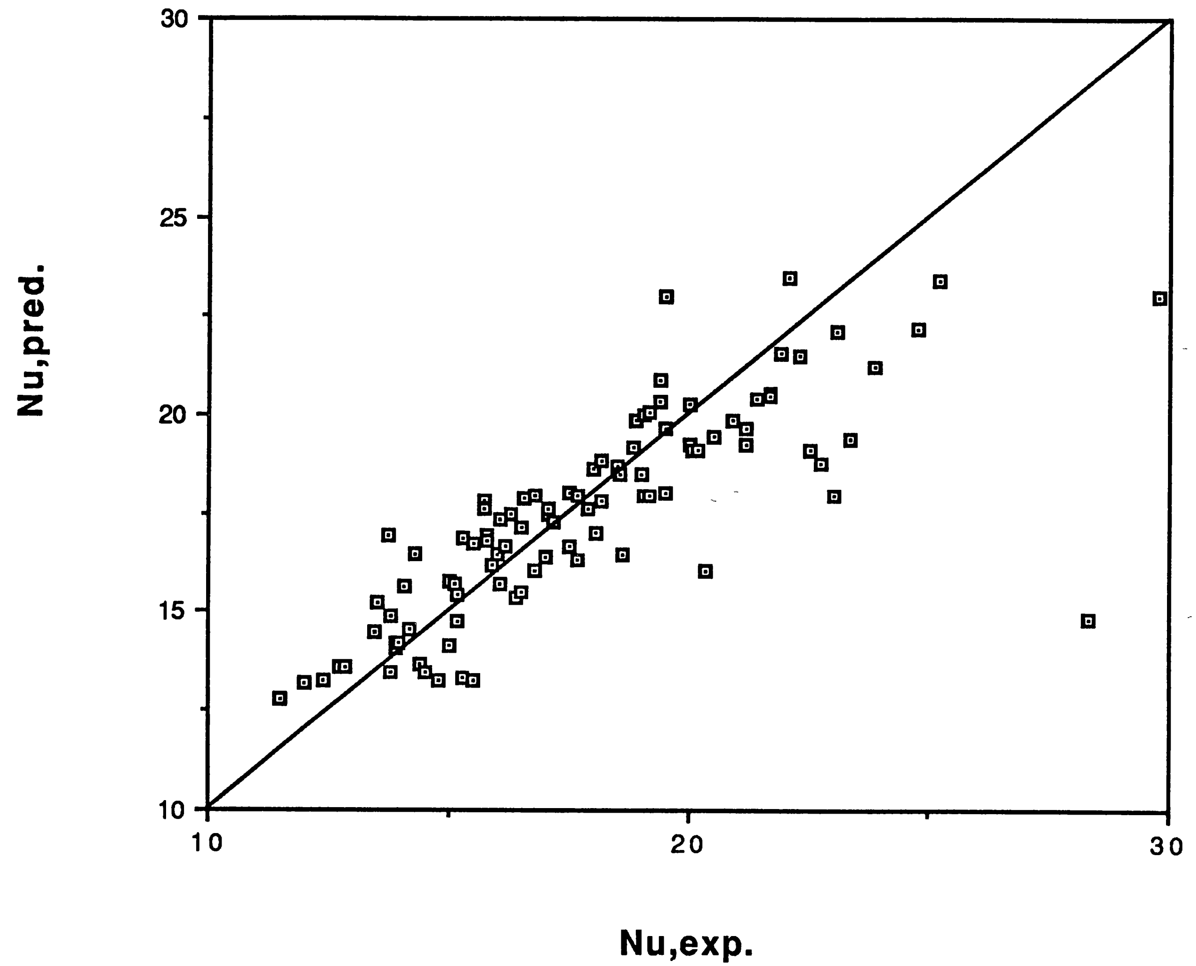

Figure 56. Comparison between experimental Nusselt numbers and those predicted by Equation (8-5)

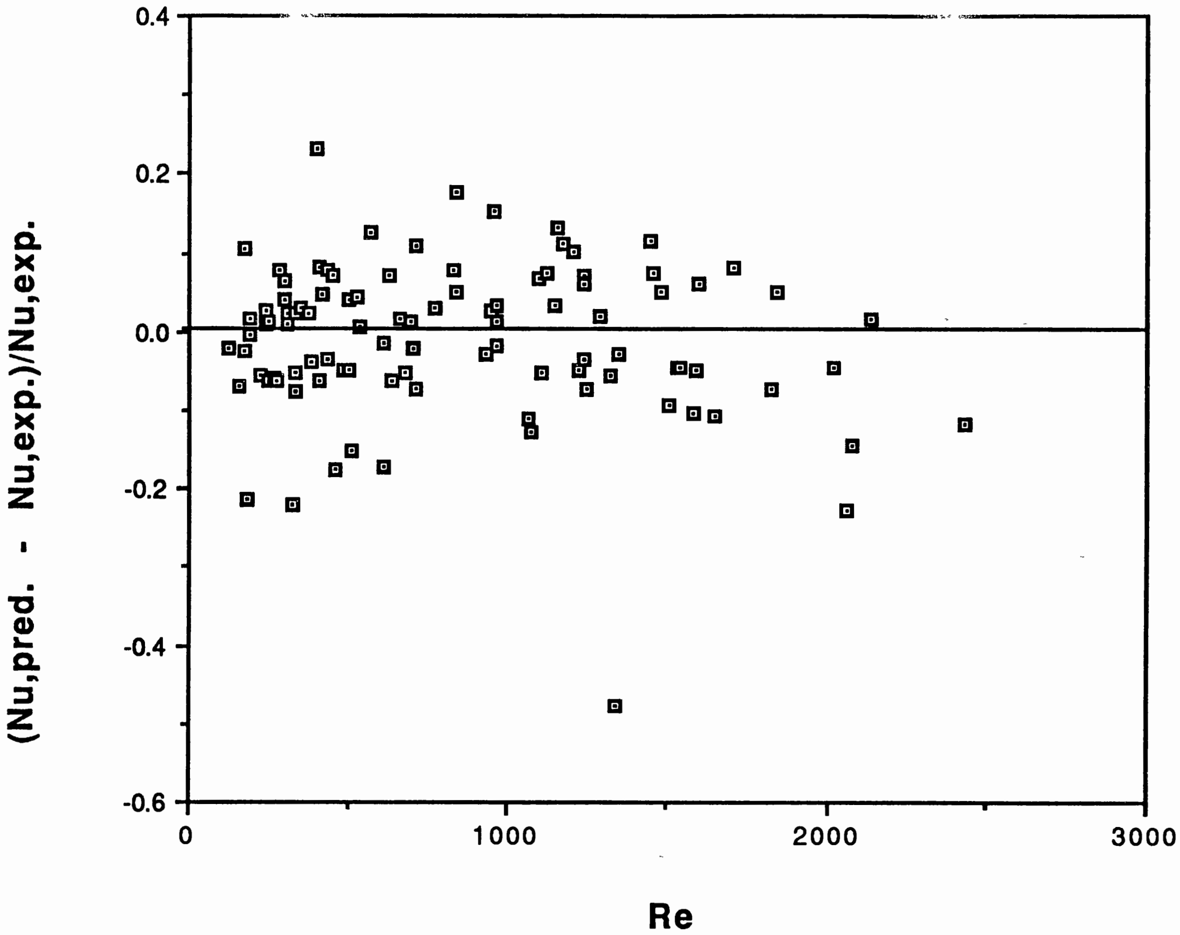

Figure 57. Comparison between experimental Nusselt numbers and those predicted by Equation(8-5), as a function of Re

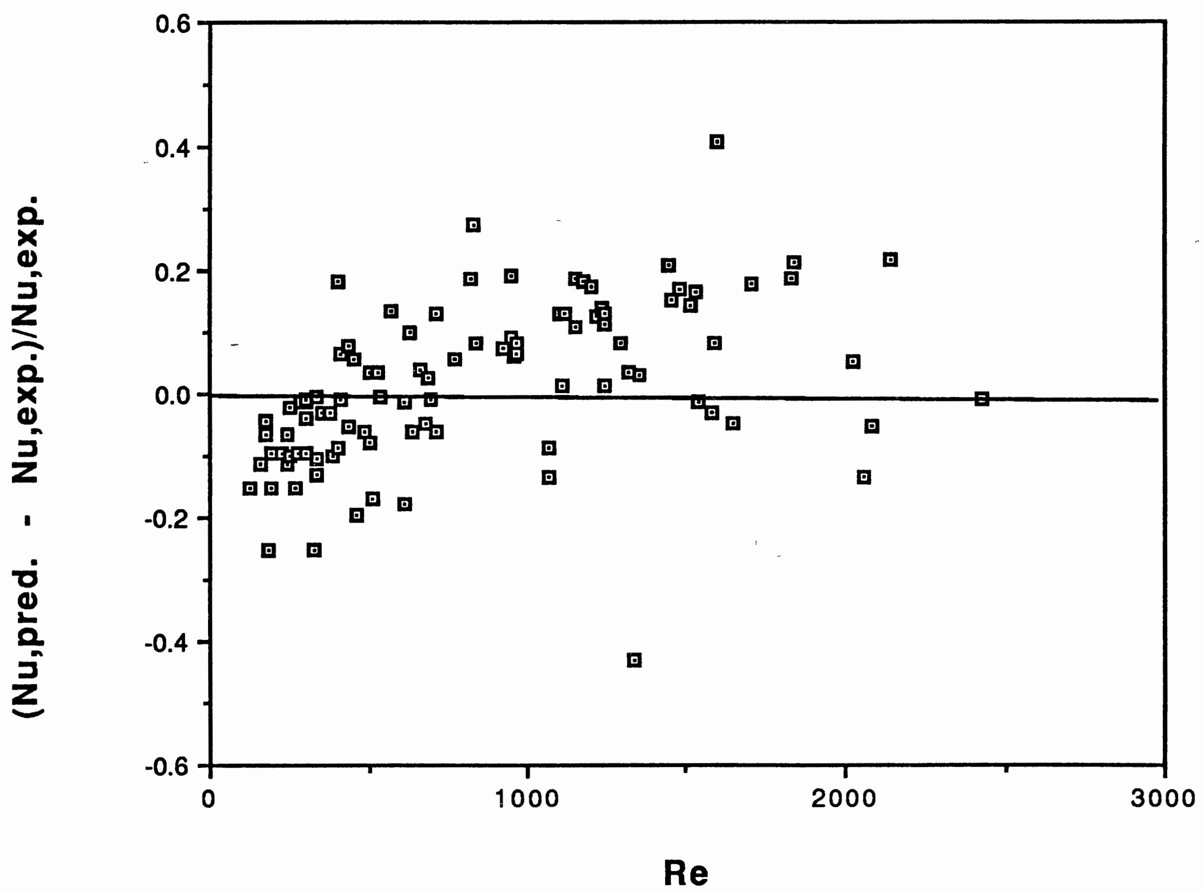

Figure 58. Comparison between experimental Nusselt numbers and those predicted by Chen (1988)

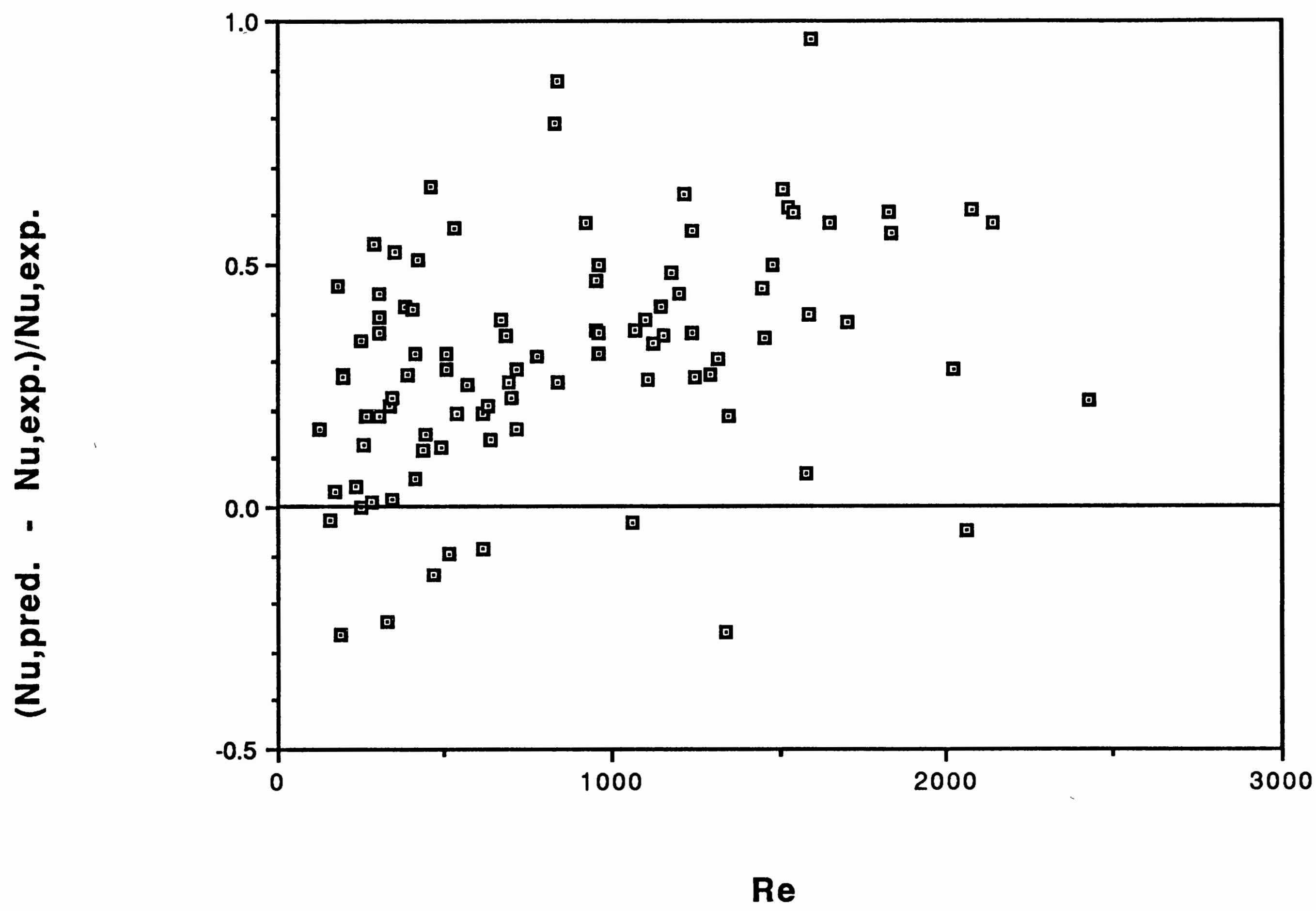

Figure 59. Comparison between experimental Nusselt numbers and those predicted by Palen and Taborek (1985)

5) has higher accuracy and a simple form, and it is recommended to use it directly in heat exchanger design practice where uniform heat flux condition exists.

CHAPTER IX

FURTHER APPLICATION OF THE COMPUTER PROGRAM

Development of the numerical method has been presented in previous chapters and the validity of the computer program has been established by comparing numerical results with corresponding experimental data. However, a more important task is how to make good use of the computer program as a tool for mixed convection study. Therefore, further application of the computer program is encouraged and the following strategy is proposed:

In order that the mapping of the flow regimes and the heat transfer correlation in previous chapters have generality, more data for various operating conditions are required. While only a very few experimental data sources with relatively narrow operating conditions are available, the computer program can generate with ease a diversified variety of data from given operating conditions.

When using numerical data to generate a heat transfer correlation for axial average Nusselt number, the computer will print out a peripheral average Nusselt number for each axial station. Then, numerical integration of those local average Nu along the tube length will give an axial average

Nusselt number for a specific run.

As for the flow regimes, the computer program will provide h_t/h_b for each axial station. Then those data at certain axial location for different runs may be plotted on figure like Figures 54 and 55, and the boundary between different flow regimes may be established.

Two major operational variables are tube diameter and the physical properties of the fluid. Since all the computational runs in this thesis are for one tube diameter, d_i=16.07mm, and water and diethylene glycol-water solutions, more computations for various operating conditions, for example, tube diameters ranging from 8 mm to 40 mm, Prandtl numbers from 300 to 10^4, and Grashof numbers from 10^6 to 20 x 10^6, are proposed.

The given values of the inside wall heat flux should be checked with the tube diameter, properties of fluid, mass flow rate, and the expected fluid bulk temperature rise. For computational runs, only a nominally uniform heat flux can be used. The mass flow rate should be selected so that the fluid flow is within the laminar region along the whole tube length.

For a working fluid other than diethylene glycol-water solution, appropriate correlations for physical properties such as density, viscosity, thermal conductivity, and specific heat, should be inserted into the program to substitute subroutines DENSE, VISCO, CONDY, and SPHT, respectively.

When a large tube diameter and high heat flux are employed, divergence or unrealistic solution may occur, unless enough attention is paid to the program. If this happens, possible treatments include adjusting the value of underrelaxation factors, RELAX(NF) and(or) using an alternative grid system. However, the smaller the underrelaxation factors, the slower the converging speed. For the computations in this thesis, the underrelaxation factors for the secondary flow velocities, u and v, and pressure correction, Δp, are all 0.5, for the axial velocity, w, and temperature, T, the factors are 0.9 or 1.

CHAPTER X

CONCLUSIONS AND RECOMMENDATIONS

Conclusions

1). Developing laminar mixed convection heat transfer in horizontal, electrically heated tubes, with variable property fluids, has been investigated theoretically. The governing equations have been solved using a three-dimensional parabolic computational technique. The computational runs covered a wide range of Prandtl number, Grashof number, and Reynolds number. Comparisons with computational and experimental results show reasonably good agreement and support the validity of the numerical solutions. The investigation presented here provides a useful device to explore the complex interaction of fluid flow and heat transfer in the entrance region of horizontal tubes with nominally uniform heat flux.

2). The buoyancy-induced secondary flow exerts a significant effect on the primary flow inside horizontal tubes. The secondary flow distorts the axial velocity profile with maximum velocity displaced toward the tube bottom or top, instead of at the center. Because the temperature difference between the tube wall and the bulk flow always exists, the secondary flow will not decay as in a UWT situation, therefore, a fully developed velocity profile would not be reached under these circumstances.

3). The influence of the secondary flow on heat transfer manifests itself mainly in two aspects. One is the peripheral variation of wall temperature, which results in a considerable peripheral wall heat conduction, and hence a nonuniformity of inside wall heat flux for electrically heated tubes. Very good agreement between experiments and computations calls into question the validity of the assertion of the infinite wall thermal conductivity case, i. e., circumferentially uniform wall temperature and axially uniform heat flux. Another aspect concerns the inconsistency between practical heat transfer applications and traditional pure forced convection, fully developed heat transfer case in which Nusselt number approaches a constant, 4.36. Because of the mixed convection, the profiles of the mean wall temperature and the bulk temperature are not parallel and the temperature difference decreased with tube length, and therefore, a constant Nusselt number would not be obtained.

4). The secondary flow strongly modified the traditional entrance effect on fluid flow and heat transfer. The entrance length is substantially shorter when mixed convection is involved.

5). By introducing a new parameter, h_t/h_b, the effect of natural convection was classified and therefore flow regimes for mixed convection could be explored. Analysis of experimental data shows that Gr and Pr have decisive influence on mixed convection, but their influences act on opposite directions. It seems better to correlate experimental data with Gr and Pr individually, instead of their product, Ra, while dealing with mixed convection inside horizontal tubes with UHF boundary condition.

6). Based on available experimental data, an improved heat transfer correlation (Equation 8-5) was developed. It is expected to be directly used in engineering design.

Recommendations

1). Numerical Approach

It is recommended to use the numerical method and the computer program presented in this thesis over a wider range of operating conditions, which would further, at least qualitively, the exploration of the mechanism of mixed convection.

The temperature problem for the solid tube wall needs to be analyzed simultaneously with that for the fluid in order to establish the actual wall-fluid heat transfer flux distribution. This conjugated problem involves the simultaneous solutions of the energy equations for both the fluid and solid wall regions. The temperature and heat fluxes at the solid-fluid interface are considered continuous.

More advanced computational techniques are worth trying. For example, concerning the treatment of the coupling between the momentum and continuity equations, the procedure SIMPLER (SIMPLE Revised) can reduce substantially the number of iterations for constant property solutions. Many other discretization schemes of combined convection and diffusion fluxes have been claimed to be better than the power-law scheme (Patankar, 1988).

2). Experimental Approach

Since the velocity of the working fluid serves as a "vehicle" for convection heat transfer, it is recommended that local velocities be measured to verify the theoretical results of this work.

In order to prove the prediction of the temperature field, it would be desirable to have some temperature data inside the tube.

More working fluids and more test tubes, other than those included in this work, are recommended, so that experiments will cover a wider range of operating conditions.

BIBLIOGRAPHY

Abdelmessih, A. 1986. Laminar flow heat transfer downstream from U-bends. PhD Thesis. Oklahoma State University.

Aihara, T., and S. Maruyama. 1986. Laminar free convective heat transfer in vertical uniform-heat-flux ducts (numerical solution with constant/temperature-dependent fluid properties). Heat Transfer Japanese Research. 15: 69-86.

Anderson, D. A., J. C. Tannehill, and R. H. Pletcher. 1984. Computational fluid mechanics and heat transfer. Hemisphere Publishing Co.

Armaly, B. F., T. S. Chen, and N. Ramachandran. 1987. Correlations for laminar mixed convection on vertical, inclined and horizontal flat plates with uniform heat flux. Int. J. Heat Mass Transfer. 30: 405-408.

Bergles, A. E., and R. R. Simonds. 1971. Combined forced and free convection for laminar flow in horizontal tubes with uniform heat flux. Int. J. Heat Mass Transfer. 14: 1989-2000.

Chen, J. H. 1988. Heat transfer in high laminar, transition and lower turbulent flow regimes for square-edged contraction entrance in a circular tube. PhD Thesis. Oklahoma State University.

Colburn, A. P. 1933. A method of correlating forced convection heat transfer data and a comparison with fluid friction. Trans. AIChE. 29: 174-210.

Chou, F. C., and G. J. Hwang. 1984. Combined free and forced laminar convection in horizontal rectangular channels for high ReRa. Canadian J. Chem. Eng. 62: 830-836.

Choudhury, D., and S. V. Patankar. 1988. Combined forced and free laminar convection in the entrance region of an inclined isothermal tube. J. Heat Transfer Trans. ASME. 110: 901-909.

Churchill, S. W., and R. Usagi. 1972. A general expression for the correlation of rates of transfer and other phenomena. AIChE J. 18: 1121-1128.

Coutier, J. P., and R. Greif. 1985. An investigation of laminar mixed convection inside a horizontal tube with isothermal wall conditions. Int. J. Heat Mass Transfer. 28: 1293-1305.

Coutier, J. P., and R. Greif. 1986. Mixed laminar convection in a horizontal tube with natural convection around its boundaries. Int. J. Heat Mass Transfer. 29: 391-402.

Croft, D. R., and D. G. Lilley. 1977. Heat transfer calculations using finite difference equations. Applied Science Publishers Ltd. London.

Depew, C. A., and S. E. August. 1971. Heat transfer due to combined free and forced convection in a horizontal and isothermal tube. J. Heat Transfer Trans. ASME. 93: 380-384.

Eckert, E. R. G., and R. M. Drake. 1972. Analysis of heat and mass transfer. McGraw-Hill.

Ede, A. J. 1961. The heat transfer for flow in a pipe. Int. J. Heat Mass Transfer. 4: 105-110.

Eubank, C. C., and W. S. Proctor. 1951. M. S. thesis in chemical engineering.M. I. T., Cambridge.

Faris, G. N., and R. Viskanta. 1969. An analysis of laminar combined forced and free convection heat transfer in a horizontal tube. Int. J. Heat Mass Transfer. 12: 1295-1309.

Gallant, R. W. 1968. Physical properties of hydrocarbons. Gulf Publisher.

Gosman, A. D., B. E. Launder, and G. J. Reece. 1985. Computer-aided engineering heat transfer and fluid flow. Ellis Horwood Ltd. England.

Hartnett, J. P., and T. F. Irvine Jr. 1967. Advances in heat transfer. Vol. 4. Academic Press.

Hessami, M. A., A. Pollard, and R. D. Rowe. 1984. Numerical calculations of natural convection heat transfer between horizontal concentric isothermal cylinders-effects of variation of fluid properties. J. Heat Transfer Trans. ASME. 106: 668-671.

Hessami, M. A., A. Pollard, R. D. Rowe, and D. W. Ruth. 1985. A study of free convective heat transfer in a horizontal annulus with a large radii ratio. J. Heat Transfer Trans. ASME. 107: 603-610.

Hieber, C. A., and S. K. Sreenivasan. 1974. Mixed convection in an isothermally heated horizontal pipe. Int. J. Heat Mass Transfer. 17: 1337-1348.

Hieber, C. A. 1981. Mixed convection in an isothermal horizontal tube: some recent theories. Int. J. Heat Mass Transfer. 24: 315-322.

Hieber, C. A. 1982. Laminar mixed convection in an isothermal horizontal tube: correlation of heat transfer data. Int. J. Heat Mass Transfer. 25: 1737-1746.

Hirt, C. W., B. D. Nichols, and N. C. Romero. 1975. SOLA-A numerical solution algorithm for transient fluid flows. Report LA-5852. Los Alamos Scientific Laboratory.

Hishida, M., Y. Nagano, and M. S. Montesclaros. 1982. Combined forced and free convection in the entrance region of an isothermally heated horizontal pipe. J. Heat Transfer Trans. ASME. 104: 153-159.

Hong, S. W., and A. E. Bergles. 1976. Theoretical solution for combined forced and free convection in horizontal tubes with temperature-dependent viscosity. J. Heat Transfer Trans. ASME. 98: 459-465.

Hussain, N. A., and S. T. McComas. 1970. Experimental investigation of combined convection in a horizontal circular tube with uniform heat flux. Heat Transfer. Vol. 4. Elsevier, Amsterdam.

Hwang, G. J., and F. C. Chou. 1987. Effect of wall conduction on combined free and forced laminar convection in horizontal rectangular channels. J. Heat Transfer Trans. ASME. 109: 936-942.

Jackson, T. W., J. M. Spurlock, and K. R. Purdy. 1961. Combined free and forced convection in a constant temperature horizontal tube. AIChE J. 7: 38-41.

Kakac, S., W.Aung, and R. Viskanta. 1985. Natural convection, fundamentals and applications. Hemisphere Publishing Co.

Kakac, S., R. K. Shah, and W. Aung. 1987. Handbook of single-phase convective heat transfer. John Wiley & Sons.

Karki, K. C., and S. V. Patankar. 1989. Laminar mixed convection in the entrance region of a horizontal annulus. Numerical Heat Transfer. 15: 87-99.

Kato, K., E. Watanabe, T. Ogura, and T.Hanzawa. 1982. Effect of natural convection on laminar flow heat transfer in horizontal circular tubes. J. Chem. Eng. Japan. 15: 355-361.

Kays, W. M., and M. E. Crawford. 1980. Convective heat and mass transfer. Second Edition. McGraw-Hill, New York.

Kern, D. Q., and D. F. Othmer. 1943. Effect of free convection on viscous heat transfer in horizontal tubes. Trans. AIChE. 39: 517-555.

Kulacki, F. A., and R. D. Boyd. 1985. Fundamentals of forced and mixed convection. HTD-Vol.42. 23rd National Heat Transfer Conference. Denver, Colorado.

Launder, B. E. 1975. Studies in convection, theory, measurement and applications. Academic Press.

Law, H. S., J. H. Masliyah, and K. Nandakumar. 1987. Effect of nonuniform heating on laminar mixed convection in ducts. J. Heat Transfer Trans. ASME. 109: 131-137.

Lilley, D. G.1989. Notes for MAE 6263: Computational fluid dynamics. Oklahoma State University.

McAdams, W. M. 1954. Heat transmission. Third Edition. Mcgraw-Hill. New York.

McComas, S. T., and E. R. G. Eckert. 1966. Combined free and forced convection in a horizontal circular tube. J. Heat Transfer Trans. ASME. 88: 147-153.

Mahaney, H. V., F. P. Incropera, and S. Ramadhyani. 1987. Development of laminar mixed convection flow in a horizontal rectangular duct with uniform bottom heating. Numerical Heat Transfer. 12: 137-143.

Metais, B. 1963. Criteria for mixed convection. HTL TR No.51. Heat Transfer Laboratory. University of Minnesota.

Metais, E., and E. R. G. Eckert. 1964. Forced, mixed, and free convection regimes. J. Heat Transfer Trans. ASME. 86: 295-296.

Morcos, S. M., and A. E. Bergles. 1975. Experimental investigation of combined forced and free laminar convection in horizontal tubes. J. Heat Transfer Trans. ASME. 97: 212-219.

Morcos, S. M., M. M. Hilal, M. M. Kamel, and M. S. Soliman. 1986. Experimental investigation of mixed-laminar convection in the entrance region of inclined rectangular channels. J. Heat Transfer Trans. ASME. 108: 574-579.

Mori, Y., K. Futagami, S. Tokuda, and M. Nakamura. 1966. Forced convective heat transfer in uniformly heated horizontal tubes. Int. J. Heat Mass Transfer. 9: 453-463.

Mori, Y., and K. Futagami. 1967. Forced convective heat transfer in uniformly heated horizontal tubes (2nd Report). Int. J. Heat Mass Transfer. 10: 1801-1812.

Morton, B. R. 1963. Laminar convection in uniformly heated horizontal pipes at low Rayleigh numbers. Quar. J. Mech. Appl. Math. 12: 410-416.

Newell, P. H., and A. E. Bergles. 1970. Analysis of combined free and forced convection for fully developed laminar flow in horizontal tubes. J. Heat Transfer Trans. ASME. 92: 83-93.

Obermeier, E., S. Fischer, and D. Bohne. 1985. Thermal conductivity, density, viscosity, and Prandtl number of Di-and Triethylene Glycol-water mixtures. Ber. Bunsenges. Phys. Chem. 89: 805-809.

Oliver, D. R. 1962. The effect of natural convection on viscous-flow heat transfer in horizontal tubes. Chem. Eng. Sci. 17: 335-350.

Ou, J. W., K. C. Cheng, and R. C. Lin. 1974. Natural convection effects on Graetz problem in horizontal rectangular channels with uniform wall temperature for large Pr. Int. J. Heat Mass Transfer. 17: 835-843.

Ou. J. W., and K. C. Cheng. 1977. Natural convection effects on Graetz problem in horizontal isothermal tubes. Int. J. Heat Mass Transfer. 20: 953-960.

Palen, J. W., and J. Taborek. 1985. An improved heat transfer correlation for laminar flow of high Prandtl number liquids in horizontal tubes. AIChE Symposium Series, No. 245, 81: 90-96.

Patankar, S. V. 1980. Numerical heat transfer and fluid flow. McGraw-Hill.

Patankar, S. V. 1981. A calculation procedure for two-dimensional elliptic situations. Numerical Heat Transfer. 4: 409-425.

Patanker, S. V. 1988. Recent developments in computational heat transfer. J. Heat Transfer Trans. ASME. 110: 1037-1045.

Patankar, S. V., and B. R. Baliga. 1984. Notes for computation of heat transfer and fluid flow. A short course for scientists and engineers. University of Minnesota.

Numerical heat transfer
VOL 4 1981. Pg 409

Main prgrme
ΔZ
No. of steps

A calculation procedure
for 2-D elliptic situation

by Patankar S.V

Patankar, S. V., S. Ramadhyani, and E. M. Sparrow. 1978. Effect of circumeferentially nonuniform heating on laminar combined convection in a horizontal tube. J. Heat Transfer Trans. ASME. 100: 63-70.

Patankar, S. V., and D. B. Spalding. 1967. Heat and mass transfer in boundary layers. Morgan-Grampian. London.

Patankar, S. V., and D. B. Spalding. 1972. A calculation procedure for heat, mass and momentum transfer in 3-D parabolic flow. Int. J. Heat Mass Transfer. 15: 1787-1806.

Petukhov, B. S., and A. F. Polyakov. 1967. Experimental investigation of viscogravitational fluid flow in a horizontal tube. High Temperature. 5: 75-81.

Petukhov, B. S., and A. F. Polyakov. 1967. Effect of free convection on heat transfer during forced flow in horizontal pipe. High Temperature. 5: 348-351.

Pratap, V. S., and D. B. Spalding. 1976. Fluid flow and heat transfer in 3-D duct flow. Int. J. Heat Mass Transfer. 19: 1183-1188.

Raithby, G. D., and G. E. Schneider. 1979. Numerical solution of problems in incompressible fluid flow: treatment of the velocity-pressure coupling. Numerical Heat Transfer. 2: 417- 440.

Reggio, M., and R. Camarero. 1986. Numerical solution procedure for viscous incompressible flows. Numerical Heat Transfer. 10: 131-146.

Reggio, M., and R. Camarero. 1987. A calculation scheme for three-dimensional viscous incompressible flows. J. Fluids Eng. 109: 345-352.

Shah, R. K., and A. L. London. 1978. Laminar flow forced convection in ducts. Academic Press.

Shannon, R. L., and C. A. Depew. 1968. Combined forced and free laminar convection in a horizontal tube with uniform heat flux. J. Heat Transfer Trans. ASME. 90: 353-357.

Shih, T. M. 1984. Numerical Heat Transfer. Hemisphere Publishing Co.

Shih, T. M. 1989. A literature survey on numerical heat transfer. Numerical Heat Transfer. 15: 1-31.

Sieder, E. N., and G. E. Tate. 1936. Heat transfer and pressure drop of liquids in tubes. Ind. and Eng. Chem. 28: 1429-1435.

Siegel, R., E. M. Sparrow, and T. M. Hallman. 1958. Steady laminar heat transfer in a circular tube with prescribed wall heat flux. Appl. Sci. Res. Sec. A. 7: 386-392.

Siegwarth, D. P., and T. J. Hanratty. 1970. Computational and experimental study of the effect of secondary flow on the temperature field and primary flow in a heated horizontal tube. Int. J. Heat Mass Transfer. 13: 27-42.

Siegwarth, D. P., Mikesell, Readal, and Hanratty. 1969. Effect of secondary flow on the temperature field and primary flow in a heated horizontal tube. Int. J. Heat Mass Transfer. 12: 1535- 1552.

Yousef, W. W., and J. D. Tarasuk. 1982. Free convection effects on laminar forced convective heat transfer in a horizontal isothermal tube. J. Heat Transfer Trans. ASME. 104: 145-152.

APPENDIX A

PROPERTIES OF TEST FLUIDS

Water

Sources of correlating equations for physical properties of testing fluids are the same as Chen's work (1988).

Density

$$\rho = 999.86 + 0.061464T - 0.0084648T^2 + 6.8794 \times 10^{-5}T^3 - 4.4214 \times 10^{-7}T^4 + 1.2505 \times 10^{-9}T^5 \qquad \text{(A-1)}$$

where ρ = density, kg/m^3

T = temperature, °C

This equation is valid for the temperature range from 0 to 100 °C and has an accuracy of ± 0.05kg/m^3.

Viscosity

$$\log(\mu_T/\mu_{20}) = [1.327(20 - T) - 0.001053(20 - T)^2]/(T + 105) \qquad \text{(A-2)}$$

where μ_{20} = viscosity of water at 20 °C, Ns/m^2

μ_T = viscosity of water at T °C, Ns/m^2

T = temperature, °C

This equation is valid within the temperature range from 10 to 100°C. It has an accuracy within 1%.

Specific Heat

$$c_p = 4.267 - 2.2 \times 10^{-3}T + 3.66 \times 10^{-5}T^2 - 1.475 \times 10^{-7}T^3 \quad \text{(A-3)}$$

where c_p = specific heat, kJ/(kgK)

T = temperature, °F

This equation has an accuracy within 1% for the range from 0 to 100°C.

Thermal Conductivity

$$k = 0.56276 + 1.874 \times 10^{-3}T - 6.8 \times 10^{-6}T^2 \quad \text{(A-4)}$$

where k = thermal conductivity, W/(m.K)

T = temperature, °C

This equation is applied in the temperature range of 0 to 100°C. It has an accuracy within 1%.

Diethylene Glycol-water Solutions

Density

$$\rho = (998.80 + 207.29x - 72.103x^2) + (-0.10357 - 1.0797x + 0.42904x^2)T + (-3.2251 \times 10^{-3} + 3.4321 \times 10^{-3}x - 4.5246 \times 10^{-3}x^2)T^2 \quad \text{(A-5)}$$

where ρ = density, kg/m^3

T = temperature, °C

x = mass fraction of DEG in DEG-water solution

This equation has an accuracy of ±0.5%. It is good for the temperature range from -10 to 140 °C.

Viscosity

$$\ln\mu = (0.63513 + 3.0176x - 0.49609x^2)^{1.3514} + (-0.029276 - 0.040815x + 0.0099051x^2)T + (1.8238 \times 10^{-6} + 5.765 \times 10^{-6}x - 2.6245 \times 10^{-6}x^2)^{0.6803}T^2 \quad \text{(A-6)}$$

where μ = viscosity, mPa.s

T = temperature

The equation has an accuracy of ±4.0%. It is good for the temperature range from -10 to 80 °C.

Thermal Conductivity

$$k = (1 - x)k_w + xk_{DEG} - \lambda(k_w - k_{DEG})(1 - x)x \quad \text{(A-7)}$$

where $k_w = 0.56276 + 1.874 \times 10^{-3}T - 6.8 \times 10^{-6}T^2$

$k_{DEG} = 0.19589 + 1.689 \times 10^{-4}T - 8.1 \times 10^{-7}T^2$

$\lambda = 0.4052 + 0.0594x - 8.4 \times 10^{-4}T$

k = thermal conductivity, W/(m.K)

T = temperature, °C

The equation has an accuracy of ±0.3%. It is good for the temperature range from -20 to 200 °C.

Specific Heat

$$c_p = (1.027 - 0.52469x + 0.021435x^2) + (-2.6187 \times 10^{-4} + 3.8054 \times 10^{-3}x - 2.5793 \times 10^{-3}x^2)T + (-2.3096 \times 10^{-7} + 6.0706 \times 10^{-7}x)T^2 \qquad \text{(A-8)}$$

where c_p = specific heat, Btu/(lb.°F)

T = temperature, °C

This equation has an accuracy of ±0.5%. It is good for temperature range from -20 to 200 °C.

APPENDIX B

A BRIEF GUIDE TO THE COMPUTER PROGRAM

A flow chart of the three-dimensional program is shown in Figure 17, Chapter V. A listing of the FORTRAN variables used in the program and their definitions is presented here. Table VI specifies the variables, which need to be changed for each specific computational run, and their locations in the program (by giving subroutine name). Run #2105 has been used as a sample for convenience of explanation.

The program is listed with all comments. The program is available from

Professor Kenneth J. Bell
School of Chemical Engineering
Oklahoma State University
Stillwater, OK 74078

Notation

ACOF	quantity to give the combined convection and diffusion effect in subroutine DIFLOW
AIM(I,J)	the coefficient a_W in Eq. (4-29)
AIP(I,J)	the coefficient a_E in Eq. (4-28)
AJM(I,J)	the coefficient a_S in Eq. (4-27)
AJP(I,J)	the coefficient a_N in Eq. (4-26)
AP(I,J)	the coefficient a_P in Eq. (4-25); also S_P in GAMSOR
AMU(I,J)	variable viscosity
AMU1	constant viscosity
ANU	Nusselt number
AREA	local variable, usually the area of a C. V. face
AREAM1 AREAM2	areas of the faces of the near-boundary C. V.
ARHO	local variable, (area) x ρ
ARX(J)	the area of the main C. V. face normal to the x direction
ARXJ(J)	the part of ARX(J) that overlaps on the C. V. for V(I,J)
ARXJP(J)	the part of ARX(J) that overlaps on the C. V. for V(I,J+1)
ASUM	$\Sigma\Delta A$
BL BLC BLM BLP	coefficients used in the block correction

P940

CON(I,J)	constant term b in Eq.(4-30); also S_C in GAMSOR
COND(I,J)	variable thermal conductivity
COND1	constant thermal conductivity
CP(I,J)	variable specific heat
CP1	constant specific heat
DENOM	temporary storage
DEZ(K)	variable steps in z-direction
DIA	inside diameter of the tube
DIFF	diffusion conductance D
DPSZ	pressure drop, dp/dz.
DQ	ΔQ, for pressure-velocity decoupling Eq.(4-46)
DU(I,J)	de influencing U(I,J)
DV(I,J)	dn inflencing V(I,J)
DX	step in x-direction
DY	step in y-direction
ERR1 ERR2 ERR4 ERR5	relative error between two iterations for u, v, T, and w, respectively
ERSUM1 ERSUM2 ERSUM4 ERSUM5	accumulative error for u, v, T, and w
F(I,J,NF)	various ϕ's
FL	temporary storage leading to FLOW
FLM	temporary storage leading to FLOW
FLOW	mass flow rate through a C.V face
FLP	temporary storage leading to FLOW

FRE	f.Re
FRSUM	$\Sigma\rho\Delta A f_p$, Eq.(4-46)
FU(I,J)	mass flow rate across the upstream face, Eq.(4-14)
FV(J) FVP(J)	interpolation factors giving the mass flow ρvr at a main grid point (I,J) as FV(J)*ρvr(I,J)+FVP(J)*ρvr(I,J+1)
FX(I) FXM(I)	interpolation factors which give the interface density RHOM (at the location of U(I,J))as FX(I)*RHO(I,J)+FXM(I)*RHO(I-1,J)
FY(J) FYM(J)	interpolation factors which give the interface density RHOM (at the location of V(I,J))as FY(J)*RHO(I,J)+FYM(I)*RHO(I,J-1)
GAM(I,J)	diffusion coefficient Γ
HTC	local average heat transfer coefficient
I	index in x-direction
II	temporary index
IPREF	the value of I for the grid point which is used as a reference for pressure
IST	the first internal point value of I
ITER	a counter for iterations
J	index in y-direction
JFL	temporary index used in PRINT
JFST	similar to IFST
JJ	temporary index
JPREF	similar to IPREF
JST	the first internal point value of J
K	index in z-direction
LAST	maximum number of iterations

LBLK(NF)	when.TRUE., the block correction for F(I,J,NF) is used
LISFIL	name of the main output file
LPRINT(NF)	when.TRUE., F(I,J,NF) is printed
LSOLVE(NF)	when.TRUE., we solve for F(I,J,NF)
LSTOP	when.TRUE., computation at a station stops
L1	the value of I for the last grid location in the x direction
L2	L1-1
L3	L1-2
MODE	index for the coordinate system MODE = 1 for xy, then x=x, y=y MODE = 2 for rz, then x=z, y=r MODE = 3 for rθ, then x=θ, y=r
M1	the value of J for the last grid location in the y direction
M2	M1-1
M3	M1-2
N	the number of axial steps; also the temporary storage for NF
NF	index denoting a particular ϕ NF=1 for u, NF=2 for v, NF=3 for p' (Eq.(4-54)) NF=4 for T, NF=5 for w, NF=6 for f (Eq.(4-47))
NFMAX	the largest value of NF for which storage is assigned
NGAM	NFMAX+3
NP	NFMAX+1
NRHO	NFMAX+2
NTIMES(NF)	the number of repetitions of the sweeps in SOLVE for the variable F(I,J,NF)
P(I,J)	the pressure p

PC(I,J)	the pressure correction p'
PI	π=3.14159
PREF	the pressure at the reference point
PT(I) or PT(J) QT(I) or QT(J)	transformed coefficients in the TDMA
QW(I,J,K)	variable inside wall heat flux
QW1	constant inside wall heat flux
R(J)	the radius r for a main grid point (I,J)
RE	Reynolds number
REL	1.-RELAX(NF)
RELAX(NF)	relaxation factor for F(I,J,NF)
RHO(I,J)	the density ρ
RHOCON	ρ for a constant-density problem
RM	0.5x(the total mass flow rate of the tube)
RMN(J)	the value of radius r for the location to which V(I,J) refers
RMSUM	$\Sigma\rho w\Delta A$, Eq.(4-41)
SMAX	the largest absolute value of the "mass source" used in the p' equation
SSUM	the algebraic sum of all the "mass source" in the p' equation
SX(J)	scale factor for the x direction at the main grid locations Y(J)
SXMN(J)	scale factor for the x direction at the interface locations YV(J)
TBULK	T_{bulk} by integration of numerical results
TB1	T_{bulk} by heat balance
TEMP	temporary storage
TIN	inlet uniform temperature

TITLE(NF)	alphameric title for F(I,J,NF)
TSUM	$\Sigma T\Delta Aw$
TW	average wall temperature
TWSUM	$\Sigma T(I,M1)$
T0	TB1 when calculating properties
U(I,J)	velocity u in x direction
V(I,J)	velocity v in y direction
VOL	volume of the C. V.
WIN	inlet uniform axial velocity
WSUM	$\Sigma w\Delta A$
X(I)	the values of the x at grid points
XCV(I)	the x-direction widths of main C. V.'s
XCVI(I)	the part of XCV(I) that overlaps on the C. V. for U(I,J)
XCVIP(I)	the part of XCV(I) that overlaps on the C. V. for U(I+1,J)
XCVS(I)	the x-direction width of the staggered C. V. for U(I,J)
XDIF(I)	the difference X(I)-X(I-1)
XL	the x-direction length of the calculation domain
XU(I)	the location of the C. V. faces; i.e., the location of U(I,J)
X1	mass fraction of DEG in DEG-water solution
Y(J)	the values of y at grid points
YCV(J)	the y-direction width of main C. V. 's
YCVR(J)	the area $r\Delta y$ for a main C. V.
YCVRS(J)	the area $r\Delta y$ for the C. V. for V(I,J)

YCVS(J)	the y-direction width of the staggered C. V. for V(I,J)
YDIF(J)	the difference Y(J)-Y(J-1)
YL	the y-direction length of the calculation domain
YV(J)	the location of C. V. faces; i.e., the location of V(I,J)
Z(K)	the values of z at grid points

TABLE VI

INPUT FOR A SPECIFIC COMPUTATIONAL RUN

Procedures	Variables	Subroutine	Run#2105	Comments
Assign Outputs	LISFIL	SETUP	R2105.SSS	main output
	- - -	OUTPUT	R2105.PL	for plotting only
Grid	MODE	GRID	3	
	L1	GRID	19	
	M1	GRID	19	
	DIA	GRID	0.016 m	
	N	MAIN	44	
	DEZ(K)	TUBE	44 data points	
Initialization	TIN	START	36.167°C	
	WIN	START	0.3 m/sec	
	RM	START	0.03925 kg/sec	
	QW1	START	12200 w/m^2	
	RHOCON	START	1090 kg/m^3	
	AMU1	START	1.4E-2 Pa.s	
	X1	START	0.09987	
	DPDZ	START	-400 Pa/m	
Iteration control	LAST	TUBE	100	for test or safety
	ITER	BOUND	5	for w
	ERSUM	BOUND	1	for u and v
	ERSUM	BOUND	1E-2	for T

* In GRID, nonuniform spacing in r-direction should be rewritten if other DIA is used.

PROGRAM LISTING

```
C
C  *****************************************************************
C  *                                                               *
C  *  A PROGRAM FOR LAMINAR MIXED CONVECTION HEAT TRANSFER INSIDE *
C  *            HORIZONTAL TUBES                                   *
C  *                                                               *
C  *  AUTHOR      : CHANGLIN ZHANG                                 *
C  *  INSTALLATION: OKLAHOMA STATE UNIVERSITY                      *
C  *  DATA        : FALL 1989                                      *
C  *  LANGUAGE    : FORTRAN 77                                     *
C  *  REFERENCE   : PATANKAR,1984                                  *
C  *                                                               *
C  *****************************************************************
      PROGRAM MAIN
      INCLUDE 'ZHANG.CMN'
      CALL GRID
      CALL SETUP1
      CALL START
      Z=0.
      N=44
      TO=TIN
      CALL SPHT
      DO 30 K=1,N
      Z=Z+DEZ(K)                          Symmetrical
      TB1=TIN+(PI*DIA*Z*QW1)/(2*RM*CP1)
      TO=TB1                          Calculat of 1/2 pipe of circle.
      CALL CONDC
      IF(K.EQ.1) GO TO 10
      CALL INPUT
   10 CALL DENSE
      CALL SPHT
      CALL CONDY
      CALL VISCO
      CALL BOUND
      CALL OUTPUT
      IF(LSTOP) GO TO 20
      CALL SETUP2
      GO TO 10
   20 CALL RESUME
   30 CONTINUE
      STOP
      END
CCCCCCCCCCCCCCCCCCCCCCCCCCCCCCCCCCCCCCCCCCCCCCCCCCCCCCCCCCCCCCCCCCC
      SUBROUTINE DIFLOW
C*******************************************************************
C-------USING POWER-LAW SCHEME-------------------------------------
      INCLUDE 'ZHANG.CMN'
      ACOF=DIFF
      IF(FLOW.EQ.0.) RETURN
      TEMP=DIFF-ABS(FLOW)*0.1
```

```
      ACOF=0.
      IF(TEMP.LE.0.) RETURN
      TEMP=TEMP/DIFF
      ACOF=DIFF*TEMP**5
      RETURN
      END
CCCCCCCCCCCCCCCCCCCCCCCCCCCCCCCCCCCCCCCCCCCCCCCCCCCCCCCCCCCCCCCCCCCC
      SUBROUTINE RESUME
C**********************************************************************
c------INITIALIZING CONTROLLERS FOR EACH MARCHING--------------------
      INCLUDE 'ZHANG.CMN'
      LSOLVE(4)=.FALSE.
      DO 60 NF=5,6
   60 LSOLVE(NF)=.TRUE.
      LSTOP=.FALSE.
      ITER=0
      SMAX=0.
      SSUM=0.
      RETURN
      END
CCCCCCCCCCCCCCCCCCCCCCCCCCCCCCCCCCCCCCCCCCCCCCCCCCCCCCCCCCCCCCCCCCCC
      SUBROUTINE SOLVE
C********************************************************************
      INCLUDE 'ZHANG.CMN'
      ISTF=IST-1
      JSTF=JST-1
      IT1=L2+IST
      IT2=L3+IST
      JT1=M2+JST
      JT2=M3+JST
C********************************************************************
      DO 999 NT=1,NTIMES(NF)
      NFF=NF
      DO 999 N=NF,NFF
C-------I-DIRECTION BLOCK CORRECTION-----------------------------
      IF(.NOT.LBLK(NF)) GO  TO 10
      PT(ISTF)=0.
      QT(ISTF)=0.
      DO 11 I=IST,L2
      BL=0.
      BLP=0.
      BLM=0.
      BLC=0.
      DO  12 J=JST,M2
      BL=BL+AP(I,J)
      IF(J.NE.M2)  BL=BL-AJP(I,J)
      IF(J.NE.JST) BL=BL-AJM(I,J)
      BLP=BLP+AIP(I,J)
      BLM=BLM+AIM(I,J)
      BLC=BLC+CON(I,J)+AIP(I,J)*F(I+1,J,N)+AIM(I,J)*F(I-1,J,N)
     1   +AJP(I,J)*F(I,J+1,N)+AJM(I,J)*F(I,J-1,N)-AP(I,J)*F(I,J,N)
   12 CONTINUE
      DENOM=BL-PT(I-1)*BLM
      IF(ABS(DENOM/BL).LT.1.E-10) DENOM=1.D30
```

```
      PT(I)=BLP/DENOM
      QT(I)=(BLC+BLM*QT(I-1))/DENOM
   11 CONTINUE
      BL=0.
      DO 13 II=IST,L2
      I=IT1-II
      BL=BL*PT(I)+QT(I)
      DO 13 J=JST,M2
   13 F(I,J,N)=F(I,J,N)+BL
C--------J-DIRECTION BLOCK CORRECTION-----------------------------------
      PT(JSTF)=0.
      QT(JSTF)=0.
      DO 21 J=JST,M2
      BL=0.
      BLP=0.
      BLM=0.
      BLC=0.
      DO 22  I=IST,L2
      BL=BL+AP(I,J)
      IF(I.NE.L2) BL=BL-AIP(I,J)
      IF(I.NE.IST) BL=BL-AIM(I,J)
      BLP=BLP+AJP(I,J)
      BLM=BLM+AJM(I,J)
      BLC=BLC+CON(I,J)+AIP(I,J)*F(I+1,J,N)+AIM(I,J)*F(I-1,J,N)
     1   +AJP(I,J)*F(I,J+1,N)+AJM(I,J)*F(I,J-1,N)-AP(I,J)*F(I,J,N)
   22 CONTINUE
      DENOM=BL-PT(J-1)*BLM
      IF(ABS(DENOM/BL).LT.1.E-10) DENOM=1.D30
      PT(J)=BLP/DENOM
      QT(J)=(BLC+BLM*QT(J-1))/DENOM
   21 CONTINUE
      BL=0.
      DO  23 JJ=JST,M2
      J=JT1-JJ
      BL=BL*PT(J)+QT(J)
      DO 23 I=IST,L2
   23 F(I,J,N)=F(I,J,N)+BL
   10 CONTINUE
C---------FORWARD I-DIRECTION TDMA-----------------------------
      DO 90 J=JST,M2
      PT(ISTF)=0.
      QT(ISTF)=F(ISTF,J,N)
      DO 70 I=IST,L2
   50 DENOM=AP(I,J)-PT(I-1)*AIM(I,J)
      PT(I)=AIP(I,J)/DENOM
      TEMP=CON(I,J)+AJP(I,J)*F(I,J+1,N)+AJM(I,J)*F(I,J-1,N)
      QT(I)=(TEMP+AIM(I,J)*QT(I-1))/DENOM
   70 CONTINUE
      DO 80 II=IST,L2
      I=IT1-II
   80 F(I,J,N)=F(I+1,J,N)*PT(I)+QT(I)
   90 CONTINUE
C-------BACKWARD I-DIRECTION TDMA-----------------------------------
      DO 190 JJ=JST,M3
```

```
      J=JT2-JJ
      PT(ISTF)=0.
      QT(ISTF)=F(ISTF,J,N)
      DO 170 I=IST,L2
  150 DENOM=AP(I,J)-PT(I-1)*AIM(I,J)
      PT(I)=AIP(I,J)/DENOM
      TEMP=CON(I,J)+AJP(I,J)*F(I,J+1,N)+AJM(I,J)*F(I,J-1,N)
      QT(I)=(TEMP+AIM(I,J)*QT(I-1))/DENOM
  170 CONTINUE
      DO 180 II=IST,L2
      I=IT1-II
  180 F(I,J,N)=F(I+1,J,N)*PT(I)+QT(I)
  190 CONTINUE
C--------FORWARD J-DIRECTION TDMA---------------------------------
      DO 290 I=IST,L2
      PT(JSTF)=0.
      QT(JSTF)=F(I,JSTF,N)
  250 DO 270 J=JST,M2
      DENOM=AP(I,J)-PT(J-1)*AJM(I,J)
      PT(J)=AJP(I,J)/DENOM
      TEMP=CON(I,J)+AIP(I,J)*F(I+1,J,N)+AIM(I,J)*F(I-1,J,N)
      QT(J)=(TEMP+AJM(I,J)*QT(J-1))/DENOM                          JM
  270 CONTINUE                                                      JP
      DO 280 JJ=JST,M2
      J=JT1-JJ
  280 F(I,J,N)=F(I,J+1,N)*PT(J)+QT(J)
  290 CONTINUE
C--------BACKWARD J-DIRECTION TDMA--------------------------------
      DO 390 II=IST,L3
      I=IT2-II
      PT(JSTF)=0.
      QT(JSTF)=F(I,JSTF,N)
  350 DO 370 J=JST,M2
      DENOM=AP(I,J)-PT(J-1)*AJM(I,J)
      PT(J)=AJP(I,J)/DENOM
      TEMP=CON(I,J)+AIP(I,J)*F(I+1,J,N)+AIM(I,J)*F(I-1,J,N)
      QT(J)=(TEMP+AJM(I,J)*QT(J-1))/DENOM
  370 CONTINUE
      DO 380 JJ=JST,M2
      J=JT1-JJ
  380 F(I,J,N)=F(I,J+1,N)*PT(J)+QT(J)
  390 CONTINUE
C*******************************************
  999 CONTINUE
      DO 400 J=2,M2
      DO 400 I=2,L2
      CON(I,J)=0.
      AP(I,J)=0.
  400 CONTINUE
      RETURN
      END
CCCCCCCCCCCCCCCCCCCCCCCCCCCCCCCCCCCCCCCCCCCCCCCCCCCCCCCCCCCCCCCCCC
      SUBROUTINE SETUP
C*****************************************************************
```

```
      INCLUDE 'ZHANG.CMN'
C***********************************************************************
    3 FORMAT('1',14X,'COMPUTATION   IN   POLAR   COORDINATES')
    4 FORMAT(14X,38(1H*),//)
      DATA LISFIL,INPUTF,SAVEF/'R2105.SSS','USER.DAT','USER.DAT'/
      DATA ZERO/0.0/
      DATA NFMAX,NP,NRHO,NGAM/LIV,LIV1,LIV2,LIV3/
      DATA LSTOP,LSOLVE,LPRINT/1*.FALSE.,LV*.FALSE.,LV*.FALSE./
      DATA LINPUT,LSAVE/LV*.FALSE.,LV*.FALSE./
      DATA LBLK/LV*.TRUE./
      DATA MODE,LAST,TIME,ITER/1,5,0.,0/
      DATA RELAX,NTIMES/LV*1.,LV*1/
      DATA DT,IPREF,JPREF,RHOCON/1.D+10,1,1,1043./
C-----------------------------------------------------------------------
      ENTRY SETUP1
      L2=L1-1
      L3=L2-1
      M2=M1-1
      M3=M2-1
      X(1)=XU(2)
      DO 5 I=2,L2
    5 X(I)=0.5*(XU(I+1)+XU(I))
      X(L1)=XU(L1)
      Y(1)=YV(2)
      DO 10 J=2,M2
   10 Y(J)=0.5*(YV(J+1)+YV(J))
      Y(M1)=YV(M1)
      DO 15 I=2,L1
   15 XDIF(I)=X(I)-X(I-1)
      DO 18 I=2,L2
   18 XCV(I)=XU(I+1)-XU(I)
      DO 20 I=3,L2
   20 XCVS(I)=XDIF(I)
      XCVS(3)=XCVS(3)+XDIF(2)
      XCVS(L2)=XCVS(L2)+XDIF(L1)
      DO 22 I=3,L3
      XCVI(I)=0.5*XCV(I)
   22 XCVIP(I)=XCVI(I)
      XCVIP(2)=XCV(2)
      XCVI(L2)=XCV(L2)
      DO 35 J=2,M1
   35 YDIF(J)=Y(J)-Y(J-1)
      DO 40 J=2,M2
   40 YCV(J)=YV(J+1)-YV(J)
      DO 45 J=3,M2
   45 YCVS(J)=YDIF(J)
      YCVS(3)=YCVS(3)+YDIF(2)
      YCVS(M2)=YCVS(M2)+YDIF(M1)
      IF(MODE.NE.1) GO TO 55
      DO 52 J=1,M1
      RMN(J)=1.0
   52 R(J)=1.0
      GO TO 56
   55 DO 50 J=2,M1
```

```
50 R(J)=R(J-1)+YDIF(J)
   RMN(2)=R(1)
   DO 60 J=3,M2
60 RMN(J)=RMN(J-1)+YCV(J-1)
   RMN(M1)=R(M1)
56 CONTINUE
   DO 57 J=1,M1
   SX(J)=1.
   SXMN(J)=1.
   IF(MODE.NE.3) GO TO 57
   SX(J)=R(J)
   IF(J.NE.1) SXMN(J)=RMN(J)
57 CONTINUE
   DO 62 J=2,M2
   YCVR(J)=R(J)*YCV(J)
   ARX(J)=YCVR(J)
   IF(MODE.NE.3) GO TO 62
   ARX(J)=YCV(J)
62 CONTINUE
   DO 64 J=4,M3
64 YCVRS(J)=0.5*(R(J)+R(J-1))*YDIF(J)
   YCVRS(3)=0.5*(R(3)+R(1))*YCVS(3)
   YCVRS(M2)=0.5*(R(M1)+R(M3))*YCVS(M2)
   IF(MODE.NE.2) GO TO 67
   DO 65 J=3,M3
   ARXJ(J)=0.25*(1.+RMN(J)/R(J))*ARX(J)
65 ARXJP(J)=ARX(J)-ARXJ(J)
   GO TO 68
67 DO 66 J=3,M3
   ARXJ(J)=0.5*ARX(J)
66 ARXJP(J)=ARXJ(J)
68 ARXJP(2)=ARX(2)
   ARXJ(M2)=ARX(M2)
   DO 70 J=3,M3
   FV(J)=ARXJP(J)/ARX(J)
70 FVP(J)=1.-FV(J)
   DO 85 I=3,L2
   FX(I)=0.5*XCV(I-1)/XDIF(I)
85 FXM(I)=1.-FX(I)
   FX(2)=0.
   FXM(2)=1.
   FX(L1)=1.
   FXM(L1)=0.
   DO 90 J=3,M2
   FY(J)=0.5*YCV(J-1)/YDIF(J)
90 FYM(J)=1.-FY(J)
   FY(2)=0.
   FYM(2)=1.
   FY(M1)=1.
   FYM(M1)=0.
   DO 95 J=1,M1
   DO 95 I=1,L1
   PC(I,J)=0.
   U(I,J)=0.
```

```
      V(I,J)=0.
      CON(I,J)=0.
      AP(I,J)=0.
      RHO(I,J)=RHOCON
      P(I,J)=0.
   95 CONTINUE
      OPEN(UNIT=1,FILE=LISFIL,STATUS='NEW')
      IF(MODE.EQ.1) WRITE (1,1)
      IF(MODE.EQ.2) WRITE (1,2)
      IF(MODE.EQ.3) WRITE (1,3)
      WRITE (1,4)
      RETURN
C-----------------------------------------------------------------
      ENTRY SETUP2
COEFFICIENTS FOR THE U EQUATION----------------------------------
      NF=1
      IF(.NOT.LSOLVE(NF)) GO TO 100
      IST=3
      JST=2
      CALL GAMSOR
      REL=1.-RELAX(NF)
      DO 102 I=3,L2
      FL=XCVI(I)*V(I,2)*RHO(I,1)
      FLM=XCVIP(I-1)*V(I-1,2)*RHO(I-1,1)
      FLOW=R(1)*(FL+FLM)
      DIFF=R(1)*(XCVI(I)*GAM(I,1)+XCVIP(I-1)*
     +GAM(I-1,1))/YDIF(2)
      CALL DIFLOW
  102 AJM(I,2)=ACOF+MAX(ZERO,FLOW)
      DO 103 J=2,M2
      FLOW=ARX(J)*U(2,J)*RHO(1,J)
      DIFF=ARX(J)*GAM(1,J)/(XCV(2)*SX(J))
      CALL DIFLOW
      AIM(3,J)=ACOF+MAX(ZERO,FLOW)
      DO 103 I=3,L2
      IF(I.EQ.L2) GO TO 104
      FL=U(I,J)*(FX(I)*RHO(I,J)+FXM(I)*RHO(I-1,J))
      FLP=U(I+1,J)*(FX(I+1)*RHO(I+1,J)+FXM(I+1)*RHO(I,J))
      FLOW=ARX(J)*0.5*(FL+FLP)
      DIFF=ARX(J)*GAM(I,J)/(XCV(I)*SX(J))
      GO TO 105
  104 FLOW=ARX(J)*U(L1,J)*RHO(L1,J)
      DIFF=ARX(J)*GAM(L1,J)/(XCV(L2)*SX(J))
  105 CALL DIFLOW
      AIM(I+1,J)=ACOF+MAX(ZERO,FLOW)
      AIP(I,J)=AIM(I+1,J)-FLOW
      IF(J.EQ.M2) GO TO 106
      FL=XCVI(I)*V(I,J+1)*(FY(J+1)*RHO(I,J+1)+FYM(J+1)*RHO(I,J))
      FLM=XCVIP(I-1)*V(I-1,J+1)*(FY(J+1)*RHO(I-1,J+1)+FYM(J+1)*
     1 RHO(I-1,J))
      GM=GAM(I,J)*GAM(I,J+1)/(YCV(J)*GAM(I,J+1)+YCV(J+1)*GAM(I,J)+
     1 1.0E-30)*XCVI(I)
      GMM=GAM(I-1,J)*GAM(I-1,J+1)/(YCV(J)*GAM(I-1,J+1)+YCV(J+1)*
     1 GAM(I-1,J)+1.E-30)*XCVIP(I-1)
```

```
      DIFF=RMN(J+1)*2.*(GM+GMM)
      GO TO 107
  106 FL=XCVI(I)*V(I,M1)*RHO(I,M1)
      FLM=XCVIP(I-1)*V(I-1,M1)*RHO(I-1,M1)
      DIFF=R(M1)*(XCVI(I)*GAM(I,M1)+XCVIP(I-1)*
     +GAM(I-1,M1))/YDIF(M1)
  107 FLOW=RMN(J+1)*(FL+FLM)
      CALL DIFLOW
      AJM(I,J+1)=ACOF+MAX(ZERO,FLOW)
      AJP(I,J)=AJM(I,J+1)-FLOW
      VOL=YCVR(J)*XCVS(I)
      CON(I,J)=CON(I,J)*VOL+FU(I,J)*F1(I,J,NF)
      AP(I,J)=(FU(I,J)-AP(I,J)*VOL+AIP(I,J)+AIM(I,J)+AJP(I,J)
     1+AJM(I,J))/RELAX(NF)
      CON(I,J)=CON(I,J)+REL*AP(I,J)*U(I,J)
      DU(I,J)=VOL/(XDIF(I)*SX(J))
      CON(I,J)=CON(I,J)+DU(I,J)*(P(I-1,J)-P(I,J))
      DU(I,J)=DU(I,J)/AP(I,J)
  103 CONTINUE
      CALL SOLVE
  100 CONTINUE
COEFFICIENTS FOR THE  V  EQUATION----------------------------------
      NF=2
      IF(.NOT.LSOLVE(NF)) GO TO 200
      IST=2
      JST=3
      CALL GAMSOR
      REL=1.-RELAX(NF)
      DO 202 I=2,L2
      AREA=R(1)*XCV(I)
      FLOW=AREA*V(I,2)*RHO(I,1)
      DIFF=AREA*GAM(I,1)/YCV(2)
      CALL DIFLOW
  202 AJM(I,3)=ACOF+MAX(ZERO,FLOW)
      DO 203 J=3,M2
      FL=ARXJ(J)*U(2,J)*RHO(1,J)
      FLM=ARXJP(J-1)*U(2,J-1)*RHO(1,J-1)
      FLOW=FL+FLM
      DIFF=(ARXJ(J)*GAM(1,J)+ARXJP(J-1)*GAM(1,J-1))
     +/(XDIF(2)*SXMN(J))
      CALL DIFLOW
      AIM(2,J)=ACOF+MAX(ZERO,FLOW)
      DO 203 I=2,L2
      IF(I.EQ.L2) GO TO 204
      FL=ARXJ(J)*U(I+1,J)*(FX(I+1)*RHO(I+1,J)+FXM(I+1)*RHO(I,J))
      FLM=ARXJP(J-1)*U(I+1,J-1)*(FX(I+1)*RHO(I+1,J-1)+FXM(I+1)*
     1 RHO(I,J-1))
      GM=GAM(I,J)*GAM(I+1,J)/(XCV(I)*GAM(I+1,J)+XCV(I+1)*GAM(I,J)+
     1 1.E-30)*ARXJ(J)
      GMM=GAM(I,J-1)*GAM(I+1,J-1)/(XCV(I)*GAM(I+1,J-1)+XCV(I+1)*
     1 GAM(I,J-1)+1.0E-30)*ARXJP(J-1)
      DIFF=2.*(GM+GMM)/SXMN(J)
      GO TO 205
  204 FL=ARXJ(J)*U(L1,J)*RHO(L1,J)
```

```
      FLM=ARXJP(J-1)*U(L1,J-1)*RHO(L1,J-1)
      DIFF=(ARXJ(J)*GAM(L1,J)+ARXJP(J-1)*GAM(L1,J-1))
     +/(XDIF(L1)*SXMN(J))
  205 FLOW=FL+FLM
      CALL DIFLOW
      AIM(I+1,J)=ACOF+MAX(ZERO,FLOW)
      AIP(I,J)=AIM(I+1,J)-FLOW
      IF(J.EQ.M2) GO TO 206
      AREA=R(J)*XCV(I)
      FL=V(I,J)*(FY(J)*RHO(I,J)+FYM(J)*RHO(I,J-1))*RMN(J)
      FLP=V(I,J+1)*(FY(J+1)*RHO(I,J+1)+FYM(J+1)*RHO(I,J))*RMN(J+1)
      FLOW=(FV(J)*FL+FVP(J)*FLP)*XCV(I)
      DIFF=AREA*GAM(I,J)/YCV(J)
      GO TO 207
  206 AREA=R(M1)*XCV(I)
      FLOW=AREA*V(I,M1)*RHO(I,M1)
      DIFF=AREA*GAM(I,M1)/YCV(M2)
  207 CALL DIFLOW
      AJM(I,J+1)=ACOF+MAX(ZERO,FLOW)
      AJP(I,J)=AJM(I,J+1)-FLOW
      VOL=YCVRS(J)*XCV(I)
      SXT=SX(J)
      IF(J.EQ.M2) SXT=SX(M1)
      SXB=SX(J-1)
      IF(J.EQ.3) SXB=SX(1)
      CON(I,J)=CON(I,J)*VOL+FU(I,J)*F1(I,J,NF)
      AP(I,J)=(FU(I,J)-AP(I,J)*VOL+AIP(I,J)+AIM(I,J)+AJP(I,J)
     1+AJM(I,J))/RELAX(NF)
      CON(I,J)=CON(I,J)+REL*AP(I,J)*V(I,J)
      DV(I,J)=VOL/YDIF(J)
      CON(I,J)=CON(I,J)+DV(I,J)*(P(I,J-1)-P(I,J))
      DV(I,J)=DV(I,J)/AP(I,J)
  203 CONTINUE
      CALL SOLVE
  200 CONTINUE
C  COEFFICIENTS FOR THE PRESSURE CORRECTION EQUATION--------------------
      NF=3
      IF(.NOT.LSOLVE(NF)) GO TO 500
      IST=2
      JST=2
      CALL GAMSOR
      SMAX=0.
      SSUM=0.
      DO 390 J=2,M2
      DO 390 I=2,L2
      VOL=YCVR(J)*XCV(I)
  390 CON(I,J)=CON(I,J)*VOL
      DO 402 I=2,L2
      ARHO=R(1)*XCV(I)*RHO(I,1)
      CON(I,2)=CON(I,2)+ARHO*V(I,2)
  402 AJM(I,2)=0.
      DO 403 J=2,M2
      ARHO=ARX(J)*RHO(1,J)
      CON(2,J)=CON(2,J)+ARHO*U(2,J)
```

```
      AIM(2,J)=0.
      DO 403 I=2,L2
      IF(I.EQ.L2) GO TO 404
      ARHO=ARX(J)*(FX(I+1)*RHO(I+1,J)+FXM(I+1)*RHO(I,J))
      FLOW=ARHO*U(I+1,J)
      CON(I,J)=CON(I,J)-FLOW
      CON(I+1,J)=CON(I+1,J)+FLOW
      AIP(I,J)=ARHO*DU(I+1,J)
      AIM(I+1,J)=AIP(I,J)
      GO TO 405
  404 ARHO=ARX(J)*RHO(L1,J)
      CON(I,J)=CON(I,J)-ARHO*U(L1,J)
      AIP(I,J)=0.
  405 IF(J.EQ.M2) GO TO 406
      ARHO=RMN(J+1)*XCV(I)*(FY(J+1)*RHO(I,J+1)+
     +FYM(J+1)*RHO(I,J))
      FLOW=ARHO*V(I,J+1)
      CON(I,J)=CON(I,J)-FLOW
      CON(I,J+1)=CON(I,J+1)+FLOW
      AJP(I,J)=ARHO*DV(I,J+1)
      AJM(I,J+1)=AJP(I,J)
      GO TO 407
  406 ARHO=RMN(M1)*XCV(I)*RHO(I,M1)
      CON(I,J)=CON(I,J)-ARHO*V(I,M1)
      AJP(I,J)=0.
  407 AP(I,J)=AIP(I,J)+AIM(I,J)+AJP(I,J)+AJM(I,J)
      PC(I,J)=0.
      SMAX=MAX(SMAX,ABS(CON(I,J)))
      SSUM=SSUM+CON(I,J)
  403 CONTINUE
      CALL SOLVE
COME HERE TO CORRECT THE PRESSURE AND VELOCITIES-------------------
      DO 501 J=2,M2
      DO 501 I=2,L2
      P(I,J)=P(I,J)+PC(I,J)*RELAX(NP)
      IF(I.NE.2) U(I,J)=U(I,J)+DU(I,J)*(PC(I-1,J)-PC(I,J))
      IF(J.NE.2) V(I,J)=V(I,J)+DV(I,J)*(PC(I,J-1)-PC(I,J))
  501 CONTINUE
  500 CONTINUE
COEFFICIENTS FOR TEMPERATURE EQUATIONS------------------------------
      IST=2
      JST=2
      NF=4
      IF(.NOT.LSOLVE(NF)) GO TO 400
      CALL GAMSOR
      REL=1.-RELAX(NF)
      DO 452 I=2,L2
      AREA=R(1)*XCV(I)
      FLOW=AREA*V(I,2)*RHO(I,1)
      DIFF=AREA*GAM(I,1)/YDIF(2)
      CALL DIFLOW
  452 AJM(I,2)=ACOF+MAX(ZERO,FLOW)
      DO 453 J=2,M2
      FLOW=ARX(J)*U(2,J)*RHO(1,J)
```

```
      DIFF=ARX(J)*GAM(1,J)/(XDIF(2)*SX(J))
      CALL DIFLOW
      AIM(2,J)=ACOF+MAX(ZERO,FLOW)
      DO 453 I=2,L2
      IF(I.EQ.L2) GO TO 454
      FLOW=ARX(J)*U(I+1,J)*(FX(I+1)*RHO(I+1,J)+
     +FXM(I+1)*RHO(I,J))
      DIFF=ARX(J)*2.*GAM(I,J)*GAM(I+1,J)/((XCV(I)*GAM(I+1,J)+
     + XCV(I+1)*GAM(I,J)+1.0E-30)*SX(J))
      GO TO 455
  454 FLOW=ARX(J)*U(L1,J)*RHO(L1,J)
      DIFF=ARX(J)*GAM(L1,J)/(XDIF(L1)*SX(J))
  455 CALL DIFLOW
      AIM(I+1,J)=ACOF+MAX(ZERO,FLOW)
      AIP(I,J)=AIM(I+1,J)-FLOW
      AREA=RMN(J+1)*XCV(I)
      IF(J.EQ.M2) GO TO 456
      FLOW=AREA*V(I,J+1)*(FY(J+1)*RHO(I,J+1)+FYM(J+1)*RHO(I,J))
      DIFF=AREA*2.*GAM(I,J)*GAM(I,J+1)/(YCV(J)*GAM(I,J+1)+
     + YCV(J+1)*GAM(I,J)+1.0E-30)
      GO TO 457
  456 FLOW=AREA*V(I,M1)*RHO(I,M1)
      DIFF=AREA*GAM(I,M1)/YDIF(M1)
  457 CALL DIFLOW
      AJM(I,J+1)=ACOF+MAX(ZERO,FLOW)
      AJP(I,J)=AJM(I,J+1)-FLOW
  453 CONTINUE
C-------------------------------------------------------------
      OMEGA=4./3.
      OMEGAM=OMEGA-1.
      DO 470 I=2,L2
      AREAM2=RMN(M2)*XCV(I)
      AREAM1=RMN(M1)*XCV(I)
      AJP(I,M2)=OMEGA*AJP(I,M2)
      AJP(I,M1)=AJP(I,M2)/AREAM1
      AJM(I,M1)=OMEGAM*AJM(I,M2)/AREAM2
      AJM(I,M2)=AJM(I,M2)*(1.+OMEGAM*AREAM1/AREAM2)
  470 CONTINUE
C-----------------------------------------------------------
      DO 475 J=2,M2
      DO 475 I=2,L2
      VOL=YCVR(J)*XCV(I)
C------------------------------------------------------------
      CON(I,J)=CON(I,J)*VOL+FU(I,J)*F1(I,J,NF)
      AP(I,J)=FU(I,J)-AP(I,J)*VOL+AIP(I,J)+AIM(I,J)+
     1AJP(I,J)+AJM(I,J)
  475 CON(I,J)=CON(I,J)
C------------------------------------------------------------
      DO 480 I=2,L2
      AP(I,M1)=AJP(I,M1)-AP(I,M1)
      AP(I,M2)=AP(I,M2)-AJP(I,M2)*(AJP(I,M1)+AJM(I,M1))/AP(I,M1)
      AJM(I,M2)=AJM(I,M2)-AJP(I,M2)*AJM(I,M1)/AP(I,M1)
      CON(I,M2)=CON(I,M2)+CON(I,M1)*AJP(I,M2)/AP(I,M1)
  480 AJP(I,M2)=0.
```

```
C--------------------------------------------------------------
      DO 482 J=2,M2
      DO 482 I=2,L2
      AP(I,J)=AP(I,J)/RELAX(NF)
  482 CON(I,J)=CON(I,J)+REL*AP(I,J)*F(I,J,NF)
      CALL SOLVE
C-----------------------------------------------------------------
      DO 485 I=2,L2
      F(I,M1,NF)=(AJP(I,M1)*F(I,M2,NF)+
     1AJM(I,M1)*(F(I,M2,NF)-F(I,M3,NF))+CON(I,M1))/AP(I,M1)
      CON(I,M1)=0.
      AP(I,M1)=0.
  485 CONTINUE
  400 CONTINUE
COEFFICIENTS FOR OTHER EQUATIONS----------------------------------
      IST=2
      JST=2
      DO 600 N=5,NFMAX
      NF=N
      IF(.NOT.LSOLVE(NF)) GO TO 600
      CALL GAMSOR
      REL=1.-RELAX(NF)
      DO 602 I=2,L2
      AREA=R(1)*XCV(I)
      FLOW=AREA*V(I,2)*RHO(I,1)
      DIFF=AREA*GAM(I,1)/YDIF(2)
      CALL DIFLOW
  602 AJM(I,2)=ACOF+MAX(ZERO,FLOW)
      DO 603 J=2,M2
      FLOW=ARX(J)*U(2,J)*RHO(1,J)
      DIFF=ARX(J)*GAM(1,J)/(XDIF(2)*SX(J))
      CALL DIFLOW
      AIM(2,J)=ACOF+MAX(ZERO,FLOW)
      DO 603 I=2,L2
      IF(I.EQ.L2) GO TO 604
      FLOW=ARX(J)*U(I+1,J)*(FX(I+1)*RHO(I+1,J)+
     +FXM(I+1)*RHO(I,J))
      DIFF=ARX(J)*2.*GAM(I,J)*GAM(I+1,J)/
     +((XCV(I)*GAM(I+1,J)+XCV(I+1)*GAM(I,J)+1.0E-30)*SX(J))
      GO TO 605
  604 FLOW=ARX(J)*U(L1,J)*RHO(L1,J)
      DIFF=ARX(J)*GAM(L1,J)/(XDIF(L1)*SX(J))
  605 CALL DIFLOW
      AIM(I+1,J)=ACOF+MAX(ZERO,FLOW)
      AIP(I,J)=AIM(I+1,J)-FLOW
      AREA=RMN(J+1)*XCV(I)
      IF(J.EQ.M2) GO TO 606
      FLOW=AREA*V(I,J+1)*(FY(J+1)*RHO(I,J+1)+FYM(J+1)*RHO(I,J))
      DIFF=AREA*2.*GAM(I,J)*GAM(I,J+1)/(YCV(J)*GAM(I,J+1)+
     + YCV(J+1)*GAM(I,J)+1.0E-30)
      GO TO 607
  606 FLOW=AREA*V(I,M1)*RHO(I,M1)
      DIFF=AREA*GAM(I,M1)/YDIF(M1)
  607 CALL DIFLOW
```

```
      AJM(I,J+1)=ACOF+MAX(ZERO,FLOW)
      AJP(I,J)=AJM(I,J+1)-FLOW
      VOL=YCVR(J)*XCV(I)
      CON(I,J)=CON(I,J)*VOL+FU(I,J)*F1(I,J,NF)
      AP(I,J)=(FU(I,J)-AP(I,J)*VOL+AIP(I,J)+AIM(I,J)+AJP(I,J)
     1+AJM(I,J))/RELAX(NF)
      CON(I,J)=CON(I,J)+REL*AP(I,J)*F(I,J,NF)
  603 CONTINUE
      CALL SOLVE
C***************************************************************
  600 CONTINUE
      ITER=ITER+1
      IF(ITER.GE.LAST) LSTOP=.TRUE.
      RETURN
      END
CCCCCCCCCCCCCCCCCCCCCCCCCCCCCCCCCCCCCCCCCCCCCCCCCCCCCCCCCCCCCCCCCCCCC
      SUBROUTINE SUPPLY
C*********************************************************************
      INCLUDE 'ZHANG.CMN'
C*********************************************************************
   10 FORMAT('1',26(1H*),3X,A10,3X,44(1H*))
   20 FORMAT(1X,4H I =,I7,8I12)
   30 FORMAT(1X,1HJ)
   40 FORMAT(1X,I2,1P9E12.2)
   50 FORMAT(1X,1H )
   51 FORMAT(1X,'I =',2X,9(I4,5X))
   52 FORMAT(1X,'X =',1P9E9.2)
   53 FORMAT(1X,'TH =',1P9E9.2)
   54 FORMAT(1X,'J =',2X,9(I4,5X))
   55 FORMAT(1X,'Y =',1P9E9.2)
C*********************************************************************
      ENTRY PRINT
      IF(.NOT.LPRINT(3)) GO TO 80
CALCULATE THE STREAM FUNCTION-------------------------------------
      F(2,2,3)=0.
      DO 82 I=2,L1
      IF(I.NE.2) F(I,2,3)=F(I-1,2,3)-RHO(I-1,1)*V(I-1,2)
     1*R(1)*XCV(I-1)
      DO 82 J=3,M1
      RHOM=FX(I)*RHO(I,J-1)+FXM(I)*RHO(I-1,J-1)
   82 F(I,J,3)=F(I,J-1,3)+RHOM*U(I,J-1)*ARX(J-1)
   80 CONTINUE
C
      IF(.NOT.LPRINT(NP)) GO TO 90
C
CONSTRUCT BOUNDARY PRESSURES BY EXTRAPOLATION
      DO 91 J=2,M2
      P(1,J)=(P(2,J)*XCVS(3)-P(3,J)*XDIF(2))/XDIF(3)
   91 P(L1,J)=(P(L2,J)*XCVS(L2)-P(L3,J)*XDIF(L1))/XDIF(L2)
      DO 92 I=2,L2
      P(I,1)=(P(I,2)*YCVS(3)-P(I,3)*YDIF(2))/YDIF(3)
   92 P(I,M1)=(P(I,M2)*YCVS(M2)-P(I,M3)*YDIF(M1))/YDIF(M2)
      P(1,1)=P(2,1)+P(1,2)-P(2,2)
      P(L1,1)=P(L2,1)+P(L1,2)-P(L2,2)
```

```
      P(1,M1)=P(2,M1)+P(1,M2)-P(2,M2)
      P(L1,M1)=P(L2,M1)+P(L1,M2)-P(L2,M2)
      PREF=P(IPREF,JPREF)
      DO 93 J=1,M1
      DO 93 I=1,L1
   93 P(I,J)=P(I,J)-PREF
   90 CONTINUE
C
      WRITE (1,50)
      IEND=0
  301 IF(IEND.EQ.L1) GO TO 310
      IBEG=IEND+1
      IEND=IEND+9
      IEND=MIN0(IEND,L1)
      WRITE (1,50)
      WRITE (1,51),(I,I=IBEG,IEND)
      IF(MODE.EQ.3) GO TO 302
      WRITE (1,52),(X(I),I=IBEG,IEND)
      GO TO 301
  302 WRITE (1,53),(X(I),I=IBEG,IEND)
      GO TO 301
  310 JEND=0
      WRITE (1,50)
  311 IF(JEND.EQ.M1) GO TO 320
      JBEG=JEND+1
      JEND=JEND+9
      JEND=MIN0(JEND,M1)
      WRITE (1,50)
      WRITE (1,54),(J,J=JBEG,JEND)
      WRITE (1,55),(Y(J),J=JBEG,JEND)
      GO TO 311
  320 CONTINUE
C
      DO 999 N=1,NGAM
      NF=N
      IF(.NOT.LPRINT(NF)) GO TO 999
      WRITE (1,50)
      WRITE (1,10),TITLE(NF)
      IFST=1
      JFST=1
      IF(NF.EQ.1.OR.NF.EQ.3) IFST=2
      IF(NF.EQ.2.OR.NF.EQ.3) JFST=2
      IBEG=IFST-9
  110 CONTINUE
      IBEG=IBEG+9
      IEND=IBEG+8
      IEND=MIN0(IEND,L1)
      WRITE (1,50)
      WRITE (1,20),(I,I=IBEG,IEND)
      WRITE (1,30)
      JFL=JFST+M1
      DO 115 JJ=JFST,M1
      J=JFL-JJ
      WRITE (1,40),J,(F(I,J,NF),I=IBEG,IEND)
```

```
  115 CONTINUE
      IF(IEND.LT.L1) GO TO 110
  999 CONTINUE
      RETURN
C
      ENTRY INPUT
      OPEN(UNIT=2,FILE=INPUTF,STATUS='OLD')
      DO 410 N=1,NGAM
      NF=N
      IF(.NOT.LINPUT(NF)) GO TO 410
      READ(2,*)
      READ(2,420)((F(I,J,NF),I=1,L1),J=1,M1)
  420 FORMAT(1X,10(E12.5,1X))
  410 CONTINUE
      CLOSE(UNIT=2)
      DO 430 NF=1,5
      DO 430 J=1,M1
      DO 430 I=1,L1
  430 F1(I,J,NF)=F(I,J,NF)
      DO 440 J=2,M2
      DO 440 I=2,L2
  440 FU(I,J)=YCVR(J)*XCV(I)/DEZ(K)*RHO(I,J)*F1(I,J,5)
      RETURN
C
      ENTRY SAVE
      OPEN(UNIT=3,FILE=SAVEF,STATUS='NEW')
      DO 500 N=1,NGAM
      NF=N
      IF(.NOT.LSAVE(NF)) GO TO 500
      WRITE(3,*)
      WRITE(3,520)((F(I,J,NF),I=1,L1),J=1,M1)
  520 FORMAT(1X,10(1PE12.5,1X))
  500 CONTINUE
      CLOSE(UNIT=3)
      RETURN
      END
CCCCCCCCCCCCCCCCCCCCCCCCCCCCCCCCCCCCCCCCCCCCCCCCCCCCCCCCCCCCCCC
      SUBROUTINE TUBE
CCCCCCCCCCCCCCCCCCCCCCCCCCCCCCCCCCCCCCCCCCCCCCCCCCCCCCCCCCCCCCC
      INCLUDE 'ZHANG.CMN'
      DIMENSION U1(30,30),V1(30,30),T1(30,30),W1(30,30)
      DIMENSION T(ID,JD)
      EQUIVALENCE (F(1,1,4),T(1,1))
      DATA TITLE(1),TITLE(2),TITLE(3),TITLE(4),TITLE(5),
     +TITLE(11)/7H  VEL U,7H  VEL V,7H STR FN,6H TEMP ,
     +7H W/WBAR,8HPRESSURE/
      DATA RELAX(1),RELAX(2),RELAX(11)/0.5,0.5,0.5/
      DATA RELAX(4)/0.9/
      DATA (LSOLVE(I),I=5,6),(LINPUT(I),LSAVE(I),LPRINT(I),I=1,5)
     +/17*.TRUE./
      DATA LAST/100/
      DATA (NTIMES(I),I=1,6)/6*3/
      DATA (DEZ(K),K=1,44)/0.0186,0.02,0.0377,0.0377,0.05,0.051,
     +0.06,0.07,0.073,0.06,0.07,0.072,0.101,0.102,0.101,0.101,
```

```
     +0.102,0.102,0.101,0.101,0.101,0.102,0.101,0.101,0.101,0.102,
     +0.101,0.101,0.101,0.101,0.101,0.101,0.101,0.103,0.105,0.105,
     +0.105,0.105,0.105,0.105,0.11,0.11,0.11,0.117/
C
      ENTRY GRID
      MODE=3
      PI=3.14159
      L1=19
      M1=19
      L3=L1-2
      XU(2)=0.
      DX=PI/DFLOAT(L3)
      DO 101 I=3,L1
  101 XU(I)=XU(I-1)+DX
C----------NONUNIFORM IN R-DIRECTION----------
      YV(2)=0.
      YV(3)=0.001
      DY=0.001
      DO 103 J=4,7
  103 YV(J)=YV(J-1)+DY
      DY=0.0004
      DO 105 J=8,13
  105 YV(J)=YV(J-1)+DY
      DY=0.0001
      DO 107 J=14,M1
  107 YV(J)=YV(J-1)+DY
      R(1)=0.
      RETURN
C
      ENTRY START
C---------------RUN #2105----------------------------
      TIN=36.167
      WIN=0.3
      DO 120 J=1,M2
      DO 120 I=1,L1
      F(I,J,4)=TIN
      F(I,M1,4)=TIN
      F(I,J,5)=WIN
  120 F(I,M1,5)=0.
C--------------------------------------------------
      RM=0.03925
      DIA=0.016
      QW1=12200.
      RHOCON=1090.
      AMU1=1.4E-2
      X1=0.9987
      DPDZ=-400.
      DO 130 J=2,M2
      DO 130 I=2,L2
      FU(I,J)=YCVR(J)*XCV(I)/DEZ(1)*RHOCON*F(I,J,5)
      F1(I,J,4)=F(I,J,4)
  130 F1(I,J,5)=F(I,J,5)
      RETURN
C
```

```
      ENTRY DENSE
      A1=998.8+207.29*X1-72.103*X1**2
      B1=-0.10357-1.0797*X1+0.42904*X1**2
      C1=-3.2251E-3+3.4321E-3*X1-4.5246E-4*X1**2
      RHOCON=A1+B1*T0+C1*T0**2
      DO 200 J=1,M1
      DO 200 I=1,L1
      RHO(I,J)=A1+B1*T(I,J)+C1*T(I,J)**2
  200 CONTINUE
      RETURN
C
      ENTRY VISCO
      A2=(0.63513+3.0176*X1-0.49609*X1**2)**1.3514
      B2=-0.029276-0.0440815*X1+0.0099051*X1**2
      C2=(1.8238E-6+5.765E-6*X1-2.6245E-6*X1**2)**0.6803
      AMU1=EXP(A2+B2*T0+C2*T0**2)*1.E-3
      DO 210 J=1,M1
      DO 210 I=1,L1
  210 AMU(I,J)=EXP(A2+B2*T(I,J)+C2*T(I,J)**2)*1.E-3
      RETURN
C
      ENTRY SPHT
      A3=1.027-0.52469*X1+0.021435*X1**2
      B3=-2.6187E-4+3.8054E-3*X1-2.5793E-3*X1**2
      C3=-2.3096E-7+6.0706E-7*X1
      CP1=4187.*(A3+B3*T0+C3*T0**2)
      DO 220 J=1,M1
      DO 220 I=1,L1
      CP(I,J)=4187.*(A3+B3*T(I,J)+C3*T(I,J)**2)
  220 CONTINUE
      RETURN
C
      ENTRY CONDC
      WK=0.56276+1.874E-3*T0-6.8E-6*T0**2
      DEGK=0.19589+1.689E-4*T0-8.1E-7*T0**2
      ALMDA=0.4052+0.0594*X1-8.4E-4*T0
      ALM=ALMDA*(WK-DEGK)*(1-X1)*X1
      COND1=WK*(1-X1)+DEGK*X1-ALM
      RETURN
C
      ENTRY CONDY
      DO 230 J=1,M1
      DO 230 I=1,L1
      WK=0.56276+1.874E-3*T(I,J)-6.8E-6*T(I,J)**2
      DEGK=0.19589+1.689E-4*T(I,J)-8.1E-7*T(I,J)**2
      ALMDA=0.4052+0.0594*X1-8.4E-4*T(I,J)
      ALM=ALMDA*(WK-DEGK)*(1-X1)*X1
  230 COND(I,J)=WK*(1-X1)+DEGK*X1-ALM
      RETURN
C
      ENTRY BOUND
      WSUM=0.
      ASUM=0.
      TSUM=0.
```

```
      FRSUM=0.
      RMSUM=0.
      TWSUM=0.
      ERSUM1=0.
      ERSUM2=0.
      ERSUM4=0.
      ERSUM5=0.
      DO 300 J=2,M2
      DO 300 I=2,L2
      AR=YCVR(J)*THCV(I)
      WSUM=WSUM+F(I,J,5)*AR
      TSUM=TSUM+AR*F(I,J,5)*F(I,J,4)
      FRSUM=FRSUM+F(I,J,6)*RHO(I,J)*AR
      RMSUM=RMSUM+F(I,J,5)*RHO(I,J)*AR
      ASUM=ASUM+AR
  300 CONTINUE
c---------VELOCITY-PRESSURE DECOUPLING IN Z-DIRECTION------------
      IF(.NOT.LSOLVE(6)) GO TO 391
      IF(ITER.LE.2) GO TO 390
      DQ=(RM-RMSUM)/FRSUM
      DPDZ=DPDZ-DQ
      DO 390 J=2,M2
      DO 390 I=2,L2
  390 F(I,J,5)=F(I,J,5)+F(I,J,6)*DQ
  391 CONTINUE
      WBAR=WSUM/ASUM
      RE=RHOCON*WBAR*DIA/AMU1
      FRE=-2.*DPDZ*DIA/(RHOCON*WBAR**2+1.D-30)*RE
      TBULK=TSUM/(WSUM+1.D-30)
C---------ERRORS BETWEEN TWO ITERATIONS-------------------------
      DO 366 J=2,M2
      DO 366 I=2,L2
      ERR1=ABS((F(I,J,1)-U1(I,J))/(U(I,J)+1.E-25))
      ERR2=ABS((F(I,J,2)-V1(I,J))/(V(I,J)+1.E-25))
      ERR4=ABS((F(I,J,4)-T1(I,J))/(F(I,J,4)+1.E-25))
      ERR5=ABS((F(I,J,5)-W1(I,J))/(F(I,J,5)+1.E-25))
      ERSUM1=ERSUM1+ERR1
      ERSUM2=ERSUM2+ERR2
      ERSUM4=ERSUM4+ERR4
  366 ERSUM5=ERSUM5+ERR5
      DO 320 J=2,M2
      U(2,J)=0.
      U(L1,J)=0.
      V(1,J)=V(2,J)
      V(L1,J)=V(L2,J)
      F(1,J,4)=F(2,J,4)
      F(L1,J,4)=F(L2,J,4)
      F(1,J,5)=F(2,J,5)
      F(L1,J,5)=F(L2,J,5)
      F(I,J,6)=F(2,J,6)
  320 F(L1,J,6)=F(L2,J,6)
      DO 330 I=2,L2
      V( ,2)=0.
      U(I,1)=U(I,2)
```

```
      F(I,1,4)=F(I,2,4)
      F(I,1,6)=F(I,2,6)
  330 F(I,1,5)=F(I,2,5)
  310 CONTINUE
C-----------------------------------------------------------------
      DO 420 J=1,M1
      DO 420 I=1,L1
      U1(I,J)=F(I,J,1)
      V1(I,J)=F(I,J,2)
      T1(I,J)=F(I,J,4)
  420 W1(I,J)=F(I,J,5)
C------------------------------------------------------------
  372 CONTINUE
      IF(ITER.LE.5) RETURN
      DO 370 NF=5,6
  370 LSOLVE(NF)=.FALSE.
      DO 360 NF=1,3
  360 LSOLVE(NF)=.TRUE.
      IF(ITER.LE.10) GO TO 382
      IF(ERSUM1.GE.1.) RETURN
      IF(ERSUM2.GE.1.) RETURN
      GO TO 383
  382 RETURN
  383 DO 362 NF=1,3
  362 LSOLVE(NF)=.FALSE.
      LSOLVE(4)=.TRUE.
      IF (ERSUM4.EQ.0.) GO TO 386
      IF(ERSUM4.LE.1E-2) LSTOP=.TRUE.
  386 CONTINUE
C---------NUSSELT NUMBER-------------------------------------
      DO 352 I=2,L2
  352 TWSUM=TWSUM+F(1,M1,4)
      TW=TWSUM/DFLOAT(L3)
      HTC=QW1/(TW-TBULK+1.D-30)
      ANU=HTC*DIA/COND1
      RETURN
C
      ENTRY OUTPUT
      IF(ITER.NE.0) GO TO 400
      PRINT 402,K,TB1
      WRITE(1,402) K,TB1
  402 FORMAT('1','*******************STATION #',I3,'*****************',
     +//' TBULK CALCULATED BY HEAT BALANCE=',1P1E12.3)
      PRINT 401
      WRITE(1,401)
  401 FORMAT(1X,//'************************************************',/
     +'  ITER',6X,'SSUM',7X,'ERR1',8X,'ERR2',8X,
     +'ERR4',6X,'DPDZ',8X,'F.RE',8X,'TBULK',8X,'TWavg',8x,'NU')
  400 PRINT 403,ITER,SSUM,ERSUM1,ERSUM2,
     +ERSUM4,DPDZ,FRE,TBULK,TW,ANU
      WRITE(1,403) ITER,SSUM,ERSUM1,ERSUM2,
     +ERSUM4,DPDZ,FRE,TBULK,TW,ANU
  403 FORMAT(I6,1P9E12.3)
      IF(.NOT.LSTOP) RETURN
```

```
C--------CREATE FILE FOR PLOTTING---------------------------------
      OPEN(UNIT=7,FILE='R2105.PL',STATUS='NEW')
      WRITE(7,450)Z,TB1,TBULK,TW,ANU,FRE,F(2,M1,4),F(L2,M1,4)
  450 FORMAT(1X,8F12.5)
C
      CALL SAVE
      DO 410 J=1,M1
      DO 410 I=1,L1
  410 F(I,J,5)=F(I,J,5)/WBAR
c----------PRINT CONTROLLER-------------------------------------
      IF(MOD(K,11).NE.0) RETURN
      CALL PRINT
      RETURN
C
      ENTRY GAMSOR
      DO 500 J=1,M1
      DO 500 I=1,L1
      GAM(I,J)=AMU(I,J)
      IF(NF.EQ.4) GAM(I,J)=COND(I,J)/CP(I,J)
      GAM(1,J)=0.
      GAM(L1,J)=0.
  500 CONTINUE
      DO 510 J=2,M2
      DO 510 I=2,L2
      IF(NF.NE.1) GO TO 520
      CON(I,J)=(F(I,M1,4)-T(I,J))*(-9.81)*(B1+2.*C1*T(I,J))*
     +SIN(TH(I))+2*AMU(I,J)*(V(I+1,J)-V(I,J))/XDIF(I)/Y(J)**2
      AP(I,J)=-RHO(I,J)*V(I,J)/Y(J)-AMU(I,J)/Y(J)**2
  520 IF(NF.EQ.2) CON(I,J)=-(F(I,M1,4)-T(I,J))*(-9.81)*(B1+
     +2.*C1*T(I,J))*COS(TH(I))+RHO(I,J)*U(I,J)**2/Y(J)-
     +2.*AMU(I,J)*(U(I+1,J)-U(I,J))/XDIF(I)/Y(J)**2
      IF(NF.EQ.2) AP(I,J)=-AMU(I,J)/Y(J)**2
      IF(NF.EQ.4) CON(I,M1)=QW1/CP(I,M1)
      IF(NF.EQ.5) CON(I,J)=-DPDZ
      IF(NF.EQ.6) CON(I,J)=1.
  510 CONTINUE
      RETURN
      END
```

Included File ZHANG.CMN

```
      IMPLICIT DOUBLE PRECISION  (A-H,O-Z)
C---- ID=I DIMENSION, JD=J DIMENSION,KD=K DIMENSION
C---- IMX=MAXIMUM OF ID AND JD
      PARAMETER ID=64,JD=60,KD=50,IMX=64
C---- LIV=NUMBER OF INDEPENDENT VARIABLES; INCLUDING U,V, AND PC
      PARAMETER LIV=10
      PARAMETER LV=LIV+3
      PARAMETER LIV1=LIV+1,LIV2=LIV+2,LIV3=LIV+3
      CHARACTER*40 INPUTF,INPUTT,SAVEF,LISFIL,DUMMY,ANS1,ANS2
      COMMON/FILE/INPUTF,INPUTT(15),SAVEF,LISFIL,TITLE(LIV3)
      LOGICAL  LSOLVE,LPRINT,LBLK,LSTOP,LINPUT,LSAVE
      COMMON/POSI/ITOTAL(2),XP(2,300),YP(2,300)
      COMMON/POINT/UIN,TURBV,PI,DIA,QW1,RM,CP1,K,COND1,RE,AMU1
      COMMON/GIVEN/ISINGLE,PR,DP,ROP,W,Z,TO,TB1,TIN,WIN,DPDZ
      COMMON F(ID,JD,LIV3),CON(ID,JD),FU(ID,JD),AMU(ID,JD),
     1 AIP(ID,JD),AIM(ID,JD),AJP(ID,JD),AJM(ID,JD),AP(ID,JD),
     2 X(ID),XU(ID),XDIF(ID),XCV(ID),XCVS(ID),F1(ID,JD,LIV3),
     3 Y(JD),YV(JD),YDIF(JD),YCV(JD),YCVS(JD),CP(ID,JD),
     4 YCVR(JD),YCVRS(JD),ARX(JD),ARXJ(JD),ARXJP(JD),COND(ID,JD),
     5 R(JD),RMN(JD),SX(JD),SXMN(JD),XCVI(ID),XCVIP(ID)
      COMMON  DU(ID,JD),DV(ID,JD), FV(JD),FVP(JD),
     1 FX(ID),FXM(ID),FY(JD),FYM(JD),PT(IMX),QT(IMX),DEZ(KD)
      COMMON/INDX/NF,NFMAX,NP,NRHO,NGAM,L1,L2,L3,M1,M2,M3,IV1,IV2,
     1 IST,JST,ITER,LAST,RELAX(LIV3),TIME,DT,XL,YL,MO,TW,
     2 IPREF,JPREF,LSOLVE(LIV3),LPRINT(LIV3),LBLK(LIV3),MODE,
     3 NTIMES(LIV3),RHOCON,LINPUT(LIV3),LSAVE(LIV3)
      COMMON/CNTL/LSTOP
      COMMON/SORC/SMAX,SSUM
      COMMON/COEF/FLOW,DIFF,ACOF
      DIMENSION U(ID,JD),V(ID,JD),PC(ID,JD)
      DIMENSION P(ID,JD),RHO(ID,JD),GAM(ID,JD),BETA(ID,JD)
      EQUIVALENCE(F(1,1,LIV+1),P(1,1)),(F(1,1,LIV+2),RHO(1,1)),
     1 (F(1,1,LIV+3),GAM(1,1))
      EQUIVALENCE(F(1,1,1),U(1,1)),(F(1,1,2),V(1,1)),(F(1,1,3),PC(1,1))
      DIMENSION TH(ID),THU(ID),THDIF(ID),THCV(ID),THCVS(ID)
      EQUIVALENCE(X,TH),(XU,THU),(XDIF,THDIF),(XCV,THCV)
     1   ,(XCVS,THCVS),(XL,THL)
```

APPENDIX C

A SAMPLE OUTPUT

Presented is a typical printout for one axial station. The first page is a record of iteration processes at the station. The following pages are distribution of velocity u, v, stream function, temperature, and dimensionless axial velocity, sequentially.

******************STATION # 44****************

TBULK CALCULATED BY HEAT BALANCE=   4 897E+01

****

ITER	SSUM	ERR1	ERR2	ERR4	DPDZ	F RE	TBULK	TWavg	NU
0	0 000E+00	1 218E-04	1 355E-04	9 148E-05	-3 300E+02	5 220E+01	4 873E+01	8 004E+01	3 079E+01
1	0 000E+00	0 000E+00	0 000E+00	0 000E+00	-3 300E+02	5 211E+01	4 875E+01	8 004E+01	3 079E+01
2	0 000E+00	0 000E+00	0 000E+00	0 000E+00	-3 300E+02	5 211E+01	4 875E+01	8 004E+01	3 079E+01
3	0 000E+00	0 000E+00	0 000E+00	0 000E+00	-3 273E+02	5 168E+01	4 875E+01	8 004E+01	3 079E+01
4	0 000E+00	0 000E+00	0 000E+00	0 000E+00	-3 273E+02	5 175E+01	4 875E+01	8 004E+01	3 079E+01
5	0 000E+00	0 000E+00	0 000E+00	0 000E+00	-3 273E+02	5 175E+01	4 875E+01	8 004E+01	3 079E+01
6	0 000E+00	0 000E+00	0 000E+00	0 000E+00	-3 273E+02	5 175E+01	4 875E+01	8 004E+01	3 079E+01
7	8 724E-20	8 998E-01	2 488E+00	0 000E+00	-3 273E+02	5 175E+01	4 875E+01	8 004E+01	3 079E+01
8	-7 073E-20	6 590E-01	1 429E+00	0 000E+00	-3 273E+02	5 175E+01	4 875E+01	8 004E+01	3 079E+01
9	4 299E-20	5 857E-01	1 312E+00	0 000E+00	-3 273E+02	5 175E+01	4 875E+01	8 004E+01	3 079E+01
10	6 956E-20	5 035E-01	1 267E+00	0 000E+00	-3 273E+02	5 175E+01	4 875E+01	8 004E+01	3 079E+01
11	-4.796E-20	4 535E-01	1 174E+00	0 000E+00	-3 273E+02	5 175E+01	4 875E+01	8 004E+01	3 079E+01
12	-2 970E-20	4 208E-01	1 066E+00	0 000E+00	-3 273E+02	5 175E+01	4 875E+01	8 004E+01	3 079E+01
13	-2 451E-20	3 970E-01	9 671E-01	0 000E+00	-3 273E+02	5 175E+01	4 875E+01	8 004E+01	3 080E+01
14	-2 451E-20	0 000E+00	0 000E+00	9 989E-01	-3 273E+02	5 175E+01	4 906E+01	8 021E+01	3 094E+01
15	-2 451E-20	0 000E+00	0 000E+00	1 554E-01	-3 273E+02	5 175E+01	4 910E+01	8 024E+01	3 095E+01
16	-2 451E-20	0 000E+00	0 000E+00	2 867E-02	-3 273E+02	5 175E+01	4 911E+01	8 025E+01	3 095E+01
17	-2 451E-20	0 000E+00	0 000E+00	6 750E-03	-3 273E+02	5 175E+01	4 911E+01	8 025E+01	3 095E+01

```
I  =     1        2        3        4        5        6        7        8        9
TH = 0 00E+00 1 21E-01 3 62E-01 6 04E-01 8 46E-01 1 09E+00 1 33E+00 1 57E+00 1 81E+00

I  =    10       11       12       13       14       15
TH = 2 05E+00 2 30E+00 2 54E+00 2 78E+00 3 02E+00 3 14E+00

J  =     1        2        3        4        5        6        7        8        9
Y  = 0 00E+00 3 08E-04 9 23E-04 1 54E-03 2 15E-03 2 77E-03 3 38E-03 4 00E-03 4 62E-03

J  =    10       11       12       13       14       15
Y  = 5 23E-03 5 85E-03 6 46E-03 7 08E-03 7 69E-03 8 00E-03
```

************************* VEL U **

I =	2	3	4	5	6	7	8	9	10
J									
15	0 00E+00	0 00E+00	0 00E+00	0 00E+00	0 00E+00	0 00E+00	0 00E+00	0 00E+00	0 00E+00
14	0 00E+00	-1 03E-03	-1 90E-03	-2 61E-03	-3 17E-03	-3 61E-03	-3 84E-03	-3 78E-03	-3 46E-03
13	0 00E+00	-3 71E-04	-8 69E-04	-1 17E-03	-1 35E-03	-1 57E-03	-1 84E-03	-2 03E-03	-2 06E-03
12	0 00E+00	-1 15E-04	-1 40E-04	-1 01E-04	-9 29E-06	-6 68E-05	-3 59E-04	-7 05E-04	-9 60E-04
11	0 00E+00	-8 32E-05	1 42E-04	3 47E-04	5 37E-04	6 13E-04	4 82E-04	1 97E-04	-1 17E-04
10	0 00E+00	-3 92E-05	2 19E-04	4 55E-04	6 46E-04	8 00E-04	8 36E-04	7 02E-04	4 66E-04
9	0 00E+00	4 56E-05	2 72E-04	4 77E-04	6 14E-04	7 67E-04	9 05E-04	9 23E-04	8 14E-04
8	0 00E+00	1 26E-04	3 28E-04	4 95E-04	5 79E-04	6 90E-04	8 58E-04	9 81E-04	9 92E-04
7	0 00E+00	1 84E-04	3 53E-04	4 88E-04	5 50E-04	6 29E-04	7 88E-04	9 61E-04	1 06E-03
6	0 00E+00	2 26E-04	3 37E-04	4 28E-04	4 86E-04	5 61E-04	7 08E-04	8 93E-04	1 04E-03
5	0 00E+00	2 66E-04	3 08E-04	3 28E-04	3 65E-04	4 41E-04	5 82E-04	7 62E-04	9 18E-04
4	0 00E+00	3 09E-04	3 20E-04	2 60E-04	2 33E-04	2 74E-04	3 86E-04	5 40E-04	6 83E-04
3	0 00E+00	3 15E-04	3 74E-04	3 03E-04	2 20E-04	1 86E-04	2 16E-04	2 93E-04	3 80E-04
2	0 00E+00	1 43E-04	2 26E-04	2 56E-04	2 54E-04	2 40E-04	2 29E-04	2 23E-04	2 19E-04
1	0 00E+00	1 43E-04	2 26E-04	2 56E-04	2 54E-04	2 40E-04	2 29E-04	2 23E-04	2 19E-04

I =	11	12	13	14	15
J					
15	0 00E+00	0 00E+00	0 00E+00	0 00E+00	0 00E+00
14	-2 96E-03	-2 32E-03	-1 58E-03	-7 69E-04	0 00E+00
13	-1 92E-03	-1 64E-03	-1 22E-03	-7 02E-04	0 00E+00
12	-1 07E-03	-1 02E-03	-8 32E-04	-5 16E-04	0 00E+00
11	-3 46E-04	-4 53E-04	-4 30E-04	-2 86E-04	0 00E+00
10	2 25E-04	4 34E-05	-4 98E-05	-5 52E-05	0 00E+00
9	6 33E-04	4 41E-04	2 76E-04	1 44E-04	0 00E+00
8	8 97E-04	7 32E-04	5 29E-04	2 97E-04	0 00E+00
7	1 04E-03	9 15E-04	6 97E-04	3 97E-04	0 00E+00
6	1 08E-03	9 87E-04	7 72E-04	4 41E-04	0 00E+00
5	9 87E-04	9 31E-04	7 40E-04	4 22E-04	0 00E+00
4	7 62E-04	7 37E-04	5 95E-04	3 40E-04	0 00E+00
3	4 38E-04	4 36E-04	3 58E-04	2 05E-04	0 00E+00
2	2 08E-04	1 83E-04	1 39E-04	7 57E-05	0 00E+00
1	2 08E-04	1 83E-04	1 39E-04	7 57E-05	0 00E+00

************************* VEL V ***

I =	1	2	3	4	5	6	7	8	9
J									
15	0 00E+00	0 00E+00	0 00E+00	0 00E+00	0 00E+00	0 00E+00	0 00E+00	0 00E+00	0 00E+00
14	-3 56E-04	-3 56E-04	-3 03E-04	-2 45E-04	-1 96E-04	-1 55E-04	-7 96E-05	1 86E-05	1 07E-04
13	-5 27E-04	-5 27E-04	-5 18E-04	-3 81E-04	-2 81E-04	-2 54E-04	-1 90E-04	-5 36E-05	1 05E-04
12	-6 26E-04	-6 26E-04	-5 80E-04	-4 02E-04	-2 71E-04	-3 03E-04	-3 30E-04	-2 03E-04	9 54E-06
11	-7 33E-04	-7 33E-04	-5 40E-04	-3 52E-04	-2 13E-04	-3 00E-04	-4 26E-04	-3 56E-04	-1 34E-04
10	-8 43E-04	-8 43E-04	-4 73E-04	-2 73E-04	-1 40E-04	-2 57E-04	-4 60E-04	-4 70E-04	-2 72E-04
9	-9 35E-04	-9 35E-04	-4 06E-04	-1 89E-04	-7 85E-05	-2 02E-04	-4 43E-04	-5 25E-04	-3 76E-04
8	-1 00E-03	-1 00E-03	-3 33E-04	-1 04E-04	-3 28E-05	-1 58E-04	-4 00E-04	-5 28E-04	-4 30E-04
7	-1 05E-03	-1 05E-03	-2 57E-04	-1 28E-05	1 30E-05	-1 23E-04	-3 48E-04	-4 90E-04	-4 35E-04
6	-1 07E-03	-1 07E-03	-2 05E-04	7 97E-05	7 70E-05	-7 48E-05	-2 82E-04	-4 20E-04	-3 96E-04
5	-1 06E-03	-1 06E-03	-2 13E-04	1 37E-04	1 54E-04	7 35E-06	-1 81E-04	-3 11E-04	-3 12E-04
4	-9 51E-04	-9 51E-04	-2 95E-04	8 22E-05	1 75E-04	9 80E-05	-3 92E-05	-1 47E-04	-1 72E-04
3	-5 92E-04	-5 92E-04	-3 46E-04	-1 24E-04	8 45E-06	5 48E-05	4 69E-05	2 41E-05	1 81E-05
2	0 00E+00	0 00E+00	0 00E+00	0 00E+00	0 00E+00	0 00E+00	0 00E+00	0 00E+00	0 00E+00

I =	10	11	12	13	14	15
J						
15	0 00E+00	0 00E+00	0 00E+00	0 00E+00	0 00E+00	0 00E+00
14	1 72E-04	2 19E-04	2 51E-04	2 79E-04	2 64E-04	2 64E-04
13	2 38E-04	3 46E-04	4 27E-04	4 99E-04	5 50E-04	5 50E-04
12	2 17E-04	4 00E-04	5 48E-04	6 79E-04	8 18E-04	8 18E-04
11	1 36E-04	3 95E-04	6 20E-04	8 21E-04	1 04E-03	1 04E-03
10	2 83E-05	3 51E-04	6 49E-04	9 21E-04	1 20E-03	1 20E-03
9	-7 43E-05	2 87E-04	6 45E-04	9 75E-04	1 29E-03	1 29E-03
8	-1 52E-04	2 21E-04	6 12E-04	9 78E-04	1 30E-03	1 30E-03
7	-1 95E-04	1 61E-04	5 55E-04	9 26E-04	1 23E-03	1 23E-03
6	-2 03E-04	1 10E-04	4 71E-04	8 15E-04	1 08E-03	1 08E-03
5	-1 74E-04	7 03E-05	3 65E-04	6 49E-04	8 55E-04	8 55E-04
4	-9 85E-05	5 54E-05	2 52E-04	4 46E-04	5 81E-04	5 81E-04
3	4 45E-05	1 03E-04	1 82E-04	2 60E-04	3 13E-04	3 13E-04
2	0 00E+00	0 00E+00	0 00E+00	0 00E+00	0 00E+00	0 00E+00

************************* STR FN ***

I =	2	3	4	5	6	7	8	9	10
J									
15	0 00E+00	-2 07E-07	-3 34E-07	-4 04E-07	-4 67E-07	-5 30E-07	-5 36E-07	-5 03E-07	-4 45E-07
14	0 00E+00	6 76E-04	1 26E-03	1 73E-03	2 11E-03	2 41E-03	2 57E-03	2 53E-03	2 32E-03
13	0 00E+00	9 21E-04	1 84E-03	2 51E-03	3 02E-03	3 47E-03	3 81E-03	3 91E-03	3 72E-03
12	0 00E+00	9 97E-04	1 93E-03	2 58E-03	3 02E-03	3 52E-03	4 06E-03	4 39E-03	4 38E-03
11	0 00E+00	1 05E-03	1 84E-03	2 35E-03	2 66E-03	3 10E-03	3 73E-03	4 26E-03	4 45E-03
10	0 00E+00	1 08E-03	1 69E-03	2 04E-03	2 23E-03	2 56E-03	3 16E-03	3 78E-03	4 14E-03
9	0 00E+00	1 05E-03	1 51E-03	1 72E-03	1 81E-03	2 04E-03	2 55E-03	3 15E-03	3 58E-03
8	0 00E+00	9 64E-04	1 29E-03	1 39E-03	1 42E-03	1 58E-03	1 97E-03	2 49E-03	2 91E-03
7	0 00E+00	8 42E-04	1 05E-03	1 06E-03	1 05E-03	1 15E-03	1 43E-03	1 84E-03	2 19E-03
6	0 00E+00	6 91E-04	8 24E-04	7 72E-04	7 22E-04	7 71E-04	9 55E-04	1 23E-03	1 49E-03
5	0 00E+00	5 14E-04	6 17E-04	5 51E-04	4 76E-04	4 72E-04	5 61E-04	7 14E-04	8 67E-04
4	0 00E+00	3 07E-04	4 03E-04	3 76E-04	3 19E-04	2 87E-04	3 00E-04	3 48E-04	4 04E-04
3	0 00E+00	9 60E-05	1 52E-04	1 72E-04	1 71E-04	1 62E-04	1 54E-04	1 50E-04	1 47E-04
2	0 00E+00	0 00E+00	0 00E+00	0 00E+00	0 00E+00	0 00E+00	0 00E+00	0 00E+00	0 00E+00

I =	11	12	13	14	15
J					
15	-3 44E-07	-2 15E-07	-1 00E-07	-3 05E-08	0 00E+00
14	1 98E-03	1 56E-03	1 06E-03	5 17E-04	0 00E+00
13	3 29E-03	2 67E-03	1 89E-03	9 93E-04	0 00E+00
12	4 02E-03	3 36E-03	2 46E-03	1 34E-03	0 00E+00
11	4 25E-03	3 67E-03	2 75E-03	1 54E-03	0 00E+00
10	4 10E-03	3 64E-03	2 79E-03	1 58E-03	0 00E+00
9	3 67E-03	3 34E-03	2 60E-03	1 48E-03	0 00E+00
8	3 06E-03	2 84E-03	2 24E-03	1 28E-03	0 00E+00
7	2 35E-03	2 22E-03	1 77E-03	1 01E-03	0 00E+00
6	1 62E-03	1 55E-03	1 24E-03	7 07E-04	0 00E+00
5	9 53E-04	9 19E-04	7 39E-04	4 20E-04	0 00E+00
4	4 37E-04	4 19E-04	3 36E-04	1 90E-04	0 00E+00
3	1 40E-04	1 23E-04	9 36E-05	5 11E-05	0 00E+00
2	0 00E+00	0 00E+00	0 00E+00	0 00E+00	0 00E+00

************************* TEMP **

J \ I =	1	2	3	4	5	6	7	8	9
15	3 62E+01	1 05E+02	9 35E+01	8 72E+01	8 28E+01	7 94E+01	7 70E+01	7 54E+01	7 45E+01
14	9 16E+01	9 16E+01	7 95E+01	7 30E+01	6 84E+01	6 47E+01	6 17E+01	5 93E+01	5 74E+01
13	8 50E+01	8 50E+01	7 05E+01	6 22E+01	5 59E+01	5 04E+01	4 56E+01	4 23E+01	4 04E+01
12	8 21E+01	8 21E+01	6 83E+01	5 98E+01	5 33E+01	4 72E+01	4 16E+01	3 85E+01	3 73E+01
11	7 95E+01	7 95E+01	6 67E+01	5 88E+01	5 29E+01	4 76E+01	4 27E+01	3 90E+01	3 71E+01
10	7 71E+01	7 71E+01	6 50E+01	5 78E+01	5 26E+01	4 81E+01	4 38E+01	4 04E+01	3 83E+01
9	7 49E+01	7 49E+01	6 32E+01	5 65E+01	5 18E+01	4 80E+01	4 44E+01	4 15E+01	3 94E+01
8	7 27E+01	7 27E+01	6 17E+01	5 52E+01	5 08E+01	4 74E+01	4 45E+01	4 21E+01	4 03E+01
7	7 04E+01	7 04E+01	6 05E+01	5 42E+01	5 00E+01	4 68E+01	4 44E+01	4 24E+01	4 09E+01
6	6 81E+01	6 81E+01	5 96E+01	5 37E+01	4 96E+01	4 66E+01	4 43E+01	4 26E+01	4 13E+01
5	6 57E+01	6 57E+01	5 91E+01	5 40E+01	5 01E+01	4 70E+01	4 47E+01	4 30E+01	4 18E+01
4	6 31E+01	6 31E+01	5 88E+01	5 49E+01	5 15E+01	4 85E+01	4 61E+01	4 43E+01	4 30E+01
3	6 02E+01	6 02E+01	5 80E+01	5 56E+01	5 32E+01	5 09E+01	4 88E+01	4 71E+01	4 59E+01
2	5 50E+01	5 50E+01	5 44E+01	5 37E+01	5 28E+01	5 20E+01	5 12E+01	5 04E+01	4 97E+01
1	3 62E+01	5 50E+01	5 44E+01	5 37E+01	5 28E+01	5 20E+01	5 12E+01	5 04E+01	4 97E+01

J \ I =	10	11	12	13	14	15
15	7 39E+01	7 36E+01	7 33E+01	7 34E+01	7 37E+01	3 62E+01
14	5 61E+01	5 53E+01	5 48E+01	5 46E+01	5 51E+01	5 51E+01
13	3 94E+01	3 91E+01	3 90E+01	3 91E+01	3 95E+01	3 95E+01
12	3 71E+01	3 72E+01	3 76E+01	3 81E+01	3 86E+01	3 86E+01
11	3 69E+01	3 71E+01	3 75E+01	3 81E+01	3 89E+01	3 89E+01
10	3 74E+01	3 73E+01	3 76E+01	3 83E+01	3 92E+01	3 92E+01
9	3 83E+01	3 79E+01	3 79E+01	3 85E+01	3 95E+01	3 95E+01
8	3 92E+01	3 86E+01	3 85E+01	3 89E+01	3 98E+01	3 98E+01
7	3 98E+01	3 92E+01	3 91E+01	3 94E+01	4 03E+01	4 03E+01
6	4 04E+01	3 99E+01	3 97E+01	4 01E+01	4 09E+01	4 09E+01
5	4 10E+01	4 07E+01	4 06E+01	4 11E+01	4 17E+01	4 17E+01
4	4 24E+01	4 21E+01	4 22E+01	4 25E+01	4 29E+01	4 29E+01
3	4 52E+01	4 48E+01	4 47E+01	4 47E+01	4 47E+01	4 47E+01
2	4 90E+01	4 85E+01	4 82E+01	4 79E+01	4 78E+01	4 78E+01
1	4 90E+01	4 85E+01	4 82E+01	4 79E+01	4 78E+01	3 62E+01

************************* W/WBAR **

J \ I =	1	2	3	4	5	6	7	8	9
15	0 00E+00	0 00E+00	0 00E+00	0 00E+00	0 00E+00	0 00E+00	0 00E+00	0 00E+00	0 00E+00
14	2 99E-01	2 99E-01	3 04E-01	3 06E-01	3 07E-01	3 09E-01	3 14E-01	3 20E-01	3 24E-01
13	6 79E-01	6 79E-01	6 58E-01	6 40E-01	6 23E-01	6 10E-01	6 02E-01	5 98E-01	5 94E-01
12	9 73E-01	9 73E-01	9 26E-01	8 85E-01	8 43E-01	8 05E-01	7 77E-01	7 61E-01	7 53E-01
11	1 21E+00	1 21E+00	1 15E+00	1 09E+00	1 03E+00	9 73E-01	9 28E-01	9 01E-01	8 90E-01
10	1 40E+00	1 40E+00	1 34E+00	1 27E+00	1 20E+00	1 13E+00	1 07E+00	1 04E+00	1 02E+00
9	1 54E+00	1 54E+00	1 48E+00	1 41E+00	1 34E+00	1 27E+00	1 21E+00	1 16E+00	1 14E+00
8	1 65E+00	1 65E+00	1 60E+00	1 53E+00	1 46E+00	1 39E+00	1 33E+00	1 28E+00	1 26E+00
7	1 72E+00	1 72E+00	1 68E+00	1 62E+00	1 55E+00	1 49E+00	1 43E+00	1 39E+00	1 36E+00
6	1 76E+00	1 76E+00	1 73E+00	1 68E+00	1 62E+00	1 57E+00	1 52E+00	1 48E+00	1 46E+00
5	1 78E+00	1 78E+00	1 75E+00	1 72E+00	1 67E+00	1 63E+00	1 59E+00	1 56E+00	1 53E+00
4	1 78E+00	1 78E+00	1 76E+00	1 73E+00	1 70E+00	1 67E+00	1 64E+00	1 62E+00	1 60E+00
3	1 75E+00	1 75E+00	1 75E+00	1 73E+00	1 72E+00	1 70E+00	1 68E+00	1 66E+00	1 65E+00
2	1 71E+00	1 71E+00	1 71E+00	1 71E+00	1 71E+00	1 70E+00	1 69E+00	1 69E+00	1 68E+00
1	8 43E-01	1 71E+00	1 71E+00	1 71E+00	1 71E+00	1 70E+00	1 69E+00	1 69E+00	1 68E+00

J \ I =	10	11	12	13	14	15
15	0 00E+00	0 00E+00	0 00E+00	0 00E+00	0 00E+00	0 00E+00
14	3 26E-01	3 27E-01	3 28E-01	3 29E-01	3 29E-01	3 29E-01
13	5 90E-01	5 89E-01	5 89E-01	5 89E-01	5 91E-01	5 91E-01
12	7 49E-01	7 48E-01	7 50E-01	7 53E-01	7 55E-01	7 55E-01
11	8 87E-01	8 89E-01	8 93E-01	8 99E-01	9 03E-01	9 03E-01
10	1 01E+00	1 02E+00	1 02E+00	1 03E+00	1 04E+00	1 04E+00
9	1 13E+00	1 13E+00	1 14E+00	1 15E+00	1 16E+00	1 16E+00
8	1 24E+00	1 24E+00	1 25E+00	1 26E+00	1 26E+00	1 26E+00
7	1 35E+00	1 34E+00	1 34E+00	1 35E+00	1 35E+00	1 35E+00
6	1 44E+00	1 43E+00	1 43E+00	1 43E+00	1 44E+00	1 44E+00
5	1 52E+00	1 51E+00	1 51E+00	1 51E+00	1 51E+00	1 51E+00
4	1 59E+00	1 58E+00	1 57E+00	1 57E+00	1 57E+00	1 57E+00
3	1 64E+00	1 63E+00	1 63E+00	1 62E+00	1 62E+00	1 62E+00
2	1 68E+00	1 68E+00	1 67E+00	1 67E+00	1 67E+00	1 67E+00
1	1 68E+00	1 68E+00	1 67E+00	1 67E+00	1 67E+00	8 43E-01

APPENDIX D

DATA FOR CORRELATION

TABLE VII

CHEN'S DATA

Run #.	q''_w, w/m^2	Nu	Re	Pr	Gr	L/d_i	μ_b/μ_w
2101	12700	23.35	611.33	167.91	7617.14	245.8	3.4359
2104	11200	22.53	509.14	167.69	7831.70	245.8	3.5000
2105	12200	22.73	463.30	161.10	8235.30	245.8	3.3400
2107	11600	23.05	327.21	151.68	8953.80	245.8	3.1360
2108	7860	20.37	186.20	165.04	5752.20	245.8	2.6590
2109	20200	23.89	1065.70	92.42	31873.6	245.8	2.9380
2110	20300	24.74	1582.30	99.99	26827.2	245.8	3.1240
2111	24400	29.77	2059.14	93.73	33086.9	245.8	3.0345
2115	5800	13.73	399.40	262.72	1847.0	245.8	2.9866
2117	8300	18.88	964.41	214.85	3074.0	245.8	3.0560
2118	8750	20.54	1107.18	215.90	2986.1	245.8	3.0100
2119	8790	21.19	1247.40	216.08	2905.3	245.8	2.9412
2121	9010	16.56	1707.73	49.38	32168.6	245.8	1.9198
2122	8790	16.29	1456.90	51.94	28049.7	245.8	1.9179
2123	9950	15.72	1152.60	59.17	25792.4	245.8	2.2252
2124	6870	14.30	953.20	57.12	21043.8	245.8	1.8781
2126	7990	13.51	568.64	53.99	16172.1	245.8	2.0876
2127	10900	15.74	1447.50	58.89	18983.9	245.8	2.3908
2128	10600	15.77	1238.77	54.12	18926.9	245.8	2.3336
2129	10400	15.54	1121.48	53.67	19115.1	245.8	2.3114
2130	8690	15.02	837.35	55.26	15679.2	245.8	2.1242
2131	8490	14.09	714.65	55.06	16147.0	245.8	2.1484
2132	6880	13.44	438.85	50.84	15895.8	245.8	1.8952
2133	11100	28.33	1339.38	57.08	8988.3	245.8	1.6068
2135	5110	12.38	627.80	22.51	30873.3	245.8	1.4899
2136	5220	12.75	1099.74	25.79	22949.3	245.8	1.5153
2137	11300	16.81	2023.24	22.90	50004.6	245.8	1.8856
2138	13100	18.65	2428.37	22.56	53582.0	245.8	1.9168
2139	3050	11.50	1177.04	20.38	23827.3	245.8	1.2781
2140	3810	11.99	1205.35	19.89	29856.8	245.8	1.3333
2141	4680	12.84	1241.60	19.28	37130.1	245.8	1.3861
2142	5970	13.96	1290.74	18.51	48971.9	245.8	1.4654
2143	7400	15.20	1352.50	17.63	62789.4	245.8	1.5354

TABLE VIII

ABDELMESSIH'S DATA

Run#	q''_w, w/m^2	Nu	Re	Pr	Gr	L/d_i	μ_b/μ_w
22	4590	14.8	1650.	5.13	151000.	76.4	1.41
23	4580	15.3	1070.	4.93	197000.	76.4	1.36
24	4580	15.5	2080.	5.15	137500.	76.4	1.42
25	4610	14.4	1540.	4.99	195000.	76.4	1.45
27	4550	16.1	126.	92.3	14500.	76.4	2.09
29	4520	15.9	191.	92.1	14750.	76.4	2.07
30	4610	16.0	247.	94.9	14100.	76.4	2.05
31	3140	15.8	303.	97.3	13800.	76.4	2.10
32	3640	16.5	305.	96.4	15100.	76.4	2.21
34	5530	17.1	377.	94.7	15950.	76.4	2.20
44	10000	20.9	506.	93.7	23750.	76.4	3.00
46	9200	20.0	386.	92.8	23200.	76.4	2.90
48	8550	20.2	339.	88.2	24900.	76.4	3.05
49	7420	19.1	266.	88.6	21600.	76.4	2.58
53	5450	19.0	926.	87.2	17850.	76.4	1.80
54	10700	21.9	960.	84.3	31300.	76.4	3.10
55	5700	20.1	1220.	87.6	17150.	76.4	1.90
56	9990	22.3	1240.	86.1	27850.	76.4	2.75
57	10200	21.7	679.	83.2	31600.	76.4	2.85
58	5430	21.2	1510.	87.5	15900.	76.4	1.77
59	10800	23.1	1530.	86.5	28750.	76.4	2.70
60	12900	25.2	1830.	86.8	31400.	76.4	3.20
102	5080	15.3	179	102.	14500.	60.1	2.40
103	9120	18.6	192.	95.4	24100.	60.1	2.80
105	8840	18.5	245.	98.5	22000.	60.1	2.80
106	5310	16.1	288.	105.	13600.	60.1	2.30
107	11200	19.5	306.	98.9	25600.	60.1	2.95
108	5430	17.1	351.	103.	13600.	60.1	2.30
111	10100	19.1	415.	102.	21700.	60.1	3.20

TABLE VIII (continued)

Run#	q''_w, w/m^2	Nu	Re	Pr	Gr	L/d_i	μ_b/μ_w
112	5570	16.8	455.	107.	13100.	60.1	2.20
114	10700	19.2	527.	104.	21500.	60.1	2.70
153	9340	19.4	826.	98.8	19800.	60.1	3.14
155	13300	19.5	835.	97.9	27600.	60.1	4.40
160	13600	22.1	1600.	98.7	24200.	60.1	3.40
201	3500	14.5	156.	92.5	6020.	174.8	1.88
202	3910	15.0	230.	95.4	6280.	174.8	2.00
203	6720	16.4	249.	88.5	10400.	174.8	2.30
204	4000	14.2	306.	96.0	6320.	174.8	2.00
205	8230	17.7	338.	87.2	12400.	174.8	2.60
207	9010	18.1	407.	90.9	12300.	174.8	2.90
208	8280	17.5	487.	91.9	11400.	174.8	2.40
211	11200	19.2	638.	93.0	13300.	174.8	2.90
212	10200	18.2	701.	95.3	12000.	174.8	2.70
254	4160	15.2	665.	105.	5130.	174.8	1.90
255	11000	19.5	712.	98.2	12000.	174.8	2.80
256	5460	16.2	951.	105.	6170.	174.8	2.08
260	15100	21.7	1320.	100.	14000.	174.8	3.60
262	12800	21.4	1590.	103.	11300.	174.8	3.40
302	3730	13.8	174.	80.6	7520.	174.2	1.73
304	4280	13.9	255.	83.4	7780.	174.2	1.81
305	7030	16.5	280.	76.3	13000.	174.2	2.30
306	4080	13.9	334.	85.3	7110.	174.2	1.76
308	4340	13.8	414.	86.3	7220.	174.2	2.10
310	5700	15.1	506.	84.9	9100.	174.2	2.21
311	8940	17.2	536.	80.3	13900.	174.2	3.02
313	9860	17.9	615.	81.7	14200.	174.2	2.98
314	8160	17.0	436.	82.1	12600.	174.2	2.51
316	10200	17.7	692.	83.1	14100.	174.2	3.10
318	10000	17.5	775.	83.5	13700.	174.2	3.05
351	11000	18.0	965.	79.9	15100.	174.2	3.20
352	11600	18.2	1150.	81.8	14800.	174.2	3.00
353	13000	18.9	1480.	83.4	15200.	174.2	3.37
354	13300	19.4	1840.	83.3	15100.	174.2	3.36
356	12800	20.0	2140.	84.9	13300.	174.2	3.13

VITA

Changlin Zhang

Candidate for the Degree of

Doctor of Philosophy

Thesis: THEORETICAL INVESTIGATION ON MIXED CONVECTION INSIDE HORIZONTAL TUBES WITH NOMINALLY UNIFORM HEAT FLUX

Major Field: Chemical Engineering

Biographical:

Education: Graduated from the Department of Chemical Engineering, Tianjin University, China (1976, no degree system at that time in China); received the Master of Science degree in Mechanical Engineering from Xi'an Jiaotong University, China (1982); completed requirements for the Doctor of Philosophy degree at Oklahoma State University in December, 1990.

Professional Experience: Graduate Assistant, School of Chemical Engineering, Oklahoma State University, August 1986 to May 1990; Faculty member, Department of Chemical Engineering, Xi'an Jiaotong University, China, May 1982 to July 1986; Faculty member, Shaanxi Petroleum and Chemical Engineering College, Xi'an, China, October 1976 to August 1979.